

THREE ESSAYS ON DECISION MAKING UNDER UNCERTAINTY IN ELECTRIC POWER SYSTEMS

by

Lizhi Wang

B.Eng., University of Science and Technology of China, 2003

B.S., University of Science and Technology of China, 2003

Submitted to the Graduate Faculty of
the School of Engineering in partial fulfillment
of the requirements for the degree of

Doctor of Philosophy

University of Pittsburgh

2007

UNIVERSITY OF PITTSBURGH

SCHOOL OF ENGINEERING

This dissertation was presented

by

Lizhi Wang

It was defended on

June 25th, 2007

and approved by

Dr. Mainak Mazumdar, Professor Emeritus, Department of Industrial Engineering,

University of Pittsburgh

Dr. Lorenz T. Biegler, Bayer Professor, Department of Chemical Engineering, Carnegie

Mellon University

Dr. Uday Rajan, Associate Professor, Stephen M. Ross School of Business, University of

Michigan

Dr. Jayant Rajgopal, Associate Professor, Department of Industrial Engineering,

University of Pittsburgh

Dr. Andrew J. Schaefer, Associate Professor, Department of Industrial Engineering,

University of Pittsburgh

Dissertation Director: Dr. Mainak Mazumdar, Professor Emeritus, Department of

Industrial Engineering, University of Pittsburgh

THREE ESSAYS ON DECISION MAKING UNDER UNCERTAINTY IN ELECTRIC POWER SYSTEMS

Lizhi Wang, PhD

University of Pittsburgh, 2007

This thesis consists of three essays, discussing three different but connected problems on decision making under uncertainty in electric power systems.

The first essay uses a system model to examine how various factors affect the market price of electricity, and decomposes the price to quantitatively evaluate the contributions of individual factors as well as their interactions. Sensitivity analysis results from a parametric quadratic program are applied in the computation.

The second essay formulates the well studied security constrained economic dispatch (SCED) problem as a Markov decision process model, where the action space is a polyhedron defined by linear generation and transmission constraints. Such a model enables the decision maker to accurately evaluate the impact of a dispatch decision to the entire future operation of the electric power system.

The third essay examines the effect of demand and supply side uncertainties on the exercise of market power. Solutions under Bertrand, Cournot, and linear supply function equilibrium (LSFE) models are derived and compared.

The three problems studied in the essays are a unique representation of different levels of the decision making process in a sophisticated deregulated electric power system, using techniques from both mathematical programming and probability/statistics.

Keywords: Decision making, uncertainty, electric power system, impact coefficient, locational marginal price (LMP), capacity expansion, sensitivity analysis, quadratic programming, probability, power system planning, load flow analysis, security constrained economic dispatch, Markov decision process, mixed integer nonlinear stochastic program, game theory, reliability.

TABLE OF CONTENTS

PREFACE	xi
1.0 INTRODUCTION	1
1.1 Introduction to Electric Power Systems	1
1.2 Introduction to “Using a System Model to Decompose the Effects of Influential Factors on Locational Marginal Prices”	4
1.3 Introduction to “Security Constrained Economic Dispatch: A Markov Decision Process Approach with Embedded Stochastic Programming”	8
1.4 Introduction to “Oligopoly Models for Market Price of Electricity under Demand Uncertainty and Unit Reliability”	11
2.0 USING A SYSTEM MODEL TO DECOMPOSE THE EFFECTS OF INFLUENTIAL FACTORS ON LOCATIONAL MARGINAL PRICES	13
2.1 Introduction	13
2.2 System Model	16
2.2.1 Transmission Network	16
2.2.2 Load Uncertainty	16
2.2.3 Thermal Limit	16
2.2.4 Capacity Reserve	17
2.2.5 Market Power	18
2.2.6 Market Clearing	18
2.2.7 Other Factors	19
2.3 Determination of Impact Coefficients	19
2.3.1 Input and Output of the System Model	19

2.3.2	Deriving Output from Input	21
2.3.3	Calculating Impact Coefficients	24
2.4	Numerical Example	26
2.4.1	Test Data	26
2.4.2	Time-Averaged Impact Coefficients	28
2.4.3	Time Variation of Impact Coefficients	37
2.5	Use of System Model in Evaluating Expansion Plans	37
2.6	Conclusion	40
3.0	SECURITY CONSTRAINED ECONOMIC DISPATCH: A MARKOV DECISION PROCESS APPROACH WITH EMBEDDED STOCHAS- TIC PROGRAMMING	46
3.1	INTRODUCTION	46
3.2	DEFINITIONS AND ASSUMPTIONS	48
3.2.1	Transmission Network	48
3.2.2	Load	48
3.2.3	Generation	48
3.2.4	Transmission Constraint	49
3.2.5	Transmission Line Failure	49
3.2.6	Cascading Failure	50
3.2.7	System Operator	51
3.2.8	Timing of the Transmission Line Failures	51
3.3	THE MARKOV DECISION PROCESS MODEL	51
3.3.1	Time Horizon $\{1, 2, \dots\}$	51
3.3.2	State Space S	51
3.3.3	Action Space A_s	52
3.3.4	Transition Probability $P(j s, a)$	52
3.3.5	Immediate Cost $c(s, a)$	54
3.3.6	Objective	54
3.4	SOLVING THE MDP MODEL	55
3.4.1	Solving Step 3 in Policy Iteration for the Normal State s_N	56

3.4.2 Solving Step 3 in Policy Iteration for Other States	59
3.4.3 Convergence of the Policy Iteration Algorithm	60
3.5 A NUMERICAL EXAMPLE	61
3.6 CONCLUSION	68
4.0 OLIGOPOLY MODELS FOR MARKET PRICE OF ELECTRICITY	
 UNDER DEMAND UNCERTAINTY AND UNIT RELIABILITY . .	69
4.1 Introduction	69
4.2 Assumptions and Objectives for the Stochastic Models	71
4.3 Cournot Model	73
4.4 Linear Supply Function Equilibrium	76
4.5 Numerical Examples	80
4.5.1 Demand and Supply	80
4.5.2 Cournot Model	80
4.5.3 LSFE Model	82
4.5.4 Model Comparisons	82
4.6 Conclusions and Discussions	91
5.0 SUMMARY, DISCUSSION, AND FUTURE RESEARCH DIRECTIONS	92
5.1 Summary	92
5.2 Interrelationships among Three Essays	94
5.3 Discussions and Future Research Directions	95
5.3.1 Discussions and Future Research Directions for Chapter 2	95
5.3.2 Discussions and Future Research Directions for Chapter 3	99
5.3.3 Discussions and Future Research Directions for Chapter 4	100
BIBLIOGRAPHY	101

LIST OF TABLES

1	Interpretation of input variables	20
2	Node data of the 30-bus example	29
3	Transmission line data of the 30-bus example	30
4	Impact coefficients for μ_{LMP}^n (part I)	31
5	Impact coefficients for μ_{LMP}^n (part II)	32
6	Impact coefficients for σ_{LMP}^n (part I)	33
7	Impact coefficients for σ_{LMP}^n (part II)	34
8	Impact coefficients for $\tilde{\mu}_{\text{LMP}}^n$ (part I)	42
9	Impact coefficients for $\tilde{\mu}_{\text{LMP}}^n$ (part II)	43
10	Impact coefficients for $\tilde{\sigma}_{\text{LMP}}^n$ (part I)	44
11	Impact coefficients for $\tilde{\sigma}_{\text{LMP}}^n$ (part II)	45
12	Node data for a five-bus example	61
13	Transmission line data for a five-bus example	62
14	Comparisons of state probabilities for the normal state s_N	67
15	Comparisons of state costs (in $\$10^6$) for the normal state s_N	67
16	Comparisons of expected long-term costs for the normal state s_N	67
17	Generator unit data	81
18	Firm unit data	82
19	Sequential search iteration results using p_{ij} and $L \sim U[769, 1154]$	86
20	Comparison of equilibrium outcomes under different models using p_{ij} and $L \sim U[769, 1154]$	87

21	Comparison of equilibrium outcomes under different models using p_{ij} and $L \sim U[769, 1154]$	87
22	Equilibrium outcomes for each firm using p_{ij} and $L \sim U[769, 1154]$	88
23	Sequential search iteration results using \bar{p}_{ij} and $L \sim U[913, 1010]$	88
24	Comparison of equilibrium outcomes under different models using \bar{p}_{ij} and $L \sim U[913, 1010]$	89
25	Comparison of equilibrium outcomes under different models using \bar{p}_{ij} and $L \sim U[913, 1010]$	89
26	Equilibrium outcomes for each firm using \bar{p}_{ij} and $L \sim U[913, 1010]$	90

LIST OF FIGURES

1	Example of load fluctuation and uncertainty	5
2	Examples of supply function and marginal cost function	7
3	Decomposition of contribution by factors i , j and k	15
4	An IEEE 30-bus network example	27
5	Normalized chronological load change	27
6	Time variation of $\mu_{\text{LMP}}(t)$ and $\sigma_{\text{LMP}}(t)$	36
7	Time variation of impact coefficients for $\mu_{\text{LMP}}(t)$	38
8	Time variation of impact coefficients for $\sigma_{\text{LMP}}(t)$	38
9	A five-bus test example	61
10	Initial generation decisions for s_N	63
11	Initial generation decisions for $s = \{\text{A-B}\}$	63
12	Optimal generation decisions for s_N	64
13	Optimal generation decisions for $s = \{\text{A-B}\}$	64
14	Total cost comparisons between optimal and initial decisions	66
15	Total cost comparisons between optimal decision and N-1 criterion	66
16	Expected profit for $q_{-3} = 480.75$ with $L \sim U(769, 1154)$ and $m = 38.5$	83
17	Best response of q_3^* to $q_{-3} = 480.75$ with $L \sim U(769, 1154)$ and $m = 38.5$	84
18	Best response function $q_3^*(q_{-3})$ with $L \sim U(769, 1154)$ and $m = 38.5$	85
19	Nash equilibrium outcome with $L \sim U(769, 1154)$ and $m = 38.5$	86
20	An example of a Pareto frontier	99

PREFACE

Knowing what I know today and given the opportunity of choosing anyone as my advisor, I would still make the same choice I did four years ago without any hesitation. I just cannot imagine a better advisor than Dr. Mazumdar. He introduced me to the area of electric power system whose cost efficiency and security are too important to take for granted. His strong background of probability/statistics, broad interests in operations research, and deep understanding of the electric power system have provided me with the unique and perfect combination of guidance through every single step towards the finish line of this thesis. He is not only a fascinating teacher in the classroom but also an excellent mentor in life where he sets an example of a successful and honorable person in every aspect. He is as caring as a parent and as frank as a best friend. He has helped me become a better person than I could ever be without him, but he probably could not even realize how much I have learned from him and how much I appreciate everything he has done for me.

The support from the National Science Foundation grant ECS-0245355 is also gratefully acknowledged.

This thesis could not have been completed without the tremendous help from other committee members: Dr. Biegler, Dr. Rajan, Dr. Rajgopal, and Dr. Schaefer. I feel much indebted for their time and effort in traveling to the committee meetings, reading the thesis, and providing me comments that greatly improved it. Needless to say, I am the only person who is responsible for any error contained in this thesis.

I have had the privilege of receiving an undeserved amount of attention and help from Dr. Schaefer, whom I consider as one of my two role models besides Dr. Mazumdar. He has almost everything I dream to have: a daughter and a son with beautiful faces and sweet personalities, an NSF CAREER award among numerous others, an unbelievable record of well

placed students working in prestigious universities and companies, a unique understanding of the big picture in his field of expertise, amazing social skills, a great sense of humor, and more importantly to me than anything else, a willingness to teach how he did it. Compared to Dr. Mazumdar's advice to me that is more on the philosophical level of how to become successful in life, Dr. Schaefer's advice has been more on the strategical and tactical level of how to do things right. Such a distinct contrast reminds me of the beauty of duality, and makes me feel extremely fortunate to have both of them as my role models.

Thanks to Dr. Bidanda for his constant support and encouragement especially during my times of confusion and frustration which every PhD student has to endure. I also thank the faculty members at Pitt: Drs. Wolfe, Shuman, Bailey, Hunsaker, Needy, Norman, Besterfield-Sacre, Bursic, Maillart, and Prokopyev, from whom I have learned the things that will be useful throughout my life. My deep gratitude also goes to Minerva, Richard, Lisa, Nora, Chalice, and Jim, whose excellent services have made the department such a nice and comfortable workplace.

Thanks to Drs. Benjamin Hobbs, Shmuel S. Oren, Jorge Valenzuela, Yihus Chen, Andrew Liu, and Uday Shanbhag. I feel honored for having the opportunity to get to know them personally whose well written papers have been the best textbook for me to learn about the complicated yet fascinating electric power system.

The CEIC seminars in CMU have well served my hunger for both the knowledge in frontier of electric power systems and free lunch. I would like to thank specifically Drs. Lester Lave, Jay Apt, Marija Ilic, Paul Hines, and Seth Blumsack.

I will miss my dear friends who have added so many pleasant memories to my life in Pittsburgh: Lin Wang, Nan Kong, Yan Wang, Zhouyan Wang, Gillian Nicholls, Chen Li, Qian Wu, Weizhe An, Shengnan Wu, Rebeca Sandino, Jennifer Kreke, Erin Gross, Natasa Vidic, Yi Zhang, Jingqiao Zhang, Xiaofei Song, Claudio Ruibal, JP Lai, WX Zhang, WJ Huang, Mike Lin, Lei Qin, Yu Wang, Ming Cheng, Man Yang, Xiao Zhu, Zhenwei Su, etc.

I also feel thankful to Ms. Vinceena DeIulus for treating my wife and me like her own children, and to the Malaysian singer Jingru Liang for her beautiful voice.

Finally and foremost, this thesis is dedicated to my parents, sister, and wife, who give me unconditional love and support through good times and bad. To my daughter (or maybe

son) to be born: please forgive me and your mother for bringing you without warning to this world where the pursuit of happiness and truth is becoming increasingly inconvenient. But we will get there. Please remember our appointment on September 27 of 2007, and be punctual.

1.0 INTRODUCTION

1.1 INTRODUCTION TO ELECTRIC POWER SYSTEMS

Electric power is delivered to widely scattered customers through a three-tiered process. It is first produced from a number of different types of generating units of varying capacities and sizes. Transmission networks then carry large amounts of power over a long distance at a high voltage level. From the transmission sources, distribution systems carry the load to a service area by forming a fine network.

With electricity being a basic need of society, the electric power industry had been regulated for almost a hundred years. Under a regulated set-up, the functions of an electric power system are provided by a given electric utility company which is responsible for supplying power over a specified geographical area and has direct relationships with customers. A major deficiency of regulation is its inefficiency. The regulator's dilemma [81] is, while he or she wishes to (a) hold price down to marginal cost and (b) minimize the cost at the same time, these two objectives can never be achieved simultaneously. On the one hand, a policy that holds price down to marginal cost and takes away any dollar saved by innovation will provide no incentive for the suppliers to improve technology and reduce cost; on the other hand, a policy that passes every dollar saved to the suppliers will soon be found to have resulted in a large gap between cost and price.

A trend of deregulation started since the 1990s, both in the US and in other countries, with the hope of introducing competition and improving efficiency. Under deregulation, electricity is traded like any other commodity, and the producers and consumers have the option to buy and sell power in a marketplace created to provide competition. Transmission networks can be viewed as consisting of nodes (or buses) and links (or lines). Power is generated and/or consumed at the nodes, and the lines connect these nodes.

Electricity has two important characteristics that distinguish it from other commodities. First, it travels at the speed of light through transmission lines, but it cannot be economically stored. Thus, it has to be generated instantaneously as it is being consumed, and at every moment, there should be sufficient generation to meet the demand (or load). Second, the amounts of power that flow through the individual transmission lines corresponding to given amounts of injections (i.e., the difference between generation and consumption) at each node cannot be set arbitrarily, but are determined by the laws of physics (e.g., Kirchhoff's laws). The maximum power flow that can be carried out over any one line in a given network is also limited by the physical characteristics of the network, known as the thermal limit.

During the last several years, different market structures have emerged but they all seem to share the feature that the generation and transmission services are unbundled from each other. Under all these schemes the generation services are competitive but the transmission services remain a regulated monopoly that provides open access to the suppliers and consumers of electricity. This latter function is provided by an impartial entity that is known as the Independent System Operator (ISO). As described in [80], "the minimum functions of the ISO should include the operation and coordination of the power system to ensure security, ... the maximum functions of the ISO will include all the reliability-related and market-related functions..."

Many decisions need to be made under uncertainty by different levels of decision makers in the electric power systems. Uncertainties in the electric power systems come from three major sources: demand, supply, and transmission. On the demand side, load is an ever changing random process that is affected by different kinds of factors, such as season, time, temperature, weather, and other ones that could affect human behavior. On the supply side, the fuel prices are changing frequently, and generators could also have unexpected

breakdowns. On the transmission level, transmission line failures impose a great threat on the reliability and security of the power systems.

This thesis examines three problems at different levels of the electric power systems where decisions need to be made under uncertainty. At a systemic planning level, a constant vigilance needs to be maintained on the price of electricity, which is such a critical element to the welfare of the society that nobody can afford to lose control of it. Investment decisions may be made once the decision makers feel a need to expand the infrastructure of the power system (e.g., building new transmission lines or adding new generators). A key consideration in such decision making processes is how to evaluate the effectiveness of the investment. The first essay examines this problem, and proposes a system model approach to assess the effect of several chosen influential factors that affect electricity prices. This approach can also be used to evaluate expansion plans and help make investment decisions.

The second essay considers decision making at the power dispatch level, where the system operator allocates existing generation and transmission resources to serve the demand. One of the major challenges is the possibility of a transmission line failure, which is a rare event, but has tremendous impact. A Markov decision process approach with embedded stochastic programming is used to model and solve the problem.

The third essay takes the power suppliers' perspective and studies their market power exercise behaviors. Market power is the ability of suppliers to raise price above marginal cost in order to maximize their profits. As deregulation introduces competition into the power market, it also gives the power suppliers a platform to exercise market power. The question of whether deregulation is more efficient than regulation has thus been under extensive scrutiny ever since the beginning of deregulation. The objective of this essay is to use game-theoretic models to formulate the market power exercise behavior in the oligopolistic power market with the hope of providing some insights on how market power affects the price of electricity. The essay is also among the first to take into account the supply side uncertainty in standard oligopoly models.

Although about different problems, these three essays are well connected. First, these problems arise from three different levels of electric power systems, and they together depict a frame of the sophisticated system. Second, the essays are all attempting to improve

the decision making process, which is complicated by the enormous amount of uncertainty involved and the critical role electricity plays to the society. Finally, all essays can serve as examples of applying optimization and probability/statistics techniques and methodologies to real world problems in electric power systems.

The remainder of this thesis is organized as follows. Sections 1.2, 1.3, and 1.4 provide background introduction and literature review on each of the three essays. Chapters 2, 3, and 4 come directly from three papers that the author has co-authored with his advisor and other faculty members. The first paper [89] has been published in the *European Journal of Operational Research*, and the other two are currently under review. Chapter 5 summarize this thesis and discusses some future research topics and directions.

1.2 INTRODUCTION TO “USING A SYSTEM MODEL TO DECOMPOSE THE EFFECTS OF INFLUENTIAL FACTORS ON LOCATIONAL MARGINAL PRICES”

The prices of electricity differ by location, because electricity is cheaper to generate in some locations than others, and generation and transmission capacity is not always sufficient to deliver the cheapest electricity to every location. From the definition of locational marginal price (LMP), a widely used pricing mechanism, the LMP at a given node is determined by the incremental cost of re-dispatching the system to serve one more unit of demand at that node [45]. In a deregulated market, the LMP at a given location is also a stochastic process driven by various endogenous and exogenous factors of the market.

Load uncertainty, for example, is one of the most influential factors. In Figure 1, the solid curve shows the fluctuation of average demand over the 24 hour period, while the dashed lines describe the range of load uncertainty within one standard deviation for each hour.

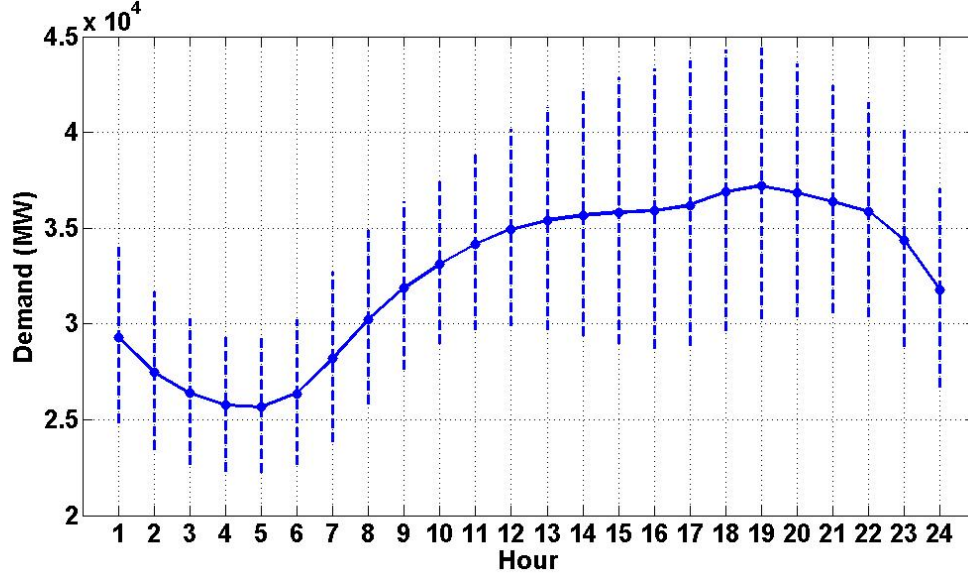


Figure 1: Example of load fluctuation and uncertainty

In the situation when loads reach a very high level, the effect of transmission capacity limitation becomes pronounced. When the transmission lines get too congested to deliver cheaper power to every node, more expensive generators need to be used to serve demand, causing significant price differences between different nodes. The transmission capacity limitation, also known as thermal limit, is the second factor that is being considered in Chapter 2.

The third factor is related to power system security. The term “system security” refers to keeping the system operating in the presence of failures of one or more components of the system. Even when a transmission network is operating within the physical limits, there always remains the possibility that the individual lines may fail due to accidents, such as a lightning strike, fire, falling trees, weather, or deliberate attack. The loss of a single transmission line would change the power flows over other operating lines, possibly exceeding the physical limits. This might result in cascading failures or even collapse of the entire network. To prevent such a catastrophic consequence, certain amounts of generation and/or transmission capacity are typically kept in reserve so that the system can withstand these

types of contingencies. The most widely used capacity reserve criterion in practice is the so called N-1 criterion, which requires the system to be able to withstand any single contingency or failure occurrence. The N-1 criterion will be discussed in more detail in Chapter 3. For the sake of simplicity, here we propose what we refer to as the 90% criterion, which means that the system operator can only use up to 90% of each generator's and transmission line's capacity, with the hope that when a contingency occurs, the reserved 10% capacity would be able to provide a buffer that will prevent the system from collapsing.

Market power is the fourth factor that is being considered. As an illustration, suppose the marginal cost function of a generator at node n is a linear function of the production quantity q_n :

$$q_n \mapsto a_n + b_n q_n,$$

where a_n and b_n are constants. In order to maximize its profit, the owner of this generator may submit a supply function to the system operator that is higher than the marginal cost function:

$$q_n \mapsto \alpha_n + b_n q_n,$$

where $\alpha_n > a_n$. This is illustrated in Figure 2. After collecting supply functions from all suppliers, the system operator then allocates the generation and transmission resources to meet the demand in the most economical way that satisfies the system security constraints.

Chapter 2 can serve as an introduction to the fundamental settings of the electric power pricing system, and it attempts to answer the following questions:

1. How can one distinguish the sole contribution of one factor from that of others?
2. How can one evaluate the interaction among factors quantitatively?
3. What would be the effects if new factors were to be introduced?

A comprehensive introduction to locational pricing can be found in part 5 of [81], which not only provides fundamentals of physical transmission limits and congestion pricing, but also discusses fallacies of congestion pricing as well as taxes and transmission rights. [76] can also serve as a good sourcebook on the theory and implementation of spot price based energy marketplace, whose appendix is especially helpful to those with interests in the detailed

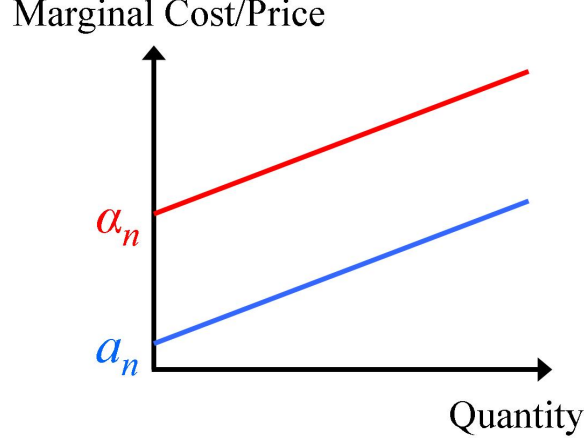


Figure 2: Examples of supply function and marginal cost function

mathematical derivations. PJM’s training center [1] is another reference for fundamentals of locational marginal pricing.

In the deregulated market, forecasting and analyzing LMPs become more and more important for all market participants. Bastian *et al.* [14] outline basic requirements for accurate computer forecast of LMPs. Hong and Hsiao propose LMP forecasting methods using a recurrent neural network [55] and artificial intelligence [56].

Investigators have also been looking at the sensitivities of LMPs to various natural and human factors. In other words, they address the question of how the LMPs evolve with respect to shifts in operational parameters. Burger *et al.* [21] propose a model that takes all the following factors into account: seasonal patterns, price spikes, mean reversion, price dependent volatilities and long term non-stationarity. The sensitivity of LMPs to demand changes throughout the network is mathematically derived in [30] from the OPF (optimal power flow) problem. Hamoud and Bradley [45] present a methodology to assess the impact of changes in system parameters and operating conditions on the LMPs using a “Probabilistic Composite System Evaluation” program.

The perspective Chapter 2 takes differs from the existing literature in the sense that, as opposed to looking at the response of LMPs to different factors as a whole, we decompose

the LMPs and quantitatively assess LMPs to the effects of individual factors as well as their interactions. The contribution of Chapter 2 is three fold. First, the decomposition approach provides insights on how much contribution does each of the factors and their interactions have on determining the prices, and in the case of abnormally high prices, points out the cause of the problem. Secondly, if or when new factors are introduced to the power system (e.g., addition or expansion of generators and/or transmission lines), the impact of each of the new factors can be quantitatively predicted to help decision makers make more effective decisions. Thirdly, sensitivity analysis results from parametric quadratic programming [15] are applied and expanded to perform the statistical computation required in the decomposition.

1.3 INTRODUCTION TO “SECURITY CONSTRAINED ECONOMIC DISPATCH: A MARKOV DECISION PROCESS APPROACH WITH EMBEDDED STOCHASTIC PROGRAMMING”

Security constrained economic dispatch refers to the program that the system operator uses to allocate generation and transmission resources to meet the demand. Economics and security are two major ingredients for an “optimal” dispatch. *Economics* means to serve demand with minimum cost, while *security* requires that electricity be delivered to the customers without interruption even in the event of component failures. Transmission line failures constitute a big threat to the electric power system security. Although such failures are rare events (e.g., 0.714 times/hundred mile-year for 230 kv transmission lines [5]), they have tremendous impacts. Without proper protection, a single component failure could disrupt the balance of the whole transmission system, cause cascading failures of other components, and result in catastrophic losses. The August 2003 blackout, for example, was initiated by the failures of three transmission lines, which caused subsequent failures of many other lines, and eventually led to the big blackout, affecting millions of people and costing billions of dollars [2].

Without the consideration of security, economic dispatch leads to a simple problem: using the existing transmission capacity to deliver power to all demand nodes at minimum

cost without violating any operational constraints. Besides generation and transmission capacity, operational constraints could also include unit commitment [86]. Chowdhury and Rahman [27] and Huneault and Galiana [57] give comprehensive surveys of economic dispatch approaches and algorithms in the literature.

System security was brought into the attention of power dispatch after the large blackout in 1965, when the North American Electric Reliability Council (NERC) was created. Another large blackout in 1977 led to wide adoption of the N-1 criterion [48]. Despite the amount of investment and effort spent by engineers and policy makers, there has been evidence that the frequency of large blackouts in the United States during the period 1984 to 2003 has not decreased, but increased [47]. The most recent large scale blackouts (August 2003 in North America and September 2003 in Italy) led to more extensive discussions on the reliability of power system infrastructure [39, 58, 77, 91] and re-examination of the N-1 criterion [29].

Peters *et al.* [69] examine the transmission line failure caused by extreme weather, and recommends strategies to improve transmission network reliability. Chen, Thorp, and Dobson [22] present a hidden failure model of the transmission line failure, and use the model to investigate the cascading behavior of the transmission systems. The PhD thesis of Chen [23] investigates the rare events in the power system that are not caused by uncontrollable natural forces, and proposes new approaches to identify, evaluate, and prevent rare events that could cause cascading failures. A summary of probabilistic approaches for power system reliability assessment is given in [6].

Various probabilistic methods have been proposed to improve or replace the deterministic N-1 criterion. Harris and Strongman [46] enhance the N-1 criterion to include the probability of overload and contingency. Bouffard, Galiana, and Arroyo [17] use the norms of Lagrange multiplier vectors associated with the post-contingency dispatch to identify credible contingencies that should be considered pre-contingency. Bouffard, Galiana, and Conejo [18, 19] use the value of unserved load to calculate the optimal power dispatch and spinning reserve, which implicitly determine the credit contingencies. The spinning reserve is the generating capacity available to the system operator by increasing the power output of generators that are already connected to the power system to meet demand in case a generator is lost or there is another disruption to the supply [92]. The importance of spinning reserve is addressed in [49] and [82].

Environmental issues have also been considered in the optimal dispatch problem. Taglag, El-Harwary, and El-Harwary [83] summarize the algorithms in environmental/economic dispatch.

Chapter 3 uses a Markov decision process (MDP) approach to address the security constrained economic dispatch problem. MDP provides a mathematical framework for modeling sequential decision-making process where the decision at each stage affects both the current outcome and future outcome. A classical introductory text to MDP is written by Puterman [71]. Compared with the existing methods, the MDP approach has the following advantages: (1) The risk of cascading failures as well as minor contingencies is converted into dollars and combined with the generation cost as a single objective for the system operator to minimize. Although cascading failures have been studied from statistical and systemic perspectives (see e.g., [37, 85]), no previous study is known to the author that addresses the preventive and corrective strategies for cascading failures and minor contingencies from the daily power dispatch perspective. (2) As an important social service, electric power dispatch should be a continuous and uninterrupted process. However, some existing literature have focused on a short period [18, 19, 20] of the process, perhaps to accommodate the limitation of the methodology. The MDP approach, on the other hand, allows one to formulate the dispatch process as an infinite horizon problem, and both the immediate and the future impact of an action is taken into account when an optimal policy is determined. (3) The objective of

most existing literature is to obtain the optimal dispatch decision for the best scenario where all components are working. However, the real practice needs a program that can provide the optimal corrective actions in case of contingency scenarios. The MDP model consists of different states, representing all possible contingency scenarios, and the optimal strategy for all states can be calculated. An introduction to the formulation and algorithms of MDP can be found in [71].

The contribution of Chapter 3 also includes the application of an MDP model with continuous action space. A stochastic programming problem thus needs to be solved in the policy improvement step of the policy iteration algorithm, since exhaustively enumerating and comparing all feasible actions is no longer an available strategy.

1.4 INTRODUCTION TO “OLIGOPOLY MODELS FOR MARKET PRICE OF ELECTRICITY UNDER DEMAND UNCERTAINTY AND UNIT RELIABILITY”

Since the beginning of deregulation, there has been a great interest in understanding the impact of introducing competition in the electricity market, and how the exercise of market power affects the electricity prices [34]. The prevailing equilibrium models of competition in the electricity market are Cournot-Nash and supply function equilibrium (SFE).

Named after the French philosopher and mathematician Antoine Augustin Cournot, the Cournot competition refers to the economic model of non-cooperative *quantity* competition. A state is said to be in Cournot-Nash equilibrium if no player has an incentive to *unilaterally* change his quantity bid. Borenstein and Bushnell [16] use a Cournot model to simulate the California electricity market with historical data. Their results indicate a potential of significant market power exercise when demand is high. Wei and Smeers [90] use a Cournot-Nash model to obtain long-run equilibrium, considering both investment and operation. Arbitrage behavior in a bilateral market is examined by Hobbs [50], who further concludes that with sufficient arbitrage, a bilateral market (a de-centralized market) yields the same Cournot equilibrium as that of a POOLCO (a centralized market). Yao, Oren, and Adler

[93] examine the Cournot competition in a two-settlement market, where the firms enter contracts in the forward market, and then get financially settled in the spot market.

In the SFE model, supply quantity is bid as a function of the price (or vice versa), in contrast to the fixed quantity bid in the Cournot model. SFE was originally introduced by Klemperer and Meyer [59] to examine competition under demand uncertainty. Although more general, realistic and flexible, the SFE model has been found to be intractable both analytically and computationally [13], and there could exist zero or multiple equilibrium solutions. Green and Newbery [40] consider a restricted symmetric duopoly model in the British electricity market, obtain the general form supply function equilibrium, and conclude that the government has underestimated the market power. Baldick, Grant and Kahn [11] use linear supply functions to model the England and Wales electricity market. Hobbs, Metzler and Pang [53] further restrict the linear supply functions to have fixed slopes, and formulate the transmission constrained competition as a bilevel game. Day, Hobbs and Pang [35] also introduce a modified version of SFE — a conjectured supply function approach, and compare it with other oligopoly models from both theoretical and computational perspectives with an application in the England-Wales system.

Depending on the assumptions made on the bidding strategy, transmission pricing, market clearing, etc., the computational effort needed to obtain a Nash equilibrium of the model varies from solving differential equations [11, 13, 40, 59], to mixed complementarity problems [35, 50] or variational inequality problems [90], to the challenging mathematical programs with equilibrium constraints (MPEC) [53, 93]. MPEC is drawing increasing interests from engineers and applied mathematicians in various fields [26, 64, 73]. Chen, Hobbs, Leyffer, and Munson [26] use the MPEC model to examine the effect of NO_x emission permits on the exercise of market power.

Chapter 4 examines the market power exercise with the following three questions in mind: (1) how does market power affect market price of electricity, (2) how do various oligopoly models differ from each other, and (3) what are the effects of demand and supply side uncertainties on the market power exercise and market price of electricity. The effects of supply side uncertainty on electricity prices using oligopoly models do not appear to have been studied previously.

2.0 USING A SYSTEM MODEL TO DECOMPOSE THE EFFECTS OF INFLUENTIAL FACTORS ON LOCATIONAL MARGINAL PRICES

2.1 INTRODUCTION

The formation of LMPs is a location dependent stochastic process [76], which is driven by a combination of various factors. Valenzuela and Mazumdar [87] categorize these factors into physical factors (which include production cost, load, generation availability, unit commitment and transmission constraints) and economic factors (which include strategic bidding and load elasticity). One approach to analyzing these factors is to derive analytical expressions for the sensitivity of LMPs with respect to the parameters of the optimal power flow models which determine those prices [30], including the sensitivity with respect to bid parameters. A similar approach has been used to identify market power in the energy market [61]. Many of these factors are stochastic by nature, and they jointly affect the LMP probability distribution. It is therefore hard to determine from historical data the sole or interactive contributions of the individual factors (see [21, 63, 70] for examples of empirical studies of LMPs).

However, such information is important and instructive in various ways. The exercise of market power, for example, has been a big concern since the beginning of electricity market deregulation, thus it will be useful to quantitatively distinguish the sole contribution of market power from that of other factors in raising the LMPs above marginal cost. Another use of this information is to accurately evaluate the effects on LMPs when generation or transmission capacity expansion plans are being made. The objective of Chapter 2 is to build a system model to analyze and decompose the effects of various influential factors on the LMP probability distributions, assuming that the factors are binary variables (inactive

or active). In this task, the property that the LMP is a piecewise linear function of demand variation turns out to be handy.

For ease of exposition, only four of the most important factors are considered: load uncertainty, thermal limit, capacity reserve and market power, numbered by 1, 2, 3 and 4, respectively. (The effects of other factors, e.g., fuel price changes, are not being studied here.) Our system model will analyze the contribution of each single and combination of factors to the means and standard deviations of LMPs at different nodes. The mean of LMPs measures the long term average level of prices, while the standard deviation is a measure of LMP variability in the same unit with LMPs (\$/MWh). The statistical models for node n in hour t are in the following two postulated linear forms:

$$\begin{aligned} & \mu_{\text{LMP}}^n(t) \\ = & \mu_0^n(t) + \mu_1^n(t) + \mu_2^n(t) + \mu_3^n(t) + \mu_4^n(t) \\ & + \mu_{12}^n(t) + \mu_{13}^n(t) + \mu_{14}^n(t) + \mu_{23}^n(t) + \mu_{24}^n(t) + \mu_{34}^n(t) \\ & + \mu_{123}^n(t) + \mu_{124}^n(t) + \mu_{134}^n(t) + \mu_{234}^n(t) + \mu_{1234}^n(t), \end{aligned} \tag{2.1}$$

$$\begin{aligned} & \sigma_{\text{LMP}}^n(t) \\ = & \sigma_0^n(t) + \sigma_1^n(t) + \sigma_2^n(t) + \sigma_3^n(t) + \sigma_4^n(t) \\ & + \sigma_{12}^n(t) + \sigma_{13}^n(t) + \sigma_{14}^n(t) + \sigma_{23}^n(t) + \sigma_{24}^n(t) + \sigma_{34}^n(t) \\ & + \sigma_{123}^n(t) + \sigma_{124}^n(t) + \sigma_{134}^n(t) + \sigma_{234}^n(t) + \sigma_{1234}^n(t). \end{aligned} \tag{2.2}$$

Here, $\mu_{\text{LMP}}^n(t)$ and $\sigma_{\text{LMP}}^n(t)$ are the realized mean and standard deviation of LMPs at node n in hour t , respectively; $\mu_0^n(t)$ and $\sigma_0^n(t)$ are, respectively, the mean and standard deviation given none of the four factors' presence; for $i, j = 1, 2, 3, 4$, $\mu_i^n(t)$ is the sole contribution of factor i to the mean of LMPs at node n in addition to $\mu_0^n(t)$, and $\sigma_{ij}^n(t)$ is the contribution resulting from (exclusively) the interaction between factors i and j to the standard deviation of LMPs at node n in addition to $\sigma_0^n(t)$. This is illustrated in Figure 3 for a three factor case. The rectangular area as a result of three interacting factors is decomposed to $\mu_0 + \mu_i + \mu_j + \mu_k + \mu_{ij} + \mu_{jk} + \mu_{ik} + \mu_{ijk}$. We will refer to the coefficients in (2.1) and (2.2) as *impact*

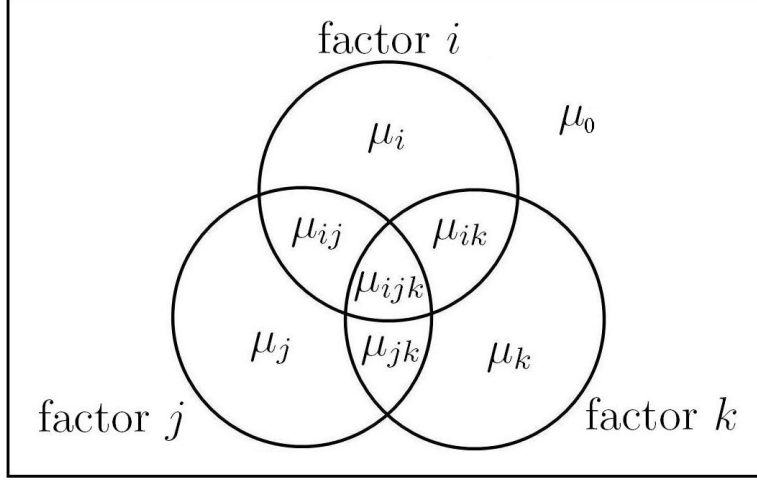


Figure 3: Decomposition of contribution by factors i , j and k

coefficients, and our primary objective is to use the system model to obtain these impact coefficients.

Section 2.2 describes the system model and the four factors in more detail. Section 2.3 first defines the inputs and outputs of the system model in 2.3.1; and then 2.3.2 describes the derivation of outputs from inputs by utilizing the piecewise linear property of LMP as a function of demand variation; the approach used in obtaining impact coefficients from input and output is given in 2.3.3. A numerical example on the IEEE 30-bus network is given in Section 2.4, where 2.4.1 gives the data of the test system, 2.4.2 and 2.4.3 present and interpret the time-averaged impact coefficients and their time variation, respectively. Use of the system model in evaluating transmission and generation capacity expansion plans is discussed and illustrated in Section 2.5. Section 2.6 concludes this chapter.

2.2 SYSTEM MODEL

2.2.1 Transmission Network

A set of nodes \mathcal{N} is connected by a set of transmission lines \mathcal{L} . The sets of nodes with demand for and supply of power are denoted by \mathcal{D} and \mathcal{S} , respectively. Depending on whether or not there is demand for or supply of power, any node in \mathcal{N} could belong to either \mathcal{D} or \mathcal{S} , or both, or neither.

2.2.2 Load Uncertainty

For a certain length of period $t = 1, 2, \dots, T$, demand is assumed to be inelastic: $d_{n,t}(1 + \epsilon_t)$, $\forall n \in \mathcal{D}, t = 1, 2, \dots, T$, where $d_{n,t}$ (in MW) is the nominal load at node n in hour t , while ϵ_t is a random variable, representing the demand uncertainty in percentage of $d_{n,t}$. Notice that for a given t , the load uncertainty ϵ_t is assumed to be the same at all nodes, which means that demands at all nodes are perfectly correlated, so that they increase or decrease universally by the same percentage.

In our system model, $d_{n,t}$'s are assumed to be known constants, and ϵ_t 's are assumed to have known probability distributions, which can be obtained from the historical load data.

2.2.3 Thermal Limit

A DC lossless load flow model is used here, which has been found to be a good approximation to the more accurate AC load flow model when thermal limits are the primary concern [54, 68].

Denote by z_n , H and T_l the net injection at node n , PTDF (power transfer distribution factors) matrix [28] and capacity of transmission line l , respectively. Net injection is the total power flow going into a node less the total power flow going out of it. PTDF matrix gives the linear relation between net injection at each node and power flow through each line. For all $l \in \mathcal{L}$, $|\sum_{n \in \mathcal{N}} H_{l,n} z_n|$ calculates the magnitude of the power flow through line l . If a transmission line's thermal limit is exceeded for a significant length of time, conductors sag

or be damaged by excessive heating, and the probability of short-circuiting with the ground increases. Therefore, the transmission constraints require that power flow going through any transmission line in either direction must be within the capacity:

$$\begin{aligned} \sum_{n \in \mathcal{N}} H_{l,n} z_n &\leq T_l, \quad \forall l \in \mathcal{L} \\ -\sum_{n \in \mathcal{N}} H_{l,n} z_n &\leq T_l, \quad \forall l \in \mathcal{L}. \end{aligned}$$

2.2.4 Capacity Reserve

As part of the ancillary services, certain amounts of generation and transmission capacities are kept in reserve to be able to re-establish the balance between load and generation in the event of a contingency. However, obtaining the exact amount of reserve capacity that is “optimal” for all stakeholders is a complex problem, and the solution may vary depending on the perspective chosen. The N-1 criterion, for example, requires that the reserve level should be sufficient to counter the loss of any single component (generator or transmission line). On the other hand, [25] and [89] simply derate the capacities by the forced outage rates to account for contingencies. As opposed to the above deterministic criteria, stochastic criteria [18, 19, 38] have also been proposed, where transmission line reliability is taken into account in determining the reserve level.

In our model, as an illustration, we use what we refer to as the 90% criterion. This criterion is to require 10% reserve capacities of all generators and transmission lines.

In considering the capacity reserve factor, our purpose is not to study the LMP probability distribution under contingencies, but simply to address the fact that when system security is taken into account, the system operator would be restricted from fully utilizing all the available generation and transmission capacities.

2.2.5 Market Power

Following [53], we assume that there is a single generator at each supply node (we will refer to the generator at node n as generator n , which should not give rise to any confusion), having a marginal cost function:

$$q_n \mapsto a_n + b_n q_n, \quad \forall n \in \mathcal{S},$$

where q_n (in MWh) is the quantity of power generation at node n , a_n (in \$/MWh) and b_n (in \$/(MWh)²) are constant parameters. The generating firms submit a linear supply function for each of their generators:

$$q_n \mapsto \alpha_n + b_n q_n, \quad \forall n \in \mathcal{S},$$

and they exercise their market power by strategically submitting α_n 's that may be different from a_n 's to maximize their profits, and they are simply assumed not to manipulate on b_n 's.

Instead of solving α_n 's using game-theoretic models as in [53], we assume them to be known parameters, and attempt to find out quantitatively the effects of their numerical differences from the a_n 's. We also assume that the supply functions stay the same for the entire time horizon.

2.2.6 Market Clearing

The electricity market is cleared each hour using the following economic dispatch:

$$\min_{q, z} \quad \sum_{n \in \mathcal{S}} (\alpha_n q_n + \frac{1}{2} b_n q_n^2) \quad (2.3)$$

$$\text{s. t.} \quad q_n - z_n = d_{n,t}(1 + \epsilon_t), \quad (p_{n,t}) \quad \forall n \in \mathcal{N} \quad (2.4)$$

$$\sum_{n \in \mathcal{N}} H_{l,n} z_n \leq 0.9 T_l, \quad \forall l \in \mathcal{L} \quad (2.5)$$

$$-\sum_{n \in \mathcal{N}} H_{l,n} z_n \leq 0.9 T_l, \quad \forall l \in \mathcal{L} \quad (2.6)$$

$$\sum_{n \in \mathcal{N}} z_n = 0 \quad (2.7)$$

$$0 \leq q_n \leq 0.9 \bar{Q}_n, \quad \forall n \in \mathcal{S}. \quad (2.8)$$

Here, \bar{Q}_n is the capacity of generator n , and dual variable $p_{n,t}$ is the LMP at node n in hour t . The objective function (2.3) is to minimize the generation cost (using the firm submitted supply functions); (2.4) comes from the definition of net injection, and the dual variable $p_{n,t}$ calculates the marginal cost of serving unit increment of demand at node n in hour t , which is consistent with the definition of LMP; (2.5) and (2.6) are transmission constraints under the 90% criterion; (2.7) is the balancing property of a network; and (2.8) is the generation capacity limit under the 90% criterion.

The economic dispatch (2.3)-(2.8) is a convex quadratic program, and is generally easy to solve in a given hour for a given value of ϵ_t . It is assumed that generation and transmission capacities are sufficient to serve demand at all scenarios, so that an optimal solution to (2.3)-(2.8) always exists.

2.2.7 Other Factors

The system model can also be used to analyze the effects of other factors. For example, we can quantitatively examine the effects of introducing new generators and/or expanding the capacities of existing transmission lines. This example will be illustrated in Section 2.5, where factors 1, 2, 3 and 4 are all assumed to be active, and four new factors 5, 6, 7 and 8 are introduced.

2.3 DETERMINATION OF IMPACT COEFFICIENTS

2.3.1 Input and Output of the System Model

We define four binary input variables x_1 , x_2 , x_3 and x_4 to represent the presence of load uncertainty, thermal limit, capacity reserve and market power, respectively. Table 1 gives the interpretation of these input variables. In reality, all the factors are active. In the system model, however, some of the factors need to be assumed absent so that the difference it makes can be obtained and used to calculate the impact coefficients.

Table 1: Interpretation of input variables

i	$x_i = 1$	$x_i = 0$
1	Demand uncertainty is active: ϵ_t is a random variable, thus $p_{n,t}(\epsilon_t)$ will be a random variable as well.	Demand has no uncertainty: ϵ_t is a constant 0, and $p_{n,t}$ will also be a constant.
2	Thermal limit is active: congestion may occur when demands are high.	Thermal limit is ignored: constraints (2.5) and (2.6) are ignored and there will be no congestion.
3	The 90% criterion is used as in constraints (2.5), (2.6) and (2.8).	The 90% criterion is not used in constraints (2.5), (2.6) and (2.8).
4	Market power is exercised to a given extent (see Table 2) as in the objective (2.3).	Market power is not exercised: firms honestly submit marginal cost functions as supply functions, thus a_n instead of α_n will be used in the objective (2.3).

For a given set of input variables $\mathbf{x} = \{x_1, x_2, x_3, x_4\}$, the output variables of the system model at node n are $p_{n,t}^*(\mathbf{x}; \epsilon_t)$, $\mu_t^n(\mathbf{x})$ and $\sigma_t^n(\mathbf{x})$. Here $p_{n,t}^*(\mathbf{x}; \epsilon_t)$ is the LMP at node n in hour t , which results from the optimal (dual) solution to the economic dispatch (2.3)-(2.8), and is also a function of ϵ_t ; $\mu_t^n(\mathbf{x})$ and $\sigma_t^n(\mathbf{x})$ are, respectively, the mean and standard deviation of $p_{n,t}^*(\mathbf{x}; \epsilon_t)$. Let the pdf (probability distribution function) of ϵ_t be $f_t(\cdot)$, then

$$\mu_t^n(\mathbf{x}) = E_{\epsilon_t}[p_{n,t}^*(\mathbf{x}; \epsilon_t)] = \int f_t(\epsilon_t) p_{n,t}^*(\mathbf{x}; \epsilon_t) d\epsilon_t,$$

and

$$\begin{aligned} \sigma_t^n(\mathbf{x}) &= \sqrt{V_{\epsilon_t}[p_{n,t}^*(\mathbf{x}; \epsilon_t)]} \\ &= \sqrt{\int f_t(\epsilon_t) [p_{n,t}^*(\mathbf{x}; \epsilon_t) - \mu_t^n(\mathbf{x})]^2 d\epsilon_t}. \end{aligned}$$

2.3.2 Deriving Output from Input

This subsection describes the algorithm for deriving $p_{n,t}^*(\mathbf{x}; \epsilon_t)$ as a function of ϵ_t from the system model for a given \mathbf{x} .

When $x_1 = 0$, the economic dispatch (2.3)-(2.8) only needs to be solved once to obtain the output for a given input. When $x_1 = 1$, regardless of the other input variables, the economic dispatch (2.3)-(2.8) can be represented by the following standard form parametric convex quadratic program (QP $_{\epsilon}$):

$$\min_x \left\{ c^\top x + \frac{1}{2} x^\top Q x : Ax = b + \epsilon \Delta b, x \geq 0 \right\},$$

where $c \in \mathbb{R}^n$, $Q \in \mathbb{R}^{n \times n}$, $A \in \mathbb{R}^{m \times n}$ and $b \in \mathbb{R}^m$ are constants, Q is a positive semi-definite matrix, $\Delta b \in \mathbb{R}^m$ is a given direction of variation, and ϵ is a scalar parameter. In the economic dispatch context, $Q = \text{diag}\{\mathbf{b}_S\}$ and $\Delta b = [d_{1,t}, \dots, d_{|N|,t}, 0, \dots, 0]^\top$. It is well known that the optimal solution $x^*(\epsilon)$ is a piecewise linear function of ϵ . [15] gives an algorithm that analytically calculates the break points and the functional form of each segment. We can use that algorithm to obtain the piecewise linear function $p_{n,t}^*(1, x_2, x_3, x_4; \epsilon_t)$, and then calculate other outputs.

We present below the algorithm that we use in our computational experiments to obtain the break points of ϵ_t . The functional form of $p_{n,t}^*(1, x_2, x_3, x_4; \epsilon_t)$ within each segment can be calculated by solving at the lower and upper limit break points, and then connecting them with a straight line. Our algorithm adopts the basic ideas from [15], but is computationally more robust.

We first review some preliminaries of parametric convex quadratic programming. Let (QD_ϵ) be the Wolfe dual of (QP_ϵ) :

$$\max_{x,y,s} \left\{ (b + \epsilon \Delta b)^\top y - \frac{1}{2} x^\top Q x : A^\top y + s - Qx = c, s \geq 0 \right\}.$$

For a given ϵ , the tripartition $\pi(\epsilon) = \{\mathcal{B}(\epsilon), \mathcal{N}(\epsilon), \mathcal{T}(\epsilon)\}$ is defined as

$$\begin{aligned} \mathcal{B}(\epsilon) &= \{i : x_i > 0 \text{ for an optimal solution } (x(\epsilon), y(\epsilon), s(\epsilon))\}, \\ \mathcal{N}(\epsilon) &= \{i : s_i > 0 \text{ for an optimal solution } (x(\epsilon), y(\epsilon), s(\epsilon))\}, \\ \mathcal{T}(\epsilon) &= \{1, \dots, n\} \setminus \{\mathcal{B}(\epsilon) \cup \mathcal{N}(\epsilon)\}. \end{aligned}$$

Define a maximal complementary solution $(x^*(\epsilon), y^*(\epsilon), s^*(\epsilon))$ as an optimal solution such that

$$x_i^*(\epsilon) > 0 \Leftrightarrow i \in \mathcal{B}(\epsilon) \text{ and } s_i^*(\epsilon) > 0 \Leftrightarrow i \in \mathcal{N}(\epsilon).$$

It has been shown in [44, 66] that a maximal complementary solution can be obtained by solving (QP_ϵ) or (QD_ϵ) using interior point methods.

We present the algorithm as pseudo codes of two functions: `main_function` and `sub_function`. The function inputs of `main_function` are coefficients of (QP_ϵ) and (QD_ϵ) , and the function output is the set of break points of ϵ within the entire range that (QP_ϵ) and (QD_ϵ) remain feasible. The function inputs of `sub_function` are coefficients of (QP_ϵ) and (QD_ϵ) and a range $(\underline{\epsilon}, \bar{\epsilon})$, and the function output is the set of break points of ϵ within $(\underline{\epsilon}, \bar{\epsilon})$.

$$\Upsilon = \text{main_function}(A, b, \Delta b, c, Q)$$

{ **Step 1:** Calculate (L_ϵ, U_ϵ) , which is the entire range of ϵ that (QP_ϵ) and (QD_ϵ) are feasible:

$$L_\epsilon = \min_{\epsilon, x, y, s} \{ \epsilon : Ax - \Delta b \epsilon = b, A^\top y + s - Qx = c, x \geq 0, s \geq 0 \},$$

$$U_\epsilon = \max_{\epsilon, x, y, s} \{ \epsilon : Ax - \Delta b \epsilon = b, A^\top y + s - Qx = c, x \geq 0, s \geq 0 \}.$$

Step 2: Call $\Upsilon = \text{sub_function}(A, b, \Delta b, c, Q, L_\epsilon, U_\epsilon)$, and return Υ .

}

$$\Upsilon = \text{sub_function}(A, b, \Delta b, c, Q, \underline{\epsilon}, \bar{\epsilon})$$

{ **Step 1:** If $(\bar{\epsilon} - \underline{\epsilon})$ is sufficiently small (or both $\bar{\epsilon}$ and $\underline{\epsilon}$ are infinity with same sign), then return $\Upsilon = \frac{1}{2}(\bar{\epsilon} + \underline{\epsilon})$. Otherwise set the initial point $\epsilon^0 = \frac{1}{2}(\bar{\epsilon} + \underline{\epsilon})$ and continue.

Step 2: Obtain the tripartition

$$\pi(\epsilon^0) = \{\mathcal{B}(\epsilon^0), \mathcal{N}(\epsilon^0), \mathcal{T}(\epsilon^0)\}$$

by solving (QP_{ϵ^0}) and (QD_{ϵ^0}) using an interior point method and obtaining a maximal complementary solution $(x^*(\epsilon^0), y^*(\epsilon^0), s^*(\epsilon^0))$.

Step 3: Calculate $(l_{\epsilon^0}, u_{\epsilon^0})$, which is the range of ϵ that (QP_ϵ) and (QD_ϵ) have the same tripartition as $\pi(\epsilon^0)$:

$$l_{\epsilon^0} = \min_{\epsilon, x, y, s} \{ \epsilon : Ax - \Delta b \epsilon = b, A^\top y + s - Qx = c,$$

$$x_{\mathcal{B}(\epsilon^0)} \geq 0, x_{\mathcal{N}(\epsilon^0) \cup \mathcal{T}(\epsilon^0)} = 0,$$

$$s_{\mathcal{N}(\epsilon^0)} \geq 0, s_{\mathcal{B}(\epsilon^0) \cup \mathcal{T}(\epsilon^0)} = 0 \},$$

$$u_{\epsilon^0} = \max_{\epsilon, x, y, s} \{ \epsilon : Ax - \Delta b \epsilon = b, A^\top y + s - Qx = c,$$

$$x_{\mathcal{B}(\epsilon^0)} \geq 0, x_{\mathcal{N}(\epsilon^0) \cup \mathcal{T}(\epsilon^0)} = 0,$$

$$s_{\mathcal{N}(\epsilon^0)} \geq 0, s_{\mathcal{B}(\epsilon^0) \cup \mathcal{T}(\epsilon^0)} = 0 \}.$$

Step 4: Recursively call

$$\Upsilon^0 = \text{sub_function}(A, b, \Delta b, c, Q, \underline{\epsilon}, l_{\epsilon^0}),$$

$$\Upsilon^1 = \text{sub_function}(A, b, \Delta b, c, Q, u_{\epsilon^0}, \bar{\epsilon}),$$

and return $\Upsilon = \Upsilon^0 \cup \{l_{\epsilon^0}, u_{\epsilon^0}\} \cup \Upsilon^1$.

}

2.3.3 Calculating Impact Coefficients

Impact coefficients can be calculated by obtaining the system model output for all possible input variables, and then solving a linear system of equations given below.

The realized values of LMPs according to the system model are determined by the combination of all factors, thus they correspond to $p_{n,t}^*(1, 1, 1, 1; \epsilon_t)$. So, $\mu_{\text{LMP}}^n(t) = \mu_t^n(1, 1, 1, 1)$ and $\sigma_{\text{LMP}}^n(t) = \sigma_t^n(1, 1, 1, 1)$, where $\mu_{\text{LMP}}^n(t)$ and $\sigma_{\text{LMP}}^n(t)$ represent, respectively, the mean and standard deviation of LMPs at node n in hour t . Moreover, for all possible binary input variables $\mathbf{x} = \{x_1, x_2, x_3, x_4\}$, we have the following relation between the outputs and the impact coefficients:

$$\begin{aligned}
& \mu_t^n(x_1, x_2, x_3, x_4) \\
= & \mu_0^n(t) + \mu_1^n(t)x_1 + \mu_2^n(t)x_2 + \mu_3^n(t)x_3 + \mu_4^n(t)x_4 \\
& + \mu_{12}^n(t)x_1x_2 + \mu_{13}^n(t)x_1x_3 + \mu_{14}^n(t)x_1x_4 \\
& + \mu_{23}^n(t)x_2x_3 + \mu_{24}^n(t)x_2x_4 + \mu_{34}^n(t)x_3x_4 \\
& + \mu_{123}^n(t)x_1x_2x_3 + \mu_{124}^n(t)x_1x_2x_4 + \mu_{134}^n(t)x_1x_3x_4 \\
& + \mu_{234}^n(t)x_2x_3x_4 + \mu_{1234}^n(t)x_1x_2x_3x_4, \\
\\
& \sigma_t^n(x_1, x_2, x_3, x_4) \\
= & \sigma_0^n(t) + \sigma_1^n(t)x_1 + \sigma_2^n(t)x_2 + \sigma_3^n(t)x_3 + \sigma_4^n(t)x_4 \\
& + \sigma_{12}^n(t)x_1x_2 + \sigma_{13}^n(t)x_1x_3 + \sigma_{14}^n(t)x_1x_4 \\
& + \sigma_{23}^n(t)x_2x_3 + \sigma_{24}^n(t)x_2x_4 + \sigma_{34}^n(t)x_3x_4 \\
& + \sigma_{123}^n(t)x_1x_2x_3 + \sigma_{124}^n(t)x_1x_2x_4 + \sigma_{134}^n(t)x_1x_3x_4 \\
& + \sigma_{234}^n(t)x_2x_3x_4 + \sigma_{1234}^n(t)x_1x_2x_3x_4,
\end{aligned}$$

where $\mu_0^n(t), \mu_1^n(t), \dots, \mu_{1234}^n(t)$ and $\sigma_0^n(t), \sigma_1^n(t), \dots, \sigma_{1234}^n(t)$ are the impact coefficients at node n in hour t .

In matrix form, we have:

$$Y = M \cdot \beta, \quad (2.9)$$

where M , Y and β are, respectively, a constant matrix, the system outputs and the impact coefficients:

$$M = \begin{bmatrix} 1 & 0 & 0 & 0 & 0 & 0 & 0 & 0 & 0 & 0 & 0 & 0 & 0 & 0 & 0 \\ 1 & 1 & 0 & 0 & 0 & 0 & 0 & 0 & 0 & 0 & 0 & 0 & 0 & 0 & 0 \\ 1 & 0 & 1 & 0 & 0 & 0 & 0 & 0 & 0 & 0 & 0 & 0 & 0 & 0 & 0 \\ 1 & 1 & 1 & 0 & 0 & 1 & 0 & 0 & 0 & 0 & 0 & 0 & 0 & 0 & 0 \\ 1 & 0 & 0 & 1 & 0 & 0 & 0 & 0 & 0 & 0 & 0 & 0 & 0 & 0 & 0 \\ 1 & 1 & 0 & 1 & 0 & 0 & 1 & 0 & 0 & 0 & 0 & 0 & 0 & 0 & 0 \\ 1 & 0 & 1 & 1 & 0 & 0 & 0 & 0 & 1 & 0 & 0 & 0 & 0 & 0 & 0 \\ 1 & 1 & 1 & 1 & 0 & 1 & 1 & 0 & 1 & 0 & 0 & 1 & 0 & 0 & 0 \\ 1 & 0 & 0 & 0 & 1 & 0 & 0 & 0 & 0 & 0 & 0 & 0 & 0 & 0 & 0 \\ 1 & 1 & 0 & 0 & 1 & 0 & 0 & 1 & 0 & 0 & 0 & 0 & 0 & 0 & 0 \\ 1 & 0 & 1 & 0 & 1 & 0 & 0 & 0 & 0 & 1 & 0 & 0 & 0 & 0 & 0 \\ 1 & 1 & 1 & 0 & 1 & 1 & 0 & 1 & 0 & 1 & 0 & 0 & 1 & 0 & 0 \\ 1 & 0 & 0 & 1 & 1 & 0 & 0 & 0 & 0 & 0 & 1 & 0 & 0 & 0 & 0 \\ 1 & 1 & 0 & 1 & 1 & 0 & 1 & 1 & 0 & 0 & 1 & 0 & 0 & 1 & 0 \\ 1 & 0 & 1 & 1 & 1 & 0 & 0 & 0 & 1 & 1 & 1 & 0 & 0 & 0 & 1 \\ 1 & 1 & 1 & 1 & 1 & 1 & 1 & 1 & 1 & 1 & 1 & 1 & 1 & 1 & 1 \end{bmatrix}, Y = \begin{bmatrix} \mu_t^n(0, 0, 0, 0) \\ \mu_t^n(1, 0, 0, 0) \\ \mu_t^n(0, 1, 0, 0) \\ \mu_t^n(1, 1, 0, 0) \\ \mu_t^n(0, 0, 1, 0) \\ \mu_t^n(1, 0, 1, 0) \\ \mu_t^n(0, 1, 1, 0) \\ \mu_t^n(1, 1, 1, 0) \\ \mu_t^n(0, 0, 0, 1) \\ \mu_t^n(1, 0, 0, 1) \\ \mu_t^n(0, 1, 0, 1) \\ \mu_t^n(1, 1, 0, 1) \\ \mu_t^n(0, 0, 1, 1) \\ \mu_t^n(1, 0, 1, 1) \\ \mu_t^n(0, 1, 1, 1) \\ \mu_t^n(1, 1, 1, 1) \end{bmatrix}, \beta = \begin{bmatrix} \mu_0^n(t) \\ \mu_1^n(t) \\ \mu_2^n(t) \\ \mu_3^n(t) \\ \mu_4^n(t) \\ \mu_{12}^n(t) \\ \mu_{13}^n(t) \\ \mu_{14}^n(t) \\ \mu_{23}^n(t) \\ \mu_{24}^n(t) \\ \mu_{34}^n(t) \\ \mu_{123}^n(t) \\ \mu_{124}^n(t) \\ \mu_{134}^n(t) \\ \mu_{234}^n(t) \\ \mu_{1234}^n(t) \end{bmatrix}.$$

The matrix form for σ is similar. Therefore, if we obtain $\mu_t^n(x_1, x_2, x_3, x_4)$ and $\sigma_t^n(x_1, x_2, x_3, x_4)$ for all 16 possible inputs, then the impact coefficients in hour t can be calculated by solving the above linear system of equations (2.9).

The inverse of matrix M is

$$M^{-1} = \begin{bmatrix} 1 & 0 & 0 & 0 & 0 & 0 & 0 & 0 & 0 & 0 & 0 & 0 & 0 & 0 & 0 & 0 \\ -1 & 1 & 0 & 0 & 0 & 0 & 0 & 0 & 0 & 0 & 0 & 0 & 0 & 0 & 0 & 0 \\ -1 & 0 & 1 & 0 & 0 & 0 & 0 & 0 & 0 & 0 & 0 & 0 & 0 & 0 & 0 & 0 \\ -1 & 0 & 0 & 0 & 1 & 0 & 0 & 0 & 0 & 0 & 0 & 0 & 0 & 0 & 0 & 0 \\ -1 & 0 & 0 & 0 & 0 & 0 & 0 & 0 & 1 & 0 & 0 & 0 & 0 & 0 & 0 & 0 \\ 1 & -1 & -1 & 1 & 0 & 0 & 0 & 0 & 0 & 0 & 0 & 0 & 0 & 0 & 0 & 0 \\ 1 & -1 & 0 & 0 & -1 & 1 & 0 & 0 & 0 & 0 & 0 & 0 & 0 & 0 & 0 & 0 \\ 1 & -1 & 0 & 0 & 0 & 0 & 0 & 0 & -1 & 1 & 0 & 0 & 0 & 0 & 0 & 0 \\ 1 & 0 & -1 & 0 & -1 & 0 & 1 & 0 & 0 & 0 & 0 & 0 & 0 & 0 & 0 & 0 \\ 1 & 0 & -1 & 0 & 0 & 0 & 0 & 0 & -1 & 0 & 1 & 0 & 0 & 0 & 0 & 0 \\ 1 & 0 & 0 & 0 & -1 & 0 & 0 & 0 & -1 & 0 & 0 & 0 & 1 & 0 & 0 & 0 \\ -1 & 1 & 1 & -1 & 1 & -1 & -1 & 1 & 0 & 0 & 0 & 0 & 0 & 0 & 0 & 0 \\ -1 & 1 & 1 & -1 & 0 & 0 & 0 & 0 & 1 & -1 & -1 & 1 & 0 & 0 & 0 & 0 \\ -1 & 1 & 0 & 0 & 1 & -1 & 0 & 0 & 1 & -1 & 0 & 0 & -1 & 1 & 0 & 0 \\ -1 & 0 & 1 & 0 & 1 & 0 & -1 & 0 & 1 & 0 & -1 & 0 & -1 & 0 & 1 & 0 \\ 1 & -1 & -1 & 1 & -1 & 1 & 1 & -1 & -1 & 1 & 1 & -1 & 1 & -1 & -1 & 1 \end{bmatrix},$$

which interprets how the impact coefficients are calculated using the outputs. For example, $\mu_1^n(t)$ is the difference of $\mu_t^n(1, 0, 0, 0)$ and $\mu_t^n(0, 0, 0, 0)$; $\mu_{12}^n(t)$ is the difference of $\mu_t^n(0, 0, 0, 0) + \mu_t^n(1, 1, 0, 0)$ and $\mu_t^n(0, 1, 0, 0) + \mu_t^n(1, 0, 0, 0)$.

2.4 NUMERICAL EXAMPLE

2.4.1 Test Data

We use the IEEE 30-bus network as an example to demonstrate our approach. As is shown in Figure 4, a supply node has a “G” in a circle representing a generator, and a demand node has an arrow. In this example, $\mathcal{D} = \{2, 3, 4, 5, 7, 8, 10, 12, 14, 15, 16, 17, 18, 19, 20, 21, 23, 24, 26, 29, 30\}$, and $\mathcal{S} = \{1, 2, 5, 8, 11, 13\}$. Node and transmission line data are given in Tables 2

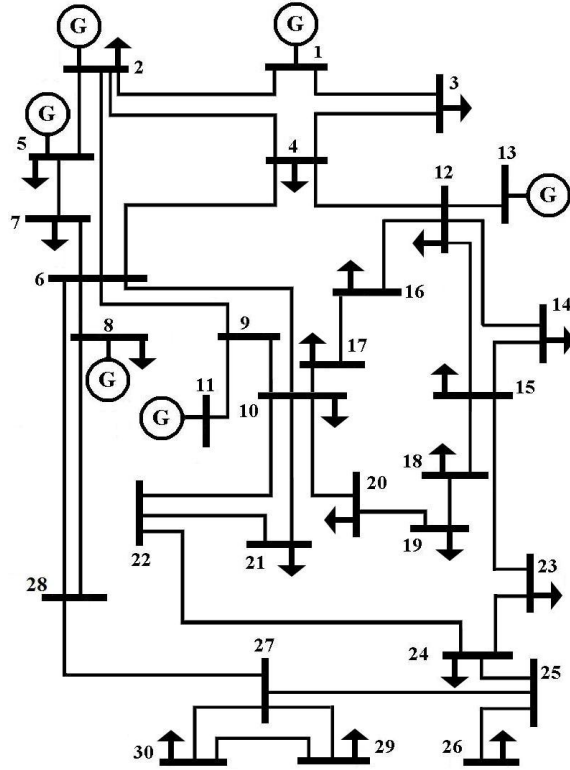


Figure 4: An IEEE 30-bus network example

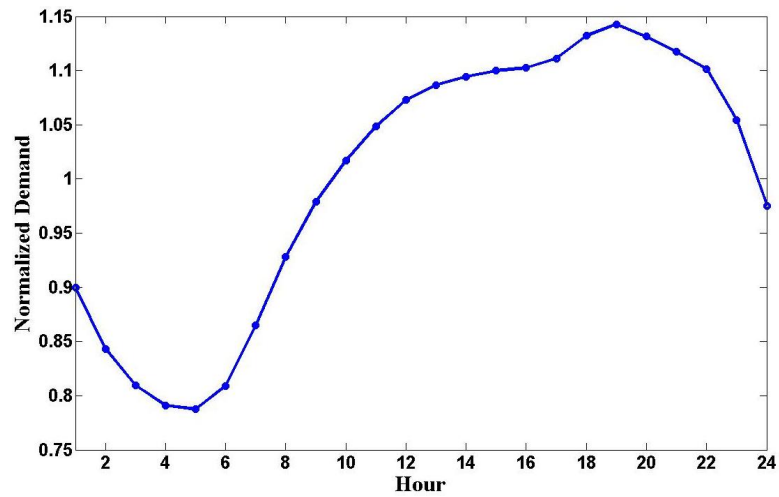


Figure 5: Normalized chronological load change

and 3, respectively. Most of these data are adopted from [53] and [7]: b_n 's, T_l 's and \overline{Q}_n 's are set to be, respectively, 50%, 60% and 80% of the values in [7]; α_n 's are set to be 50% of the equilibrium values in [53]. For all $n \in \mathcal{D}$, the average nominal load over time horizon is set to be 70% of d_n in [7]; the relative load chronological changes, shown in Figure 5, are estimated using the load data of PJM-E [1]; the demand uncertainty ϵ_t in each hour is assumed to have a truncated normal distribution also estimated using the load data of PJM-E. Let $f_N(\cdot)$ be the pdf of a normal distribution, then the pdf of a truncated normal distribution $f_T(\cdot)$ with the same mean and standard deviation within $[\underline{x}, \overline{x}]$ is

$$f_T(x) = \begin{cases} f_N(x) / \int_{\underline{x}}^{\overline{x}} f_N(y) dy & \underline{x} \leq x \leq \overline{x}, \\ 0 & \text{otherwise.} \end{cases}$$

2.4.2 Time-Averaged Impact Coefficients

We obtain the impact coefficients for both mean and standard deviation of LMPs at all nodes $n \in \mathcal{D} \cup \mathcal{S}$ in hour $t = 1, \dots, 24$. The computational time was around 24 minutes on a Pentium 4 PC with CPU 3.2 GHz and 1.00 GB of RAM. Tables 4 & 5 and 6 & 7 show the time-averaged impact coefficients for μ_{LMP}^n and σ_{LMP}^n , respectively. Here,

$$\mu_{\text{LMP}}^n = \frac{1}{24} \sum_{t=1}^{24} \mu_{\text{LMP}}^n(t).$$

Time-averages are also taken in the same manner for other impact coefficients. The “average” rows are the average values over all nodes in $n \in \mathcal{D} \cup \mathcal{S}$. We have the following observations and interpretations based on these results:

1. Had none of the four factors existed, the LMPs would have been constantly and universally \$39.61/MWh, compared to the realized mean of \$62.43/MWh with a \$6.11/MWh standard deviation on average.
2. As the sole contributions of the individual factors, load uncertainty, capacity reserve and market power raise the mean of LMPs by $\mu_1^n = \$2.09/\text{MWh}$, $\mu_3^n = \$3.57/\text{MWh}$ and $\mu_4^n = \$14.12/\text{MWh}$, respectively.

Table 2: Node data of the 30-bus example

n	d_n	a_n	α_n	b_n	\overline{Q}_n
1	—	0	14.00	1.00	160
2	15.19	0	12.10	0.88	64
3	1.68	—	—	—	—
4	5.32	—	—	—	—
5	65.94	0	8.28	0.50	40
6	—	—	—	—	—
7	15.96	—	—	—	—
8	21	0	16.58	1.63	28
9	—	—	—	—	—
10	4.06	—	—	—	—
11	—	0	15.41	1.50	24
12	7.84	—	—	—	—
13	—	0	15.39	1.50	32
14	4.34	—	—	—	—
15	5.74	—	—	—	—
16	2.45	—	—	—	—
17	6.3	—	—	—	—
18	2.24	—	—	—	—
19	6.65	—	—	—	—
20	1.54	—	—	—	—
21	12.25	—	—	—	—
22	—	—	—	—	—
23	2.24	—	—	—	—
24	6.09	—	—	—	—
25	—	—	—	—	—
26	2.45	—	—	—	—
27	—	—	—	—	—
28	—	—	—	—	—
29	1.68	—	—	—	—
30	7.42	—	—	—	—

Table 3: Transmission line data of the 30-bus example

line	resistance R (Ω)	reactance X (Ω)	thermal limit (MW)
1-2	0.0192	0.0575	78
1-3	0.0452	0.1852	78
2-4	0.0570	0.1737	39
3-4	0.0132	0.0379	78
2-5	0.0472	0.1983	78
2-6	0.0581	0.1763	39
4-6	0.0119	0.0414	54
5-7	0.0460	0.1160	42
6-7	0.0267	0.0820	78
6-8	0.0120	0.0420	19.2
6-9	0	0.2080	39
6-10	0	0.5560	19.2
9-11	0	0.2080	39
9-10	0	0.1100	39
4-12	0	0.2560	39
12-13	0	0.1400	39
12-14	0.1231	0.2559	19.2
12-15	0.0662	0.1304	19.2
12-16	0.0945	0.1987	19.2
14-15	0.2210	0.1997	9.6
16-17	0.0824	0.1932	9.6
15-18	0.1070	0.2185	9.6
18-19	0.0639	0.1292	9.6
19-20	0.0340	0.0680	19.2
10-20	0.0936	0.2090	19.2
10-17	0.0324	0.0845	19.2
10-21	0.0348	0.0749	19.2
10-22	0.0727	0.1499	19.2
21-22	0.0116	0.0236	19.2
15-23	0.1000	0.2020	9.6
22-24	0.1150	0.1790	9.6
23-24	0.1320	0.2700	9.6
24-25	0.1885	0.3292	9.6
25-26	0.2544	0.3800	9.6
25-27	0.1093	0.2087	9.6
28-27	0	0.3960	39
27-29	0.2198	0.4153	9.6
27-30	0.3202	0.6027	9.6
29-30	0.2399	0.4533	9.6
8-28	0.0636	0.2000	19.2
6-28	0.0169	0.0599	19.2

Table 4: Impact coefficients for μ_{LMP}^n (part I)

n	μ_{LMP}^n	μ_0^n	μ_1^n	μ_2^n	μ_3^n	μ_4^n	μ_{12}^n	μ_{13}^n	μ_{14}^n
1	61.80	39.61	2.09	0	3.57	14.12	0	2.66	-0.11
2	61.81	39.61	2.09	0	3.57	14.12	0	2.66	-0.11
3	61.75	39.61	2.09	0	3.57	14.12	0	2.66	-0.11
4	61.74	39.61	2.09	0	3.57	14.12	0	2.66	-0.11
5	61.85	39.61	2.09	0	3.57	14.12	0	2.66	-0.11
7	61.87	39.61	2.09	0	3.57	14.12	0	2.66	-0.11
8	61.89	39.61	2.09	0	3.57	14.12	0	2.66	-0.11
10	62.42	39.61	2.09	0	3.57	14.12	0	2.66	-0.11
11	62.23	39.61	2.09	0	3.57	14.12	0	2.66	-0.11
12	60.80	39.61	2.09	0	3.57	14.12	0	2.66	-0.11
13	60.80	39.61	2.09	0	3.57	14.12	0	2.66	-0.11
14	62.54	39.61	2.09	0	3.57	14.12	0	2.66	-0.11
15	64.99	39.61	2.09	0	3.57	14.12	0	2.66	-0.11
16	61.49	39.61	2.09	0	3.57	14.12	0	2.66	-0.11
17	62.14	39.61	2.09	0	3.57	14.12	0	2.66	-0.11
18	64.08	39.61	2.09	0	3.57	14.12	0	2.66	-0.11
19	63.54	39.61	2.09	0	3.57	14.12	0	2.66	-0.11
20	63.26	39.61	2.09	0	3.57	14.12	0	2.66	-0.11
21	62.54	39.61	2.09	0	3.57	14.12	0	2.66	-0.11
23	64.18	39.61	2.09	0	3.57	14.12	0	2.66	-0.11
24	63.11	39.61	2.09	0	3.57	14.12	0	2.66	-0.11
26	62.65	39.61	2.09	0	3.57	14.12	0	2.66	-0.11
29	62.36	39.61	2.09	0	3.57	14.12	0	2.66	-0.11
30	62.36	39.61	2.09	0	3.57	14.12	0	2.66	-0.11
average	62.43	39.61	2.09	0	3.57	14.12	0	2.66	-0.11

Table 5: Impact coefficients for μ_{LMP}^n (part II)

n	μ_{23}^n	μ_{24}^n	μ_{34}^n	μ_{123}^n	μ_{124}^n	μ_{134}^n	μ_{234}^n	μ_{1234}^n
1	0	0	-0.32	-0.01	0	0.19	0	0.00
2	0	0	-0.32	0.02	0	0.19	0	-0.01
3	0	0	-0.32	-0.11	0	0.19	0	0.06
4	0	0	-0.32	-0.13	0	0.19	0	0.07
5	0	0	-0.32	0.10	0	0.19	0	-0.06
7	0	0	-0.32	0.15	0	0.19	0	-0.09
8	0	0	-0.32	0.21	0	0.19	0	-0.12
10	0	0	-0.32	1.39	0	0.19	0	-0.78
11	0	0	-0.32	0.97	0	0.19	0	-0.55
12	0	0	-0.32	-2.26	0	0.19	0	1.26
13	0	0	-0.32	-2.26	0	0.19	0	1.26
14	0	0	-0.32	1.65	0	0.19	0	-0.93
15	0	0	-0.32	7.18	0	0.19	0	-4.00
16	0	0	-0.32	-0.70	0	0.19	0	0.38
17	0	0	-0.32	0.77	0	0.19	0	-0.43
18	0	0	-0.32	5.14	0	0.19	0	-2.86
19	0	0	-0.32	3.92	0	0.19	0	-2.19
20	0	0	-0.32	3.28	0	0.19	0	-1.83
21	0	0	-0.32	1.65	0	0.19	0	-0.92
23	0	0	-0.32	5.37	0	0.19	0	-2.99
24	0	0	-0.32	2.95	0	0.19	0	-1.65
26	0	0	-0.32	1.90	0	0.19	0	-1.06
29	0	0	-0.32	1.26	0	0.19	0	-0.71
30	0	0	-0.32	1.26	0	0.19	0	-0.71
average	0	0	-0.32	1.40	0	0.19	0	-0.79

Table 6: Impact coefficients for σ_{LMP}^n (part I)

n	σ_{LMP}^n	σ_0^n	σ_1^n	σ_2^n	σ_3^n	σ_4^n	σ_{12}^n	σ_{13}^n	σ_{14}^n
1	5.62	0	3.24	0	0	0	0	2.34	-0.11
2	5.63	0	3.24	0	0	0	0	2.34	-0.11
3	5.59	0	3.24	0	0	0	0	2.34	-0.11
4	5.59	0	3.24	0	0	0	0	2.34	-0.11
5	5.66	0	3.24	0	0	0	0	2.34	-0.11
7	5.67	0	3.24	0	0	0	0	2.34	-0.11
8	5.69	0	3.24	0	0	0	0	2.34	-0.11
10	6.08	0	3.24	0	0	0	0	2.34	-0.11
11	5.94	0	3.24	0	0	0	0	2.34	-0.11
12	5.01	0	3.24	0	0	0	0	2.34	-0.11
13	5.01	0	3.24	0	0	0	0	2.34	-0.11
14	6.17	0	3.24	0	0	0	0	2.34	-0.11
15	8.09	0	3.24	0	0	0	0	2.34	-0.11
16	5.41	0	3.24	0	0	0	0	2.34	-0.11
17	5.87	0	3.24	0	0	0	0	2.34	-0.11
18	7.37	0	3.24	0	0	0	0	2.34	-0.11
19	6.95	0	3.24	0	0	0	0	2.34	-0.11
20	6.73	0	3.24	0	0	0	0	2.34	-0.11
21	6.17	0	3.24	0	0	0	0	2.34	-0.11
23	7.45	0	3.24	0	0	0	0	2.34	-0.11
24	6.61	0	3.24	0	0	0	0	2.34	-0.11
26	6.25	0	3.24	0	0	0	0	2.34	-0.11
29	6.04	0	3.24	0	0	0	0	2.34	-0.11
30	6.04	0	3.24	0	0	0	0	2.34	-0.11
average	6.11	0	3.24	0	0	0	0	2.34	-0.11

Table 7: Impact coefficients for σ_{LMP}^n (part II)

n	σ_{23}^n	σ_{24}^n	σ_{34}^n	σ_{123}^n	σ_{124}^n	σ_{134}^n	σ_{234}^n	σ_{1234}^n
1	0	0	0	0.00	0	0.16	0	0.00
2	0	0	0	0.02	0	0.16	0	-0.01
3	0	0	0	-0.06	0	0.16	0	0.03
4	0	0	0	-0.08	0	0.16	0	0.04
5	0	0	0	0.07	0	0.16	0	-0.03
7	0	0	0	0.10	0	0.16	0	-0.05
8	0	0	0	0.14	0	0.16	0	-0.07
10	0	0	0	0.89	0	0.16	0	-0.43
11	0	0	0	0.63	0	0.16	0	-0.31
12	0	0	0	-1.36	0	0.16	0	0.75
13	0	0	0	-1.36	0	0.16	0	0.75
14	0	0	0	1.06	0	0.16	0	-0.51
15	0	0	0	4.58	0	0.16	0	-2.11
16	0	0	0	-0.44	0	0.16	0	0.23
17	0	0	0	0.49	0	0.16	0	-0.24
18	0	0	0	3.28	0	0.16	0	-1.53
19	0	0	0	2.51	0	0.16	0	-1.18
20	0	0	0	2.10	0	0.16	0	-1.00
21	0	0	0	1.06	0	0.16	0	-0.51
23	0	0	0	3.43	0	0.16	0	-1.60
24	0	0	0	1.89	0	0.16	0	-0.90
26	0	0	0	1.22	0	0.16	0	-0.59
29	0	0	0	0.81	0	0.16	0	-0.40
30	0	0	0	0.81	0	0.16	0	-0.40
average	0	0	0	0.91	0	0.16	0	-0.42

3. The factor thermal limit does not increase LMPs by itself ($\mu_2^n = \$0/\text{MWh}$), nor does the interaction between load uncertainty and thermal limit ($\mu_{12}^n = \$0/\text{MWh}$). This is because in this particular example, the transmission capacity is sufficient when 90% criterion is inactive. This result, however, may not necessarily hold in general, and μ_2^n and/or μ_{12}^n could become non-zeros for other network settings.
4. Price difference between nodes is an indication of congestion. Only two impact coefficients μ_{123}^n and μ_{1234}^n in Tables 4 & 5 take different values over different nodes, which means that congestion is not caused by a single factor, rather it is a result of the interaction among three or four factors. For the same reason as explained above, there may exist other combinations of factors that also contribute to the congestion, but the significant source of congestion is still believed to be μ_{123}^n and μ_{1234}^n . However, those columns where factor 2 does not appear ($\mu_0^n, \mu_1^n, \mu_{34}^n$, etc.) can be proven to be constant across nodes regardless of system parameters, because the only cause of price difference in a DC lossless model, thermal limit (factor 2), is set to be inactive in the computation of these columns.
5. It is also interesting to observe that μ_{1234}^n 's have smaller magnitudes with opposite signs than those of μ_{123}^n 's. This means that, given the existence of the first three factors, the incremental effect of market power mitigates congestion. One possible interpretation of this phenomenon is that market power reduces the relative differences among supply functions, and thus diminishes the preference for less expensive generators. Comparing the supply function parameters α_n 's and b_n 's in Table 2, we find that they have a positive correlation, but α_n 's are less spread out than b_n 's:

$$\begin{aligned}
& b_5 : b_2 : b_1 : b_{13} : b_{11} : b_8 \\
= & 1 : 1.75 : 2 : 3 : 3 : 3.25, \\
& \alpha_5 : \alpha_2 : \alpha_1 : \alpha_{13} : \alpha_{11} : \alpha_8 \\
= & 1 : 1.46 : 1.69 : 1.86 : 1.86 : 2.00.
\end{aligned}$$

Without market power, the ratio of supply functions of a more expensive generator i and a less expensive one j is

$$\frac{a_i q + b_i q^2/2}{a_j q + b_j q^2/2} = \frac{b_i}{b_j} > 1,$$

noticing that $a_n = 0, \forall n \in \mathcal{S}$ in this example. When market power becomes active, α_n 's substitute zero-valued a_n 's, and this ratio becomes

$$\frac{\alpha_i q + \frac{1}{2} b_i q^2}{\alpha_j q + \frac{1}{2} b_j q^2} < \frac{\left(\alpha_j \frac{b_i}{b_j} \right) q + \frac{1}{2} b_i q^2}{\alpha_j q + \frac{1}{2} b_j q^2} = \frac{b_i}{b_j},$$

which means that the relative differences among supply functions shrink. This phenomenon has also been observed and discussed in [62]. However, we can only conclude that market power could mitigate congestion in certain cases under certain assumptions (e.g., how market power is exercised), but not necessarily so in all circumstances.

6. Load uncertainty is the single primary and decisive source of LMP volatility, contributing an average standard deviation of $\sigma_1^n = \$3.24/\text{MWh}$ to the realized $\$6.11/\text{MWh}$ in total. The absence of sole contributions of other factors ($\sigma_2^n = \sigma_3^n = \sigma_4^n = \$0/\text{MWh}$) is due to their assumed deterministic characteristics. The interactions between these factors and load uncertainty, however, have significant contribution to the LMP volatility. It is also indicated in Tables 6 & 7 that congestion is a result of the interaction among factors.

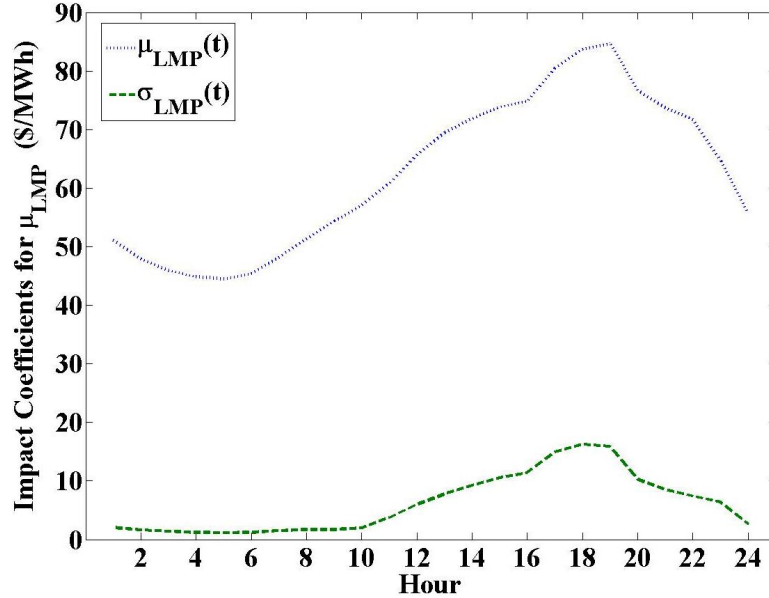


Figure 6: Time variation of $\mu_{\text{LMP}}(t)$ and $\sigma_{\text{LMP}}(t)$

2.4.3 Time Variation of Impact Coefficients

We show in Figure 6 how the node-averaged mean and standard deviation of LMPs vary from hour to hour. In Figure 6,

$$\mu_{\text{LMP}}(t) = \frac{1}{|\mathcal{D} \cup \mathcal{S}|} \sum_{n \in \mathcal{D} \cup \mathcal{S}} \mu_{\text{LMP}}^n(t).$$

Node-averages are also taken in the same manner for the impact coefficients, which are shown in Figures 7 and 8. Only some of the impact coefficients are plotted; the omitted ones have little or no variation over time.

We have the following observations:

1. Coefficients $\mu_{\text{LMP}}(t)$ and $\mu_1(t)$ follow a similar pattern of time variation with $d_{n,t}$. Recall that $\mu_1(t)$ represents the sole contribution of factor 1 at node n in hour t , and is the difference between $\mu_t(x_1 = 1, x_2 = 0, x_3 = 0, x_4 = 0)$ and $\mu_t(x_1 = 0, x_2 = 0, x_3 = 0, x_4 = 0)$, which represent the two situations with demand at node n in hour t being $d_{n,t}(1 + \epsilon_t)$ and $d_{n,t}$.
2. Coefficient $\mu_{13}(t)$, interaction between factors 1 and 3, becomes significant when demand is high.
3. We can see from $\mu_{123}(t)$ and $\mu_{1234}(t)$ that congestion occurs during peak hours and that market power mitigates the congestion.
4. The observations on the impact coefficients for σ_{LMP} are similar.

2.5 USE OF SYSTEM MODEL IN EVALUATING EXPANSION PLANS

The system model approach described in Section 2.3 can be used to perform sensitivity analysis for the current system, or to analyze the effects of other factors or system upgrading decisions. As an illustration, we use the network example in Section 2.4 to analyze the effects of generator and transmission line capacity expansion plans.

Suppose investment decisions are to be made to introduce new generators at nodes 15, 18 and 23, where highest means and largest standard deviations of LMPs are observed. The

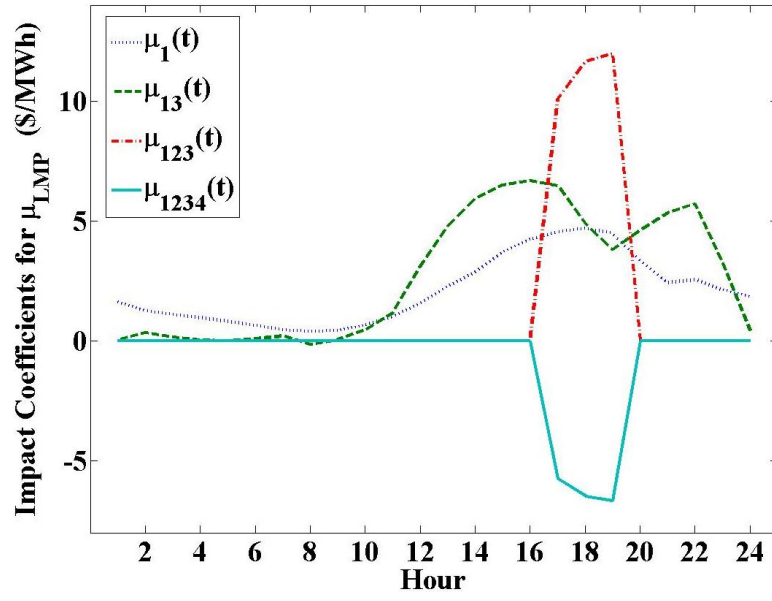


Figure 7: Time variation of impact coefficients for $\mu_{LMP}(t)$

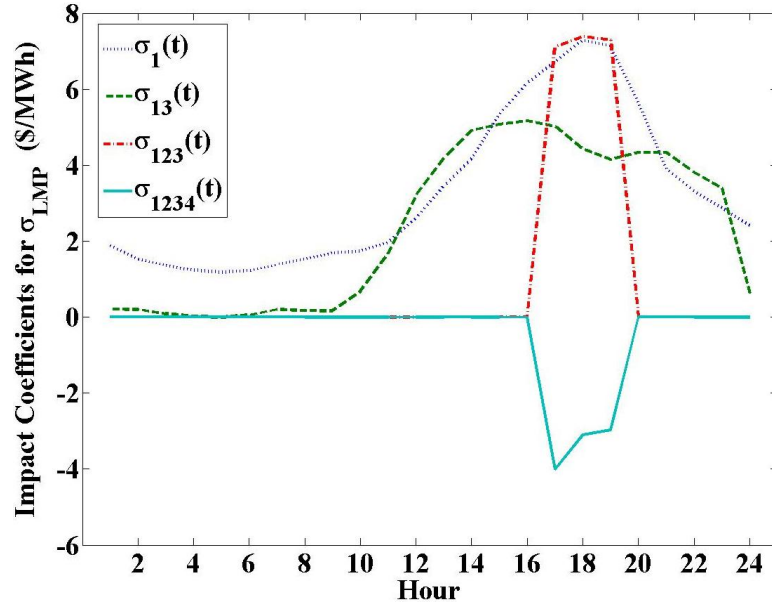


Figure 8: Time variation of impact coefficients for $\sigma_{LMP}(t)$

supply function parameters of the new generators are all assumed to take the average values of the previously existing ones, i.e., $a_n = 0, \alpha_n = 13.63, b_n = 1.17, \bar{Q}_n = 52.2, \forall n = 15, 18, 23$. Transmission line 12-15 is also planned to be expanded by 15% of its current capacity. The questions are: (1) how would the LMPs be affected, and (2) how effective would the capacity expansion of each component (generator or transmission line) be?

Keeping all of the previous factors (load uncertainty, thermal limit, capacity reserve and market power) active, we define another four factors, numbered 5, 6, 7 and 8, as the introduction of generators 15, 18 and 23, and capacity expansions of transmission line 12-15, respectively.

The statistical models for this problem become:

$$\begin{aligned}
& \tilde{\mu}_{\text{LMP}}^n(t) \\
= & \mu_{\text{LMP}}^n(t) + \mu_5^n(t) + \mu_6^n(t) + \mu_7^n(t) + \mu_8^n(t) \\
& + \mu_{56}^n(t) + \mu_{57}^n(t) + \mu_{58}^n(t) + \mu_{67}^n(t) + \mu_{68}^n(t) + \mu_{78}^n(t) \\
& + \mu_{567}^n(t) + \mu_{568}^n(t) + \mu_{578}^n(t) + \mu_{678}^n(t) + \mu_{5678}^n(t), \\
& \tilde{\sigma}_{\text{LMP}}^n(t) \\
= & \sigma_{\text{LMP}}^n(t) + \sigma_5^n(t) + \sigma_6^n(t) + \sigma_7^n(t) + \sigma_8^n(t) \\
& + \sigma_{56}^n(t) + \sigma_{57}^n(t) + \sigma_{58}^n(t) + \sigma_{67}^n(t) + \sigma_{68}^n(t) + \sigma_{78}^n(t) \\
& + \sigma_{567}^n(t) + \sigma_{568}^n(t) + \sigma_{578}^n(t) + \sigma_{678}^n(t) + \sigma_{5678}^n(t),
\end{aligned}$$

where $\tilde{\mu}_{\text{LMP}}^n(t)$ and $\tilde{\sigma}_{\text{LMP}}^n(t)$ are, respectively, the forecasted mean and standard deviation of LMP at node n as a result of these additional factors; as has been defined before, $\mu_{\text{LMP}}^n(t)$ and $\sigma_{\text{LMP}}^n(t)$ are, respectively, the realized mean and standard deviation before the introduction of new factors.

We obtain the impact coefficients at all nodes $n \in \mathcal{D} \cup \mathcal{S}$ in each hour $t = 1, \dots, 24$. Tables 8 & 9 and 10 & 11 show the time-averaged impact coefficients for $\tilde{\mu}_{\text{LMP}}^n$ and $\tilde{\sigma}_{\text{LMP}}^n$, respectively. As a result of the combined effect of these four factors, the mean and standard deviation of LMPs are reduced on average from \$62.43/MWh and \$6.11/MWh to \$49.18/MWh and \$3.24/MWh, respectively. The individual contributions of factors 5, 6, 7 and 8 to $\tilde{\mu}_{\text{LMP}}^n$

are, respectively, $-\$6.71/\text{MWh}$, $-\$7.61/\text{MWh}$, $-\$8.84/\text{MWh}$ and $-\$0.62/\text{MWh}$ on average; and their individual contributions to $\tilde{\sigma}_{\text{LMP}}^n$ are, respectively, $-\$0.49/\text{MWh}$, $-\$1.82/\text{MWh}$, $-\$2.19/\text{MWh}$ and $-\$0.49/\text{MWh}$ on average.

Tables 8 & 9 and 10 & 11 can also provide information for any subset of factors 5, 6, 7 and 8. For example, to answer the question of “what is the incremental value of expanding the capacity of transmission line 12-15 by 15% after new generators have been introduced at nodes 15, 18 and 23?”, we select those columns in Tables 8 & 9 that contain factor 8: $\{\mu_8, \mu_{58}, \mu_{68}, \mu_{78}, \mu_{568}, \mu_{578}, \mu_{678}, \mu_{5678}\}$. The summation of these columns is zero. The same result is observed for Tables 10 & 11. It indicates that the incremental value of expanding the capacity of transmission line 12-15 beyond introducing new generators is zero. This information is useful for decision makers to avoid redundant investments.

By re-defining the factors as unit increments of certain system parameters (e.g., b_n ’s as fuel prices increase or α_n ’s as more severe market power), sensitivity analysis for the current system can also be performed in a similar way as illustrated in this section.

2.6 CONCLUSION

This chapter builds a system model to decompose the effects of influential factors on locational marginal prices. Four factors (load uncertainty, thermal limit, capacity reserve and market power) are considered, and the impact coefficients are calculated to estimate the contribution of each single factor and their interactions to the mean and standard deviation of LMPs at each node.

An IEEE 30-bus network is used as an example to demonstrate this approach. The system model approach can also be used to perform sensitivity analysis or to evaluate the effectiveness of investment plans, e.g, introducing new generators and/or expanding capacities of transmission lines.

The main contributions of this chapter include:

1. The system model enables one to answer “what if” questions which are generally hard to answer using historical data.

2. Piecewise linear property of LMPs as functions of demand variation has been explored. For a given continuous probability distribution of demand uncertainty and input variables, the mean and standard deviation of LMPs can be obtained exactly and efficiently using integration, which is equivalent to infinitely many simulation samples if Monte Carlo simulation were to be used instead.
3. Impact coefficients provide insights on the composition of LMP probability distribution, in terms of mean and standard deviation. They can also inform and assist power system evaluation and investment decision making. The techniques used in this chapter can also be applied for a more complete analysis of the LMP probability distribution (e.g., on higher moments).

It is worth mentioning that our observations and analyses are based on the consideration of only four factors with simplifying assumptions, and are only derived for some specified system parameters. Further research should (1) consider other factors that affect LMP probability distributions, e.g., fuel prices fluctuation, generator or transmission line outage; (2) relax the assumption of perfect load correlation among nodes (according to the load data from PJM [1], the correlation between PJM-E and PJM-W is 0.8632); (3) relax the assumption that supply functions stay the same over the entire time horizon, and study the dynamic gaming behavior of market power exercise under different scenarios and inputs; (4) examine the hypothesis that market power would in general reduce the difference among supply functions and mitigate congestion; and (5) compare the analyses from the system model to real world observations.

Table 8: Impact coefficients for $\tilde{\mu}_{\text{LMP}}^n$ (part I)

n	$\tilde{\mu}_{\text{LMP}}^n$	μ_{LMP}^n	μ_5^n	μ_6^n	μ_7^n	μ_8^n	μ_{56}^n	μ_{57}^n	μ_{58}^n
1	50.10	61.80	-8.82	-6.79	-7.44	0.01	5.53	6.37	-0.01
2	50.24	61.81	-8.74	-6.73	-7.38	0.00	5.50	6.34	
3	49.68	61.75	-9.06	-6.96	-7.62	0.05	5.63	6.44	-0.05
4	49.59	61.74	-9.12	-7.00	-7.67	0.06	5.65	6.46	-0.06
5	50.60	61.85	-8.53	-6.58	-7.22	-0.04	5.42	6.28	0.04
7	50.83	61.87	-8.39	-6.48	-7.12	-0.06	5.36	6.24	0.06
8	51.08	61.89	-8.32	-6.43	-6.95	-0.09	5.41	6.23	0.09
10	56.28	62.42	-3.54	-2.93	-5.94	-0.61	1.79	4.49	0.61
11	54.45	62.23	-5.18	-4.13	-6.32	-0.43	3.01	5.09	0.43
12	40.20	60.80	-14.62	-10.93	-11.83	1.01	7.79	8.08	-1.01
13	40.20	60.80	-14.62	-10.93	-11.83	1.01	7.79	8.08	-1.01
14	36.56	62.54	-19.01	-14.68	-15.42	-0.73	10.95	10.90	0.73
15	31.43	64.99	-25.21	-19.97	-20.48	-3.18	15.41	14.86	3.18
16	47.08	61.49	-9.87	-7.50	-9.31	0.32	5.22	6.54	-0.32
17	53.54	62.14	-5.42	-4.29	-6.94	-0.33	2.81	5.10	0.33
18	22.36	64.08	28.72	-33.19	-15.35	-2.27	-36.82	-9.29	2.27
19	67.53	63.54	18.28	13.47	-12.31	-1.74	-22.15	-4.83	1.73
20	64.69	63.26	12.76	9.32	-10.70	-1.45	-16.10	-2.47	1.45
21	57.43	62.54	-4.75	-3.89	-4.03	-0.73	4.17	5.21	0.73
23	23.53	64.18	-18.70	-15.10	-31.94	-2.38	33.38	10.59	2.38
24	63.09	63.11	-10.68	-8.62	5.38	-1.31	15.86	8.70	1.31
26	58.49	62.65	-9.78	-7.78	0.66	-0.84	11.86	7.76	0.84
29	55.70	62.36	-9.23	-7.27	-2.21	-0.56	9.43	7.18	0.56
30	55.70	62.36	-9.23	-7.27	-2.21	-0.56	9.43	7.18	0.56
average	49.18	62.43	-6.71	-7.61	-8.84	-0.62	4.26	5.73	0.62

Table 9: Impact coefficients for $\tilde{\mu}_{\text{LMP}}^n$ (part II)

n	μ_{67}^n	μ_{68}^n	μ_{78}^n	μ_{567}^n	μ_{568}^n	μ_{578}^n	μ_{678}^n	μ_{5678}^n
1	3.91	-0.01	-0.01	-4.46	0.01	0.01	0.01	-0.01
2	3.89	0.00	0.00	-4.47	0.00	0.00	0.00	0.00
3	3.96	-0.05	-0.05	-4.45	0.05	0.05	0.05	-0.05
4	3.98	-0.06	-0.06	-4.45	0.06	0.06	0.06	-0.06
5	3.85	0.04	0.04	-4.48	-0.04	-0.04	-0.04	0.04
7	3.82	0.06	0.06	-4.48	-0.06	-0.06	-0.06	0.06
8	3.79	0.09	0.09	-4.55	-0.09	-0.09	-0.09	0.09
10	3.17	0.61	0.61	-3.18	-0.61	-0.61	-0.61	0.61
11	3.39	0.43	0.43	-3.63	-0.43	-0.43	-0.43	0.43
12	5.14	-1.01	-1.01	-4.24	1.01	1.01	1.01	-1.01
13	5.14	-1.01	-1.01	-4.24	1.01	1.01	1.01	-1.01
14	7.69	0.73	0.73	-6.40	-0.73	-0.73	-0.73	0.73
15	11.29	3.18	3.18	-9.44	-3.18	-3.18	-3.18	3.18
16	4.29	-0.32	-0.32	-3.78	0.32	0.32	0.32	-0.32
17	3.50	0.33	0.33	-3.36	-0.33	-0.33	-0.33	0.33
18	12.26	2.27	2.27	11.94	-2.27	-2.27	-2.27	2.27
19	1.97	1.74	1.74	9.57	-1.74	-1.73	-1.74	1.73
20	2.27	1.45	1.45	6.34	-1.45	-1.45	-1.45	1.45
21	3.00	0.73	0.73	-4.82	-0.73	-0.73	-0.73	0.73
23	12.40	2.38	2.38	-31.29	-2.38	-2.38	-2.38	2.38
24	2.19	1.31	1.31	-12.86	-1.31	-1.31	-1.31	1.31
26	2.80	0.84	0.84	-9.68	-0.84	-0.84	-0.84	0.84
29	3.17	0.56	0.56	-7.74	-0.56	-0.56	-0.56	0.56
30	3.17	0.56	0.56	-7.74	-0.56	-0.56	-0.56	0.56
average	4.75	0.62	0.62	-4.83	-0.62	-0.62	-0.62	0.62

Table 10: Impact coefficients for $\tilde{\sigma}_{\text{LMP}}^n$ (part I)

n	$\tilde{\sigma}_{\text{LMP}}^n$	σ_{LMP}^n	σ_5^n	σ_6^n	σ_7^n	σ_8^n	σ_{56}^n	σ_{57}^n	σ_{58}^n
1	3.28	5.62	-1.24	-1.33	-1.58	0.00	0.99	1.35	0.00
2	3.30	5.63	-1.22	-1.32	-1.58	-0.01	0.98	1.34	0.01
3	3.22	5.59	-1.33	-1.34	-1.60	0.03	1.01	1.37	-0.03
4	3.21	5.59	-1.35	-1.34	-1.60	0.04	1.01	1.37	-0.04
5	3.35	5.66	-1.14	-1.31	-1.56	-0.03	0.96	1.32	0.03
7	3.38	5.67	-1.09	-1.30	-1.56	-0.05	0.95	1.31	0.05
8	3.42	5.69	-1.07	-1.31	-1.54	-0.07	1.00	1.30	0.07
10	4.14	6.08	0.69	-0.91	-1.62	-0.46	-0.63	1.17	0.46
11	3.88	5.94	0.08	-1.04	-1.59	-0.32	-0.09	1.21	0.32
12	1.89	5.01	-3.38	-1.73	-2.06	0.61	1.57	1.90	-0.61
13	1.89	5.01	-3.38	-1.73	-2.06	0.61	1.57	1.90	-0.61
14	1.37	6.17	-5.60	-3.27	-3.59	-0.55	3.30	3.52	0.55
15	0.66	8.09	-6.53	-5.75	-6.04	-2.47	5.45	5.99	2.47
16	2.85	5.41	-1.58	-1.32	-1.81	0.21	0.57	1.53	-0.21
17	3.75	5.87	0.02	-1.02	-1.67	-0.25	-0.28	1.27	0.25
18	0.54	7.37	113.23	-6.94	-4.47	-1.75	-13.33	1.65	1.75
19	5.62	6.95	9.17	1.66	-3.54	-1.32	-13.31	1.49	1.32
20	5.25	6.73	7.02	1.01	-3.05	-1.10	-10.10	1.41	1.10
21	4.31	6.17	0.15	-1.16	-1.29	-0.55	0.83	1.02	0.55
23	0.53	7.45	-5.67	-4.32	-7.03	-1.83	18.43	5.77	1.83
24	5.17	6.61	-2.42	-2.42	0.27	-0.99	7.92	0.26	0.99
26	4.50	6.25	-1.91	-1.99	-0.41	-0.63	5.28	0.66	0.63
29	4.09	6.04	-1.59	-1.73	-0.83	-0.41	3.66	0.90	0.41
30	4.09	6.04	-1.59	-1.73	-0.83	-0.41	3.66	0.90	0.41
average	3.24	6.11	-0.49	-1.82	-2.19	-0.49	0.89	1.75	0.49

Table 11: Impact coefficients for $\tilde{\sigma}_{\text{LMP}}^n$ (part II)

n	σ_{67}^n	σ_{68}^n	σ_{78}^n	σ_{567}^n	σ_{568}^n	σ_{578}^n	σ_{678}^n	σ_{5678}^n
1	0.79	0.00	0.00	-1.31	0.00	0.00	0.00	0.00
2	0.79	0.01	0.01	-1.32	-0.01	-0.01	-0.01	0.01
3	0.78	-0.03	-0.03	-1.26	0.03	0.03	0.03	-0.03
4	0.78	-0.04	-0.04	-1.25	0.04	0.04	0.04	-0.04
5	0.79	0.03	0.03	-1.36	-0.03	-0.03	-0.03	0.03
7	0.79	0.05	0.05	-1.39	-0.05	-0.05	-0.05	0.05
8	0.79	0.07	0.07	-1.44	-0.07	-0.07	-0.07	0.07
10	0.80	0.46	0.46	-1.45	-0.46	-0.46	-0.46	0.46
11	0.80	0.32	0.32	-1.43	-0.32	-0.32	-0.32	0.32
12	0.87	-0.61	-0.61	-0.31	0.61	0.61	0.61	-0.61
13	0.87	-0.61	-0.61	-0.31	0.61	0.61	0.61	-0.61
14	2.28	0.55	0.55	-1.43	-0.55	-0.55	-0.55	0.55
15	4.56	2.47	2.47	-5.12	-2.47	-2.47	-2.47	2.47
16	0.78	-0.21	-0.21	-0.73	0.21	0.21	0.21	-0.21
17	0.79	0.25	0.25	-1.23	-0.25	-0.25	-0.25	0.25
18	4.39	1.75	1.75	-1.37	-1.75	-1.75	-1.75	1.75
19	0.80	1.32	1.32	2.41	-1.32	-1.32	-1.32	1.32
20	0.80	1.10	1.10	1.43	-1.10	-1.10	-1.10	1.10
21	0.82	0.55	0.55	-2.22	-0.55	-0.55	-0.55	0.55
23	4.22	1.83	1.83	-18.32	-1.83	-1.83	-1.83	1.83
24	0.93	0.99	0.99	-5.99	-0.99	-0.99	-0.99	0.99
26	0.87	0.63	0.63	-4.25	-0.63	-0.63	-0.63	0.63
29	0.83	0.41	0.41	-3.19	-0.41	-0.41	-0.41	0.41
30	0.83	0.41	0.41	-3.19	-0.41	-0.41	-0.41	0.41
average	1.32	0.49	0.49	-2.33	-0.49	-0.49	-0.49	0.49

3.0 SECURITY CONSTRAINED ECONOMIC DISPATCH: A MARKOV DECISION PROCESS APPROACH WITH EMBEDDED STOCHASTIC PROGRAMMING

3.1 INTRODUCTION

In a pool-based electricity market, security constrained economic dispatch is the process of allocating generation and transmission resources so as to serve the system load with low cost and high reliability. The goals of cost efficiency and reliability, however, are oftentimes conflicting. On the one hand, in order to serve the demand most cost efficiently, the capacities of transmission lines and the cheapest generators should be fully utilized. On the other hand, the consideration of reliability would suggest using local generators, which may not be the cheapest, but the supply has less dependence on the reliability of transmission lines; a considerable amount of generation and transmission capacities should also be reserved for contingency use. A compromise between low cost and high reliability is thus inevitable.

In practice, the “optimal” tradeoff for all stakeholders is a complex problem, and the solution may vary depending on the perspective chosen. The N-1 criterion, for example, requires that the system be able to withstand the failure of any single component (generator or transmission line). Various stochastic criteria have also been proposed. [18, 19] review some of the recent publications on the probabilistic criteria, and propose a stochastic security approach to market clearing where the probabilities of generator and transmission line failures are taken into consideration.

This chapter presents another stochastic approach to security constrained economic dispatch, which has some significant differences with [18, 19], and is able to address some important questions that have yet to be answered in the existing literature. First, cascading

failures are taken into consideration. Although a rare event, the impact of a cascading failure could be tremendous [10], and the frequency of large blackouts in the United States has been observed to increase during the recent years [47]. A great amount of research has been conducted on modeling, monitoring and managing the risk of cascading failures (see e.g., [24, 48, 84]). [94] proposes an operational criterion to minimize the risk of subsequent line failures, whereas the generation cost is not being considered. We adopt the hidden failure model [22] and take both the probability and the economic cost of a cascading failure into consideration of power dispatch.

Secondly, in our model, the dispatch decisions are made with an infinitely repeated 24-hour time horizon taken into account, as opposed to [18, 19], where an isolated 24-hour period is studied. The advantage of far-sighted decision making is that the long-term economic cost of a potential contingency is not underestimated when compared with the immediate reward of taking the risk.

Thirdly, the optimal policy from the MDP model provides the optimal dispatch not only for the normal scenario, but also for contingency scenarios. A remarkable property of the MDP approach is that the optimal decision is provided for all possible scenarios that are being considered. [79] uses an MDP approach to study the bidding decision of power suppliers in the spot market, and [72] uses a competitive MDP model to examine the market power exercise in deregulated power markets.

The remaining sections are organized as follows. Section 3.2 explains the optimization problem and makes necessary definitions and assumptions. The MDP model is formulated in Section 3.3, and the policy iteration algorithm is introduced in Section 3.4 to solve the MDP model. Section 3.5 demonstrates the approach with a numerical example, and compares the results with those of other approaches. Section 3.6 concludes this chapter.

3.2 DEFINITIONS AND ASSUMPTIONS

3.2.1 Transmission Network

A set of nodes \mathcal{N} is connected by a set of transmission lines \mathcal{L} . The sets of nodes with demand for and supply of power are denoted by \mathcal{D} and \mathcal{S} , respectively. Depending on whether there is demand for or supply of power, any node in \mathcal{N} could belong to either \mathcal{D} or \mathcal{S} , or both, or neither.

A DC lossless load flow model is used here, which has been found to be a good approximation to the more accurate AC load flow model when thermal limit is the primary concern [54, 68].

3.2.2 Load

Hourly load fluctuation is considered. Locational demands are assumed to be inelastic, deterministic and constant within each hour. The demand (in MW) at node n in hour t is denoted by $D_{n,t}, \forall n \in \mathcal{D}, t = 1, 2, \dots, 24$.

In case the generation and transmission capacity is not sufficient to meet all the demands, a certain amount of load will be involuntarily left unserved. The amount of involuntarily unserved load is called load shedding. The associated cost of unit amount of load shedding is denoted by c_n^{LS} (in \$/MWh).

3.2.3 Generation

Following [53], we assume that there is at most one generator at a node (as a result, the generator at node n can be referred to as generator n), and that power suppliers will submit a linear supply function for each of their generators to the system operator. The supply function for generator n is denoted by

$$q_n \mapsto a_n + b_n q_n, \quad \forall n \in \mathcal{S},$$

where q_n (in MWh) is the quantity of power generation at node n , a_n (in \$/MWh) and b_n (in \$/(MWh)²) are constant parameters. Each generator n has a maximum generation

capacity \overline{Q}_n . No minimum generation, fixed cost, or other unit commitment requirements are considered. For modeling simplicity, we also ignore generator failures, which could be considered without much additional modeling effort.

3.2.4 Transmission Constraint

Denote by z_n , T_l , and H the net injection at node n , the thermal limit of line l , and the PTDF (power transfer distribution factors) matrix, respectively. Net injection is the total power flow going into a node less the total power flow going out of it. PTDF matrix gives the linear relation between net injection at each node and power flow through each line. For all $l \in \mathcal{L}$, $|\sum_{n \in \mathcal{N}} H_{l,n} z_n|$ calculates the magnitude of the power flow through line l . The transmission constraints require that power flow going through any transmission line in either direction must be within the capacity:

$$\begin{aligned} \sum_{n \in \mathcal{N}} H_{l,n} z_n &\leq T_l, \quad \forall l \in \mathcal{L}, \\ -\sum_{n \in \mathcal{N}} H_{l,n} z_n &\leq T_l, \quad \forall l \in \mathcal{L}. \end{aligned}$$

These two constraints will be presented as

$$\pm \sum_{n \in \mathcal{N}} H_{l,n} z_n \leq T_l, \quad \forall l \in \mathcal{L}$$

for short in the remainder of this chapter.

3.2.5 Transmission Line Failure

A transmission line can be in either of two states: working or failed. There are two types of transmission line failures: (a) When the power flow is within the thermal limit, the risk comes from unexpected events, e.g., fire, falling tree, bad weather, etc. Failures of the transmission lines in such situation are assumed to be independent of each other. The state transition between failed and working (repaired) states of a transmission line is assumed to be a continuous time Markov chain, and the availability of the lines can be calculated using the historical data on MTTF (mean time to failure) and MTTR (mean time to repair). Denote by λ_l and μ_l (both in #/hour) the rates of failure and repair of line l , respectively.

(b) When the power flow exceeds the thermal limit of line l , there is an additional risk of failure due to the overflow. The system operator makes the dispatch decision in such a way that the power flows do not exceed the thermal limits. However, once a transmission line has failed due to an unexpected event, the power flows will instantaneously change their routes according to the new network topology, which may cause overflows on some other lines. [22] proposes a hidden failure model to estimate the probability of a type (b) failure on line l as a function $f(v_l)$:

$$f(v_l) := \begin{cases} 2.5v_l & 0 \leq v_l \leq 0.4, \\ 1 & v_l > 0.4, \end{cases}$$

where v_l is the *percentages* of overflow with respect to the thermal limit of line l . If the power flow through line l is t_l , then

$$v_l = \max \left\{ 0, \frac{|t_l| - T_l}{T_l} \right\} \times 100\%.$$

This assumption is reported to be “consistent with the observed NERC events.” [67]

3.2.6 Cascading Failure

We assume that a cascading failure occurs whenever two or more transmission lines have failed in a single hour. This could occur in the following two situations: (i) two or more lines have failed due to unexpected events, and (ii) the failure of one line causes overflow and then failure of another line. Once one line has failed due to an unexpected event, which could cause overflows on all other lines, we assume that the probability of a cascading failure caused by the overflow is a function $f(\mathbf{v})$:

$$f(\mathbf{v}) := \begin{cases} 2.5 \max\{\mathbf{v}\} & 0 \leq \max\{\mathbf{v}\} \leq 0.4, \\ 1 & \max\{\mathbf{v}\} > 0.4, \end{cases} \quad (3.1)$$

where \mathbf{v} is the vector of *percentages* of overflows with respect to the thermal limits.

3.2.7 System Operator

The task of the system operator is assumed to be to make dispatch decisions using existing generation and transmission resources to serve the demand at minimum long term expected cost, which includes cost of generation, load shedding and cascading failures. The system operator re-dispatches the system once every hour to adjust for the demand change and possible transmission line failure and repair. In case of a cascading failure, the system operator should shut down the entire system until the system has been restored (all components examined and all failed lines repaired). The rate of system restoration is denoted by $\tilde{\mu}$ (in #/hour).

3.2.8 Timing of the Transmission Line Failures

We make two assumptions about the timing of the transmission line failures:

- (A1) A single transmission line failure may only occur at the beginning of each hour, after the system operator has already made the dispatch decision without expectation of that failure.
- (A2) A cascading failure occurs at the end of the hour, so that the cost of blackout is calculated from the next hour.

3.3 THE MARKOV DECISION PROCESS MODEL

3.3.1 Time Horizon $\{1, 2, \dots\}$

We consider infinitely repeated 24-hour cycles. The time cycle will be incorporated into the state space, thus the decision making time horizon is: $\{1, 2, \dots\}$.

3.3.2 State Space S

There are three types of states: a normal state s_N , a set of contingency states S_C , and a blackout state s_B . In the normal state s_N , all transmission lines are working; in a contingency

state $s \in S_C$, exactly one transmission line has failed; s_B represents the blackout state caused by a cascading failure. A contingency state is represented by the failed transmission line: $S_C = \{\{1\}, \{2\}, \dots, \{|\mathcal{L}|\}\}$. To incorporate the repeated time cycles, we include the demand vector $D_{n,t}$ as an additional dimension to the state space, and set $D_{n,t} = D_{n,t+24}$ for all $t = 1, 2, \dots$. As a result, the size of the entire state space is $(1 + |\mathcal{L}| + 1) \times 24$.

3.3.3 Action Space A_s

An action $a_s \in A_s$ at a given state s is an admissible dispatch decision of using the generators and working transmission lines (denoted by \mathcal{L}_s) to serve the demand $D_{n,t}$ of all nodes in hour t . More specifically, it is a polyhedron of admissible actions $\{q_n, \forall n \in \mathcal{S}; d_n, \forall n \in \mathcal{D}\}$ defined by the following constraints:

$$\begin{aligned}
A_s &= \{q, d : \\
&\pm \left[\sum_{n \in \mathcal{S}} H_{l,n}^s q_n - \sum_{n \in \mathcal{D}} H_{l,n}^s (D_{n,t} - d_n) \right] \leq T_l, \forall l \in \mathcal{L}_s \\
&\sum_{n \in \mathcal{S}} q_n = \sum_{n \in \mathcal{D}} (D_{n,t} - d_n) \\
&0 \leq q_n \leq \overline{Q}_n, \forall n \in \mathcal{S}; d_n \geq 0, \forall n \in \mathcal{D}\},
\end{aligned}$$

where d_n is the amount of load shedding at node n .

3.3.4 Transition Probability $P(j|s, a)$

In an MDP model, the transition probability $P(j|s, a)$ is the probability that the system moves from state s to state j within an hour given action a . In the remainder, when this probability does not depend on the action a (as long as $a \in A_s$ is a feasible action), it may be denoted as $P(j|s)$.

- The transition of staying at the normal state s_N means that no failure occurs in this hour, so

$$P(s_{t+1} = s_N | s_t = s_N) = \prod_{l \in \mathcal{L}} e^{-\lambda_l}.$$

- The transition from the normal state s_N to a contingency state $s \in S_C$ means that (i) line s has failed in this hour due to an unexpected event, and that (ii) this failure does not cause a type (b) failure of another line. The latter depends on the action (dispatch decision). Therefore,

$$P(s_{t+1} = s | s_t = s_N, a) = [1 - f(a)] (1 - e^{-\lambda_s}) \prod_{l \in \mathcal{L} \setminus s} e^{-\lambda_l}, \forall s \in S_C,$$

where the probability of a type (b) failure, $f(\cdot)$, is written as a function of the action a , because the percentage of overflow can be calculated from the action $a = \{q_n, \forall n \in \mathcal{S}; d_n, \forall n \in \mathcal{D}\}$:

$$v_l = \left(\frac{|\sum_{n \in \mathcal{S}} H_{l,n}^s q_n - \sum_{n \in \mathcal{D}} H_{l,n}^s (D_n - d_n)| - T_l}{T_l} \right)^+ \times 100\%, \forall l \in \mathcal{L}_s.$$

- The probability of transition from the normal state s_N to the blackout state s_B is

$$P(s_{t+1} = s_B | s_t = s_N, a) = 1 - P(s_{t+1} = s_N | s_t = s_N) - \sum_{l \in S_C} P(s_{t+1} = l | s_t = s_N, a).$$

- The transition from a contingency state $s \in S_C$ to the normal state s_N implies that, during this hour no line has failed and line s has been repaired:

$$P(s_{t+1} = s_N | s_t = s) = (1 - e^{-\mu_s}) \prod_{k \in \mathcal{L} \setminus s} e^{-\lambda_k}, \forall s \in S_C.$$

- The transition of staying at the same contingency state $s \in S_C$ implies that, during this hour no line has failed and line s has not been repaired:

$$P(s_{t+1} = s | s_t = s) = e^{-\mu_s} \prod_{k \in \mathcal{L} \setminus s} e^{-\lambda_k}, \forall s \in S_C.$$

- The transition from a contingency state $s \in S_C$ to another contingency state $k \in S_C$ implies that, during this hour line k has failed, line s has been repaired, and no other line has failed:

$$P(s_{t+1} = k | s_t = s, a) = [1 - f(a)] (1 - e^{-\mu_s}) (1 - e^{-\lambda_k}) \prod_{j \in \mathcal{L} \setminus \{k, s\}} e^{-\lambda_j}, \forall s, k (\neq s) \in S_C.$$

- The probability of transition from a contingency state $s \in S_C$ to the blackout state s_B is

$$P(s_{t+1} = s_B | s_t = s, a) = 1 - P(s_{t+1} = s_N | s_t = s) - \sum_{k \in S_C} P(s_{t+1} = k | s_t = s, a), \forall s \in S_C.$$

- The probability of transition from the blackout state s_B to the normal state s_N is

$$P(s_{t+1} = s_N | s_t = s_B) = e^{-\tilde{\mu}}.$$

- The probability of transition from the blackout state s_B to a contingency state $s \in S_C$ is

$$P(s_{t+1} = s | s_t = s_B) = 0, \forall s \in S_C.$$

- The probability of staying at the blackout state s_B is

$$P(s_{t+1} = s_B | s_t = s_B) = 1 - e^{-\tilde{\mu}}.$$

3.3.5 Immediate Cost $c(s, a)$

The immediate cost includes generation cost and cost of load shedding of this hour. For a given dispatch decision $a_s = \{q_n, \forall n \in \mathcal{S}; d_n, \forall n \in \mathcal{D}\}$, the immediate cost is

$$c(s, a) = \int_0^{q_n} (a_n + b_n q) dq + \sum_{n \in \mathcal{D}} c_n^{\text{LS}} d_n = \left(a_n q_n + \frac{1}{2} b_n q_n^2 \right) + \sum_{n \in \mathcal{D}} c_n^{\text{LS}} d_n.$$

3.3.6 Objective

The objective of the MDP model is to minimize the total cost, including immediate cost and discounted future cost. The optimality equations are:

$$V(s) = \inf_{a \in A_s} \left\{ c(s, a) + \sum_{j \in S} \beta P(j | s, a) V(j) \right\}, \forall s \in S \quad (3.2)$$

where $V(s)$ is the value (total cost) at state s , and β is the discount rate.

3.4 SOLVING THE MDP MODEL

We present here the steps of the policy iteration [71], which is a commonly used method for solving MDPs:

Step 1: Set $i = 0$, and select an initial decision rule $a_s^0, \forall s \in \{\{s_N\} \cup S_C \cup \{s_B\}\}$.

Step 2: Obtain V^i by solving

$$(I - \beta P(a^i))V^i = c(a^i).$$

Step 3: For all $s \in \{\{s_N\} \cup S_C \cup \{s_B\}\}$, choose a_s^{i+1} to satisfy

$$a_s^{i+1} \in \operatorname{argmin} \{c(a_s^{i+1}) + \beta P_{a_s^{i+1}}(\cdot|s)V^i\},$$

setting $a_s^{i+1} = a_s^i$ if possible.

Step 4: If $a_s^{i+1} = a_s^i, \forall s \in \{\{s_N\} \cup S_C \cup \{s_B\}\}$, stop and set $a_s^* = a_s^i, \forall s \in \{\{s_N\} \cup S_C \cup \{s_B\}\}$. Otherwise increment i by 1 and return to Step 2.

In this algorithm, I is the identity matrix, a^i is the action vector for all states in iteration i , $c(a^i)$ is the immediate cost vector for all states given action vector a^i , V^i is the value vector for all states in iteration i , and $P(a^i)$ is the transition probability matrix given action vector a^i . The value vector V^i is updated in Step 2, but is treated as a constant vector in the policy improvement Step 3.

Since the action space for each state $s \in \{\{s_N\} \cup S_C\}$ is a polyhedron, the decision improvement in Step 3 cannot be done by enumerating all infinitely many possible actions as in the case with a finite discrete action space, thus an optimization problem needs to be solved in Step 3 for each state $s \in \{\{s_N\} \cup S_C\}$. In the following sections, the optimization problems are derived and structured as two-stage stochastic programs with convex quadratic objective functions and binary variables. Extensive forms of the stochastic programs can be solved by a Cplex [3] solver.

3.4.1 Solving Step 3 in Policy Iteration for the Normal State s_N

For the normal state s_N , the optimization problem is:

$$\begin{aligned}
\min_{q, d, v, v_{\max}} \quad & V^{i+1}(s_N) = \sum_{n \in \mathcal{S}} \left(a_n q_n + \frac{1}{2} b_n q_n^2 \right) + \sum_{n \in \mathcal{D}} c_n^{\text{LS}} d_n \\
& + \beta P(s_N | s_N) V^i(s_N) + \beta \sum_{s \in S_C} P(s | s_N, v_{\max}^s) V^i(s) + \beta P(s_B | s_N, v_{\max}^s) V^i(s_B) \\
\text{s. t.} \quad & \pm \left[\sum_{n \in \mathcal{S}} H_{l,n} q_n - \sum_{n \in \mathcal{D}} H_{l,n} (D_n - d_n) \right] \leq T_l, \quad \forall l \in \mathcal{L} \\
& \pm \left[\sum_{n \in \mathcal{S}} H_{l,n}^s q_n - \sum_{n \in \mathcal{D}} H_{l,n}^s (D_n - d_n) \right] \leq (1 + v_l^s) T_l, \quad \forall l \in \mathcal{L}_s, \forall s \in S_C \\
& \sum_{n \in \mathcal{S}} q_n = \sum_{n \in \mathcal{D}} (D_n - d_n) \\
& v_l^s \leq v_{\max}^s, \quad \forall l \in \mathcal{L}_s, \forall s \in S_C; \\
& 0 \leq q_n \leq \bar{Q}_n, \forall n \in \mathcal{S}; d_n \geq 0, \forall n \in \mathcal{D}; v_l^s \geq 0, \forall l \in \mathcal{L}_s, \forall s \in S_C; v_{\max}^s \geq 0, \forall s \in S_C.
\end{aligned}$$

Here v_l^s calculates the percentage of thermal limit violation on line l caused by the failure of line s , and v_{\max}^s is the maximum of such percentages on all working line $l \in \mathcal{L}_s$. The state values $V^i(s)$ for all $s \in \{\{s_N\} \cup S_C \cup \{s_B\}\}$ from the last iteration i are treated as constants. This formulation can be equivalently simplified by substituting v_l^s with v_{\max}^s for all $l \in \mathcal{L}_s, s \in S_C$ and then replacing v_{\max}^s with a simpler notation v^s :

$$\begin{aligned}
\min_{q, d, v} \quad & V^{i+1}(s_N) = \sum_{n \in \mathcal{S}} \left(a_n q_n + \frac{1}{2} b_n q_n^2 \right) + \sum_{n \in \mathcal{D}} c_n^{\text{LS}} d_n \\
& + \beta P(s_N | s_N) V^i(s_N) + \beta \sum_{s \in S_C} P(s | s_N, v^s) V^i(s) + \beta P(s_B | s_N, v^s) V^i(s_B) \\
\text{s. t.} \quad & \pm \left[\sum_{n \in \mathcal{S}} H_{l,n} q_n - \sum_{n \in \mathcal{D}} H_{l,n} (D_n - d_n) \right] \leq T_l, \quad \forall l \in \mathcal{L} \\
& \pm \left[\sum_{n \in \mathcal{S}} H_{l,n}^s q_n - \sum_{n \in \mathcal{D}} H_{l,n}^s (D_n - d_n) \right] \leq (1 + v^s) T_l, \quad \forall l \in \mathcal{L}_s, \forall s \in S_C \\
& \sum_{n \in \mathcal{S}} q_n = \sum_{n \in \mathcal{D}} (D_n - d_n) \\
& 0 \leq q_n \leq \bar{Q}_n, \forall n \in \mathcal{S}; d_n \geq 0, \forall n \in \mathcal{D}; v^s \geq 0, \forall s \in S_C.
\end{aligned}$$

In this stochastic program, \mathbf{q} and \mathbf{d} are the first stage variables representing *a priori* contingency dispatch decisions, whereas \mathbf{v} can be perceived as the second stage variables representing post contingency percentage violations. The definition of the transition probabilities in the objective function contains the piecewise linear function $f(\cdot)$, which can be formulated by using the standard SOS-2 (special order set constraint of type 2) technique [32, 36]. The piecewise linear function

$$f(v) = \begin{cases} 2.5v & 0 \leq v \leq 0.4, \\ 1 & v > 0.4. \end{cases}$$

can be modeled as:

$$\begin{aligned} v &= 0.4(1 - u_1 - u_2) + Mu_2 \\ f(v) &= 1 - u_1 \\ u_1 &\leq w \\ u_2 + w &\leq 1 \\ u_1, u_2 &\geq 0, w \in \{0, 1\}, \end{aligned}$$

where v plays the role of $\max\{\mathbf{v}\}$ in (3.1), and M is a sufficiently large number. By substituting the transition probabilities and the $f(\cdot)$ function, we can rewrite the stochastic programs as the following:

$$\begin{aligned}
\min_{q,d,u,w} \quad & V^{i+1}(s_N) = \sum_{n \in \mathcal{S}} \left(a_n q_n + \frac{1}{2} b_n q_n^2 \right) + \sum_{n \in \mathcal{D}} c_n^{\text{LS}} d_n \\
& + \beta \sum_{s \in S_C} \left\{ u_1^s \prod_{l \in \mathcal{L} \setminus s} e^{-\lambda_l} (1 - e^{-\lambda_s}) [V^i(s) - V^i(s_B)] \right\} + v_c \\
\text{s. t.} \quad & \pm \left[\sum_{n \in \mathcal{S}} H_{l,n} q_n - \sum_{n \in \mathcal{D}} H_{l,n} (D_n - d_n) \right] \leq T_l, \quad \forall l \in \mathcal{L} \\
& \pm \left[\sum_{n \in \mathcal{S}} H_{l,n}^s q_n - \sum_{n \in \mathcal{D}} H_{l,n}^s (D_n - d_n) \right] \leq [1 + 0.4(1 - u_1^s - u_2^s) + M u_2^s] T_l, \quad \forall l \in \mathcal{L}_s, \forall s \in S_C \\
& \sum_{n \in \mathcal{S}} q_n = \sum_{n \in \mathcal{D}} (D_n - d_n) \\
& u_1^s \leq w^s, \quad \forall s \in S_C \\
& u_2^s + w^s \leq 1, \quad \forall s \in S_C \\
& 0 \leq q_n \leq \bar{Q}_n, \quad \forall n \in \mathcal{S}; \quad d_n \geq 0, \quad \forall n \in \mathcal{D}; \quad u_1^s, u_2^s \geq 0, w^s \in \{0, 1\}, \quad \forall s \in S_C,
\end{aligned} \tag{3.3}$$

where v_c is a constant term that appears in the objective function but does not affect the optimal solution. When it appears in other formulations of this chapter, v_c may or may not represent the same value of constant.

In this formulation, the binary variable w^s indicates whether ($w^s = 0$) or not ($w^s = 1$) the type (a) failure (defined in Section 3.2.5) of transmission line s will *surely* result in a cascading failure. If $w^s = 1$, the probability of a cascading failure is calculated by $1 - u_1^s$. A lower bound of M can be obtained as:

$$M \geq \frac{\sum_{n \in \mathcal{D}} D_n}{\min_{l \in \mathcal{L}} \{T_l\}}.$$

Any value above this bound can guarantee the validity of the formulation, since the maximal percentage of violation $\max\{\mathbf{v}\}$ is bounded by the largest possible amount of power flow $\sum_{n \in \mathcal{D}} D_n$ divided by the minimal thermal limit $\min_{l \in \mathcal{L}} \{T_l\}$.

3.4.2 Solving Step 3 in Policy Iteration for Other States

For a contingency state $s \in S_C$, the optimization problem is:

$$\begin{aligned}
\min_{q,d,v} \quad & V^{i+1}(s) = \sum_{n \in \mathcal{S}} \left(a_n q_n + \frac{1}{2} b_n q_n^2 \right) + \sum_{n \in \mathcal{D}} c_n^{\text{LS}} d_n \\
& + \beta P(s_N | s) V^i(s_N) + \beta \sum_{k \in S_C} P(k | s, v^k) V^i(k) + \beta P(s_B | s, v) V^i(s_B) \\
\text{s. t.} \quad & \pm \left[\sum_{n \in \mathcal{S}} H_{l,n}^s q_n - \sum_{n \in \mathcal{D}} H_{l,n}^s (D_n - d_n) \right] \leq T_l, \quad \forall l \in \mathcal{L}_s \\
& \pm \left[\sum_{n \in \mathcal{S}} H_{l,n}^k q_n - \sum_{n \in \mathcal{D}} H_{l,n}^k (D_n - d_n) \right] \leq (1 + v^k) T_l, \quad \forall l \in \mathcal{L}_s \setminus k, \forall k \in S_C \setminus s \\
& \sum_{n \in \mathcal{S}} q_n = \sum_{n \in \mathcal{D}} (D_n - d_n) \\
& 0 \leq q_n \leq \bar{Q}_n, \forall n \in \mathcal{S}; \quad d_n \geq 0, \forall n \in \mathcal{D}; \quad v^k \geq 0, \forall k \in S_C \setminus s.
\end{aligned}$$

Similar to Section 3.4.1, this stochastic programs can be rewritten by substituting the transition probabilities and the $f(\cdot)$ function as the following:

$$\begin{aligned}
\min_{q,d,u,w} \quad & V^{i+1}(s) = \sum_{n \in \mathcal{S}} \left(a_n q_n + \frac{1}{2} b_n q_n^2 \right) + \sum_{n \in \mathcal{D}} c_n^{\text{LS}} d_n \tag{3.4} \\
& + \beta \sum_{k \in S_C \setminus s} \left\{ u_1^k \prod_{j \in \mathcal{L} \setminus \{k, s\}} e^{-\lambda_j} (1 - e^{-\mu_s}) (1 - e^{-\lambda_k}) [V^i(k) - V^i(s_B)] \right\} + v_c \\
\text{s. t.} \quad & \pm \left[\sum_{n \in \mathcal{S}} H_{l,n}^s q_n - \sum_{n \in \mathcal{D}} H_{l,n}^s (D_n - d_n) \right] \leq T_l, \quad \forall l \in \mathcal{L}_s \\
& \pm \left[\sum_{n \in \mathcal{S}} H_{l,n}^k q_n - \sum_{n \in \mathcal{D}} H_{l,n}^k (D_n - d_n) \right] \leq [1 + 0.4(1 - u_1^k - u_2^k) + M u_2^k] T_l, \\
& \quad \quad \quad \forall l \in \mathcal{L}_s \setminus k, \forall k \in S_C \setminus s \\
& \sum_{n \in \mathcal{S}} q_n = \sum_{n \in \mathcal{D}} (D_n - d_n) \\
& u_1^k \leq w^k, \quad \forall k \in S_C \setminus s \\
& u_2^k + w^k \leq 1, \quad \forall k \in S_C \setminus s \\
& 0 \leq q_n \leq \bar{Q}_n, \forall n \in \mathcal{S}; \quad d_n \geq 0, \forall n \in \mathcal{D}; \quad u_1^k, u_2^k \geq 0, w^k \in \{0, 1\}, \forall k \in S_C \setminus s.
\end{aligned}$$

For the blackout state s_B , the action affects neither the transition probability nor the immediate cost, thus no optimization problem needs to be solved.

3.4.3 Convergence of the Policy Iteration Algorithm

For an MDP with a finite state space and a finite action space, the policy iteration has been proved to converge finitely (Theorem 6.4.2 in [71]). However, the proposed model has a continuous action space, thus in general the policy iteration algorithm may not converge. An alternative theorem establishes the convergence of policy iteration for arbitrary state and action spaces under the assumption that there is a minimizing decision rule at each value vector V [71]:

Theorem 1. (*Theorem 6.4.6 in [71]*)

The sequence of value vectors $\{V^i\}$ generated by policy iteration converges monotonically and in norm to $\{V_\beta^\}$, which solves the optimality equation (3.2).*

It is mentioned on page 180 in [71] that Theorem 1 holds for models with action space A_s compact, transition probability matrix $P(j|s, a)$ and immediate cost function $c(s, a)$ continuous in a for each $s \in S$, and S either finite or compact. It can be confirmed from Section 3.3 that the action space A_s is compact, transition probability $P(j|s, a)$ and immediate cost $c(s, a)$ are continuous in a for each $s \in \{\{s_N\} \cup S_C \cup \{s_B\}\}$, and the state space $\{\{s_N\} \cup S_C \cup \{s_B\}\}$ is finite. Therefore, the convergence of policy iteration for this model can be established.

Corollary 1. *As long as stochastic programs (3.3) and (3.4) are solved to optimality, the sequence of value vectors $\{V^i\}$ generated by the policy iteration in Section 3.4 converges monotonically and in norm to $\{V_\beta^*\}$, which solves the optimality equation (3.2).*

3.5 A NUMERICAL EXAMPLE

Figure 9 shows a five-bus network example from the website (<http://www.pjm.com>) of PJM (Pennsylvania–New Jersey–Maryland Interconnection), which is a regional transmission organization (RTO) in the eastern United States that operates the world’s largest competitive wholesale electricity market. In Figure 9, a ‘G’ in a circle represents a generator, and an arrow represents demand. In this example, $\mathcal{N} = \{A, B, C, D, E\}$, $\mathcal{D} = \{B, C, D\}$, $\mathcal{S} = \{A, C, D, E\}$, $\mathcal{L} = \{A-B, B-C, C-D, D-E, E-A, A-D\}$. Node and transmission line data are given in Tables 12 and 13. Discount rate β is set to be 0.99.

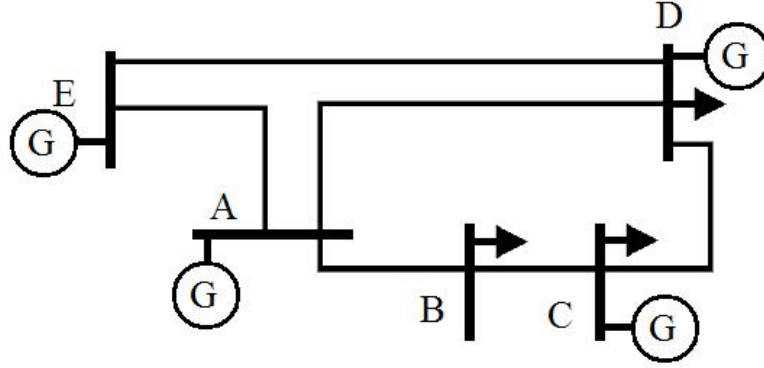


Figure 9: A five-bus test example

Table 12: Node data for a five-bus example

n	D_n	a_n	b_n	\overline{Q}_n
A	–	7	0.0452	210
B	250	–	–	–
C	350	13.51	0.0700	520
D	250	15	0.1210	200
E	–	9	0.0920	600

Table 13: Transmission line data for a five-bus example

line	resistance	reactance	thermal limit	MTTF	MTTR
	R (Ω)	X (Ω)	(MW)	(Hour)	(Hour)
A-B	0	0.0281	377	18015	43
B-C	0	0.0108	77	6924	17
C-D	0	0.0297	223	19041	46
D-E	0	0.0297	240	19041	46
E-A	0	0.0064	360	4103	10
A-D	0	0.0304	159	19490	47

Policy iteration is implemented in Matlab [4] and Cplex [3]. We present the results of this example and answer the following questions.

- **How is the initial decision rule determined?**

The initial decision rule (in Step 1 of policy iteration) is obtained by solving the non-security constrained economic dispatch for all $s \in \{\{s_N\} \cup S_C \cup \{s_B\}\}$:

$$\begin{aligned}
\min_{q,d} \quad & \sum_{n \in \mathcal{S}} \left(a_n q_n + \frac{1}{2} b_n q_n^2 \right) + \sum_{n \in \mathcal{D}} c_n^{\text{LS}} d_n \\
\text{s. t.} \quad & \pm \left[\sum_{n \in \mathcal{S}} H_{l,n}^s q_n - \sum_{n \in \mathcal{D}} H_{l,n}^s (D_n - d_n) \right] \leq T_l, \quad \forall l \in \mathcal{L}_s \\
& \sum_{n \in \mathcal{S}} q_n = \sum_{n \in \mathcal{D}} (D_n - d_n) \\
& 0 \leq q_n \leq \bar{Q}_n, \quad \forall n \in \mathcal{S}; \quad d_n \geq 0, \quad \forall n \in \mathcal{D}.
\end{aligned}$$

The objective here is only to minimize the immediate cost, ignoring the future cost. The initial generation decisions at the normal state s_N and the contingency state $s = \{\text{A-B}\}$ for the 24-hour period are shown in Figures 10 and 11, respectively.

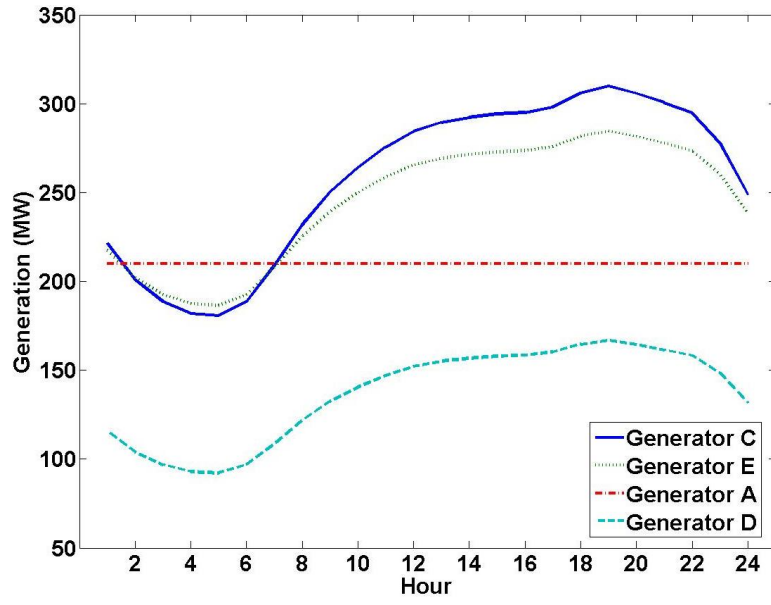


Figure 10: Initial generation decisions for s_N

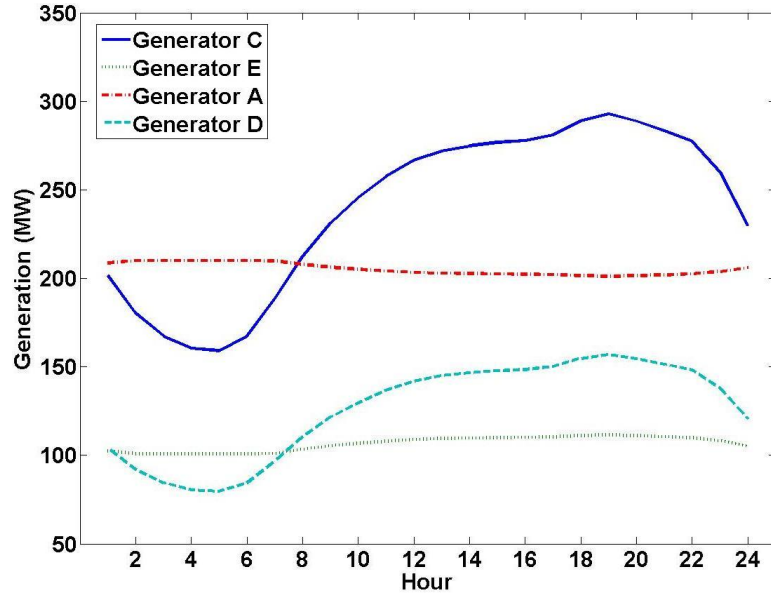


Figure 11: Initial generation decisions for $s = \{A-B\}$

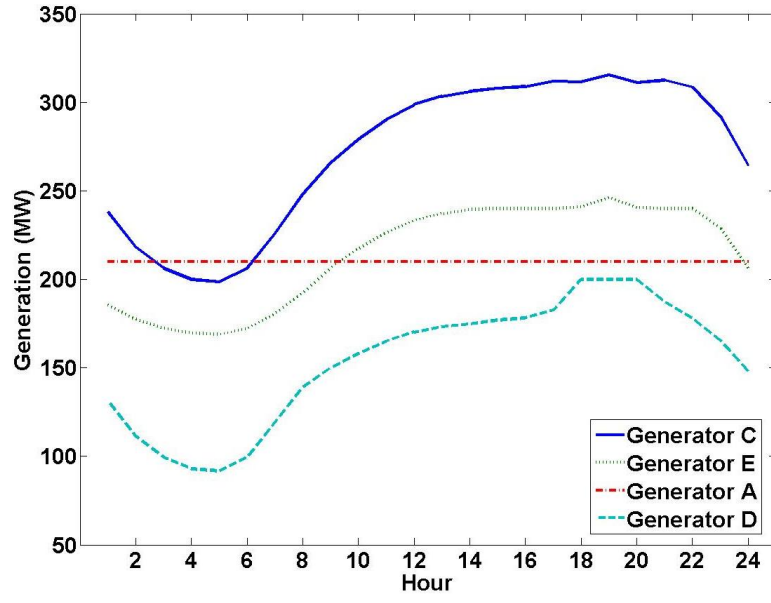


Figure 12: Optimal generation decisions for s_N

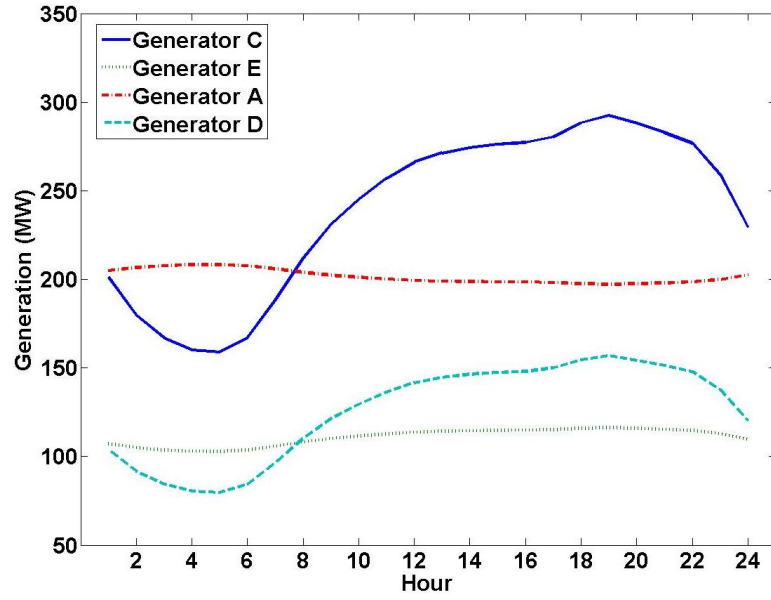


Figure 13: Optimal generation decisions for $s = \{A-B\}$

- **How fast does the policy iteration algorithm converge?**

The algorithm converges in two iterations within a few seconds. The optimal generation decisions at the normal state s_N and the contingency state $s = \{A-B\}$ for the 24-hour period are shown in Figures 12 and 13, respectively.

Compared to the initial generation decisions, the optimal ones at the normal state use generators C and D more, but use generator E less. This is because generator E depends on transmission lines to supply, which has some risk that the optimal generation decisions are trying to avoid. The optimal generation decisions at the contingency state $s = \{A-B\}$ have similar changes over the initial ones, but the differences are very small. This is because the failure of line $\{A-B\}$ has already reduced the use of generator E significantly even in the non-security constrained economic dispatch.

- **How are the values of the initial decisions and N-1 criterion evaluated?**

The values of the initial decisions and N-1 criterion are evaluated by solving the linear system of equations given in Step 2 of the policy iteration, where the action a^i is obtained using the initial dispatch decision and N-1 criterion, respectively.

- **How much improvement do the optimal decisions have over the initial decisions and the N-1 criterion?**

The comparison of total costs between optimal and initial decisions are given for the normal state s_N and the contingency state $s = \{A-B\}$ in Figure 14. The N-1 criterion, as has been explained, requires that the system withstands any single line failure. From the comparison of total costs between optimal decisions and N-1 criterion in Figure 15, we can see that the expected total cost of the optimal decisions is significantly less (in the order of million dollars) than that of the N-1 criterion.

For the normal state s_N , we also compare the probability that a system is in each of the possible states in Table 14, and the expected total cost of being in each of the possible states in Table 15. The stationary probability is obtained by solving the following equation

$$\pi^\top P(a^*) = \pi^\top,$$

where π is the stationary probability vector, while $P(a^*)$ is the transition probability matrix under the optimal policy a^* . The stationary cost is given by the optimal solution

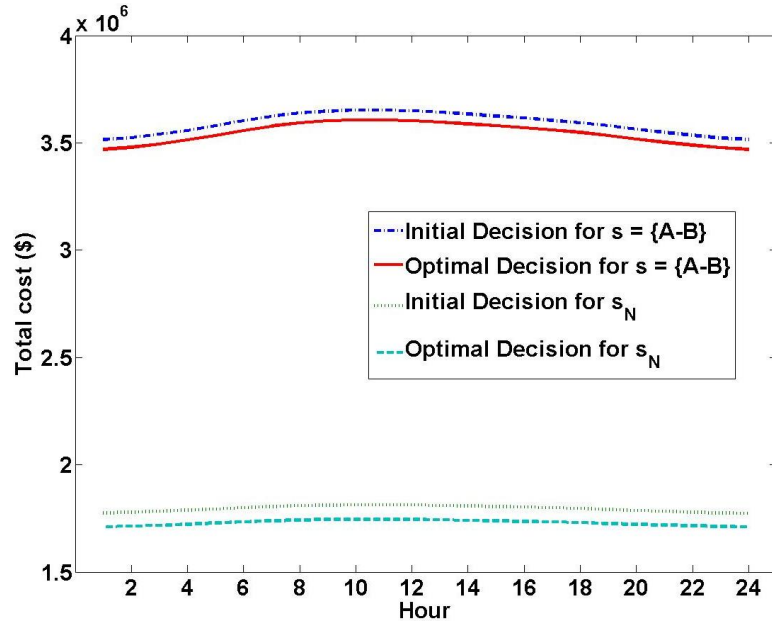


Figure 14: Total cost comparisons between optimal and initial decisions

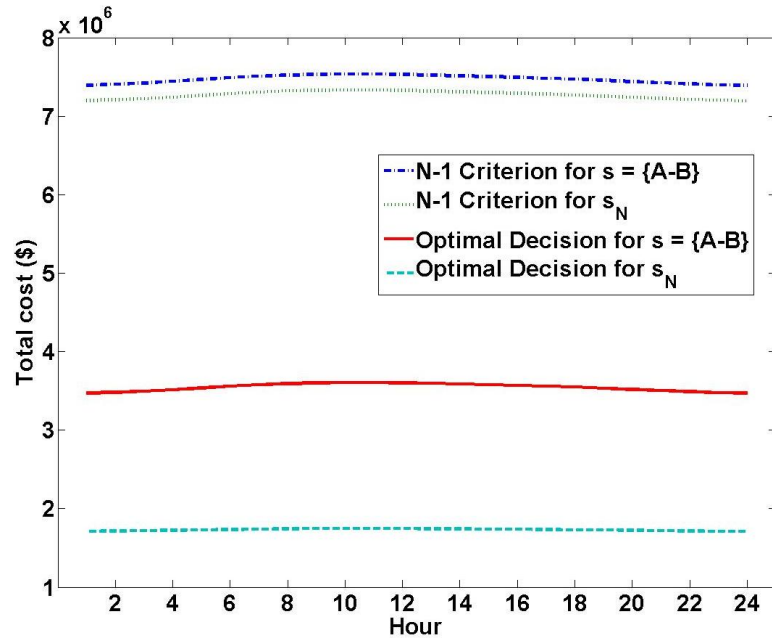


Figure 15: Total cost comparisons between optimal decision and N-1 criterion

Table 14: Comparisons of state probabilities for the normal state s_N

	Normal	A-B	B-C	C-D	D-E	E-A	A-D	Blackout
Initial	0.917	0.012	0.002	0.014	0.014	0.002	0.016	0.023
MDP	0.918	0.012	0.002	0.015	0.015	0.002	0.016	0.020
N-1	0.918	0.014	0.002	0.015	0.015	0.002	0.016	0.018

Table 15: Comparisons of state costs (in $\$10^6$) for the normal state s_N

	Normal	A-B	B-C	C-D	D-E	E-A	A-D	Blackout
Initial	1.796	3.590	1.831	1.906	1.911	1.807	1.908	10.830
MDP	1.796	3.590	1.831	1.906	1.911	1.807	1.908	10.830
N-1	7.269	7.470	6.493	7.392	7.482	7.288	7.486	14.535

of the state value V^* to the MDP model. It can be seen from Tables 14 and 15 that the MDP solution is almost as cost efficient as the initial economic dispatch solution, but it also has a security level almost as high as the N-1 criterion. Therefore, the long-term expected cost for the MDP solution outperforms both of the other approaches, as is confirmed in Table 16.

Table 16: Comparisons of expected long-term costs for the normal state s_N

	Long-term Expected Cost
Initial	$2.0326 \times 10^6 \$$
MDP	$2.0062 \times 10^6 \\$
N-1	$7.4101 \times 10^6 \$$

3.6 CONCLUSION

We have introduced a Markov Decision Process model for the security constrained economic dispatch problem. This approach quantitatively takes the cascading failure into modeling consideration, and minimizes the long-term expected total cost. The optimal solution of the model provides the cost-minimizing decision rules not only for the normal state but also for all contingency states. The numerical example demonstrates the advantage of this model over non-security constrained economic dispatch and N-1 criterion.

4.0 OLIGOPOLY MODELS FOR MARKET PRICE OF ELECTRICITY UNDER DEMAND UNCERTAINTY AND UNIT RELIABILITY

4.1 INTRODUCTION

In the new deregulated environment, the price of electricity is no longer set by regulators; instead it is set by market forces. Since investment and operating decisions will be made based on the anticipated prices, there is a strong interest in modeling them using available engineering and economic information [78]. In the recent literature, three oligopoly models (together with their various variants and extensions) have been proposed to depict the behavior of market prices. These are the Bertrand, Cournot, and SFE models [12, 33, 40, 75]. For the most part, with the exception of the SFE, these models are deterministic. The electricity price, however, depends on a variety of physical and economic factors, many of which are stochastic by nature. The physical factors include production cost, load, generation and transmission reliability, unit commitment, and transmission constraints. The economic factors include strategic bidding and load elasticity. In this chapter, we enhance the oligopoly models by incorporating the stochasticity associated with the load and the generation availabilities. We obtain the Nash equilibrium solutions for the Cournot and SFE models, in which generating firms compete with each other to maximize their own expected profits. The current literature on these models primarily considers random factors on the demand side, but it does not consider random factors present in the supply side of the market [40, 59].

In their elegant formulation of the SFE, Klemperer and Meyer [59] consider a stochastic demand function by assuming that the quantity demanded is a function of both the price p and a scalar random variable ϵ . Thus, the demand function is represented by $D(p, \epsilon)$. Under the assumption that the second partial derivative $D_{p\epsilon} = 0$, they express the Nash

equilibrium solution in terms of differential equations. Their solution does not apply without this condition or when there are uncertainties associated with the supply side such as fuel prices and production cost functions. Our contribution is to include some of these sources of uncertainties in the oligopoly models for electricity prices. We conjecture that when these sources of uncertainties are included, a supply function equilibrium as general as that of Klemperer and Meyer may not exist. Cournot model can be seen as a restricted special case of SFE. Using the best response function, our approach obtains the Nash Cournot equilibrium solution, taking into account both demand and supply side uncertainties.

Theoretical research and computational studies on SFE models have shown considerable difficulties in computing equilibrium solutions [12, 40, 59]. In fact, multiple equilibrium solutions may exist, which carry additional equilibrium selection problem. Thus, most of the SFE studies have been designed assuming a linear supply function [41, 42, 74]. Klemperer and Meyer [59] have shown that in the special case of symmetric firms with linear marginal costs and random shock with full support ($\epsilon \geq 0$), a unique equilibrium solution exists, and this solution is a linear function. If the random shock does not have full support, which is a more realistic assumption, the linear supply function is not the unique equilibrium. Nevertheless, according to Green [41], a linear supply function is more tractable and for low levels of demand, it can be seen as an approximation to a set of equilibrium supply functions. The assumption of linear supply functions has been used in Green [42] to study the effects of the contract market on a pool market. It has also been used by Rudkevich [74] in his investigation of the bidding learning process. The learning model consists of generating companies adjusting their supply functions as aggregated-bid information on the market is revealed. Rudkevich shows that if the initial supply functions submitted by the firms are based on their marginal costs, the sequence of supply functions converges to a linear SFE. In this chapter, we have thus restricted ourselves to linear supply functions and attempted to obtain an equilibrium solution for this class (LSFE).

The numerical examples given here are based on a linear demand function with multiple asymmetric firms. Our model assumes that the transmission grid is free of congestion. In the Cournot model, adding transmission constraints to the market models would involve solving a mixed complementarity problem [51]. These constraints in conjunction with supply and

demand uncertainties would make the models hard to solve. A similar difficulty would occur with the SFE model. Our assumption is reasonable under low demand conditions (off-peak hours) during which the power system remains unconstrained by congested lines. We use best response function approach to obtain the Nash Cournot equilibrium, and nonlinear optimization for LSFE.

Section 4.2 states the assumptions used to represent the supply and demand sides for the electricity market. Section 4.3 provides the derivation of the Nash Cournot equilibrium under the stochastic setup. Section 4.4 gives the corresponding approach for the LSFE model. Section 4.5 gives numerical examples for a market consisting of three asymmetric firms. We compare here the results of the mean and standard deviation of equilibrium prices, profits, and the quantities supplied under these two models. As an added comparison, we also provide the corresponding statistics resulting from the perfect SFE and Bertrand models. Section 4.6 concludes this chapter.

4.2 ASSUMPTIONS AND OBJECTIVES FOR THE STOCHASTIC MODELS

This chapter considers the following decision situation in the face of uncertainty. A commitment is being made at some point in time (either to quantity, in the case of the Cournot model, or to the slope and intercept of the bid curve in the case of the SFE model), before the bidder knows the exact load level or generator availabilities. For example, assume that bids are taken hour by hour, and the commitment is “day ahead” (such as 12 noon the previous day, as in the PJM market [www.pjm.com]). The load uncertainty is due to errors in the short term load forecasts (typically with a standard deviation of 2-5% [8, 9]). The generator availability uncertainty is about generators that are currently available, but might have a forced outage between the time of making the bid and 24 hours away. We have obtained the appropriate estimates of generator availabilities using the failure and repair rates given for the IEEE Reliability Test System [43] and using the Markov process assumption as described in the following paragraph.

We assume that there are n competing asymmetric firms with firm i having $N_i - 1$ units available for production. The capacity of the j^{th} unit, $j = 1, \dots, N_i - 1$ of firm i is represented by c_{ij} . To account for a firm's ability to purchase energy at a higher cost from an outside source, we define an N_i^{th} unit which represents this available source. As a result, we assume $c_{iN_i} = \infty, \forall i = 1, \dots, n$. We assume that each firm's units are dispatched according to their constant marginal cost, which is represented by d_{ij} . The operating state of generator j for firm i at time t is denoted by a two-state stochastic process $Y_{ij}(t)$ that takes the value 1 when the unit is up and 0 otherwise. For the purpose of the numerical examples given in Section 4.5, we will assume that this process is a continuous time Markov chain with a failure rate λ_{ij} and a repair rate μ_{ij} . The steady state availability of the unit which we denote by p_{ij} is given by

$$p_{ij} = P[Y_{ij}(\infty) = 1] = \frac{\mu_{ij}}{\lambda_{ij} + \mu_{ij}}.$$

We will abbreviate $Y_{ij}(\infty)$ by Y_{ij} , thus we have $P[Y_{ij} = 1] = p_{ij}$. We assume $p_{iN_i} = 1$. That is, the outside source is always available. We also assume that the Y_{ij} 's and the load L are independent. It is well known [60] that under the Markov assumption,

$$p_{ij}(t) \equiv P[Y_{ij}(t) | Y_{ij}(0) = 1] = \frac{\mu_{ij}}{\lambda_{ij} + \mu_{ij}} + \frac{\lambda_{ij}}{\lambda_{ij} + \mu_{ij}} e^{-(\lambda_{ij} + \mu_{ij})t}.$$

Thus the average availability during the interval $[0, T]$ given that the unit (i, j) was up at time 0 is given by

$$\begin{aligned} \bar{p}_{ij}(T) &= \frac{1}{T} \int_0^T \left[\frac{\mu_{ij}}{\lambda_{ij} + \mu_{ij}} + \frac{\lambda_{ij}}{\lambda_{ij} + \mu_{ij}} e^{-(\lambda_{ij} + \mu_{ij})t} \right] dt \\ &= \frac{\mu_{ij}}{\lambda_{ij} + \mu_{ij}} + \frac{1}{T} \frac{\lambda_{ij}}{(\lambda_{ij} + \mu_{ij})^2} [1 - e^{-(\lambda_{ij} + \mu_{ij})T}]. \end{aligned}$$

In Section 4.5, the first example uses the steady-state availability term p_{ij} whereas the second one gives results for day ahead bids using the quantity $\bar{p}_{ij}(T)$ for the average availability where $T = 24$ hours.

We assume a constant marginal cost for each generating unit (i, j) . This results in a piecewise linear production cost function for each firm i . Our model also makes several simplifying assumptions. First, it does not consider unit commitment. Uncertainty in load by itself (due to 24 hour-ahead load forecast error) can make an important difference in

unit commitment. Wrong unit commitments can have negative economic consequences [52]. Uncertainty in generator availability would certainly magnify this effect. The zero-one nature of commitment, along with minimum run levels and ramp rates, may make it impossible to stack units in merit order. Secondly, we have assumed that if a firm commits one of its generators to provide a specified quantity ahead, but one of its own generators fails, it will access the balancing market if its quantity commitment is greater than the sum of their available capacities, and the cost for this transaction is fixed. But, in reality, it will go into the real time market and buy at the prevailing market price to make up for the shortfall. This may be a price that is quite low, or it might be very high if the system is in a shortage state. Also, if the balancing energy prices are below the generating costs, the firm will surely opt to access the market even if it has ample generation. Inclusion of this exogenous factor will make our model complicated, and we do not consider this here.

At price P , the actual demand function $Q = D(L, P)$ is a random variable, where the load L is the source of uncertainty. It is assumed that L has a known probability distribution. Each firm will select its bid to maximize its expected profit. We describe this process in detail and provide Nash equilibrium solution for each of the bidding models.

4.3 COURNOT MODEL

In the Cournot model, we assume $\frac{\partial D(L, P)}{\partial P} < 0$ and denote the inverse function of $D(L, P)$ as $P(L, D)$. In this model, each firm simultaneously bids a quantity q_i that it is willing to supply. Notice that q_i is an MWh variable, and it represents the firm amount of generation that the firm commits itself to. The market clearing price P^* is determined after the actual demand is observed. We denote the market clearing price P^* as the price where $D(l, P^*) = \sum_{i=1}^n q_i$ or $P^* = P(l, \sum_{i=1}^n q_i)$, where l is the realization of L . We assume that if $P^* < 0$, no trade is made.

Firms choose their bids q_i in order to maximize their expected profits. Given the sum of other firms' bids q_{-i} , the profit of firm i is a function of q_i :

$$\pi_i(q_i \mid q_{-i}) = q_i P(L, q_{-i} + q_i)^+ - \text{Cost}_i(q_i),$$

where $\text{Cost}_i(q_i)$ is the cost for firm i to produce the quantity of q_i , and $P(L, q_{-i} + q_i)^+ := \max\{P(L, q_{-i} + q_i), 0\}$. Clearly, the cost is a random variable due to uncertainty resulting from supply side unit availabilities. Therefore, each firm's objective is to select a q_i to maximize its expected profit, which is the expected revenue less the expected costs:

$$E[\pi_i(q_i \mid q_{-i})] = q_i \int_{-\infty}^{\infty} P(l, q_{-i} + q_i)^+ f(l) dl - E_Y[\text{Cost}_i(q_i)]. \quad (4.1)$$

where $E_Y[\cdot]$ indicates that expectation is taking in terms of random variable Y .

For ease of exposition, we assume that $D(L, P)$ is a linear function, i.e. $Q = D(L, P) = L - mP$ for a constant $m > 0$, and then $P(L, Q) = \frac{(L-Q)}{m}$. We assume that L is uniformly distributed on $[L_1, L_2]$. This assumption allows us to obtain closed form expressions for the solutions of the integrals that appear in the computations, although the basic idea of the approach also applies to more general distributions (In the literature, the normal distribution has been considered to be more representative of actual forecast errors). Assuming further that $L_2 > Q$, we can directly compute the expected revenue

$$q_i \int_{-\infty}^{\infty} P(l, q_{-i} + q_i)^+ f(l) dl = q_i \frac{[L_2 - \max(L_1, q_{-i} + q_i)][L_2 + \max(L_1, q_{-i} + q_i) - 2(q_{-i} + q_i)]}{2m(L_2 - L_1)}.$$

To aid in the computation of a firm's expected cost, we define the following expression:

$$C_{i,j}(q) := \begin{cases} E_Y[\text{Cost}_i(q)] & \text{if } j = 1, \\ E_Y[\text{Cost}_i(q) \mid Y_{ik} = 0, \text{ for } k = 1, \dots, j-1] & \text{for } j = 2, \dots, N_i. \end{cases}$$

Here $C_{ij}(q)$ represents the expected cost of firm i producing q units of energy when generating units $1, \dots, j-1$ are not available. Then we have

$$C_{i,N_i}(q) = qd_{iN_i},$$

and for $k = 1, 2, \dots, N_i - 1$, we obtain the following recursive relationship:

$$C_{i,j}(q) = \begin{cases} p_{ij}d_{ij}q + (1 - p_{ij})C_{i,j+1}(q) & 0 \leq q \leq c_{ij}; \\ p_{ij}\{d_{ij}c_{ij} + C_{i,j+1}(q - c_{ij})\} + (1 - p_{ij})C_{i,j+1}(q) & q > c_{ij}. \end{cases}$$

Therefore, $C_{i,j}(\cdot)$ is a piecewise linear function and $E_Y[Cost_i(q_i)] = C_{i,1}(q_i)$ can be calculated recursively. We then rewrite the expected profit function as

$$E[\pi_i(q_i | q_{-i})] = q_i \int_{-\infty}^{\infty} P(l, q_{-i} + q_i)^+ f(l) dl - E_Y[Cost_i(q_i)] =: R_i(q_i | q_{-i}) - C_{i,1}(q_i).$$

Here, the term $R_i(q_i | q_{-i})$ is the expected revenue function and the $C_{i,1}(q_i)$ is the expected production costs. Equation (4.1) is the expected profit given the total bid of the other firms. The best response for firm i is to bid a quantity q_i^* in order to maximize (4.1). Therefore, q_i^* is a function of q_{-i} , in other words, if firm i observes the other firms' total bids q_{-i} , then $q_i^*(q_{-i})$ is its optimal bid. Thus $q_i^*(\cdot)$ is the best response function for firm i . We can further derive the best response function in terms of $Q = q_{-i} + q_i^*(q_{-i})$, so $q_i^*(Q) = q_i^*[q_{-i} + q_i^*(q_{-i})]$. It means that if the market total bid is Q , then firm i must have bid $q_i^*(Q)$. Under the uniform distribution assumption of load uncertainty L , best response functions $q_i^*(q_{-i})$ and $q_i^*(Q)$ are piecewise linear and can be analytically obtained. Then the Nash Cournot equilibrium outcome Q^* can be either determined analytically by the solution to $Q = \sum_{i=1}^n q_i^*(Q)$, or graphically by the intersection of $q(Q) = \sum_{i=1}^n q_i^*(Q)$ and the 45 degree line $q(Q) = Q$. Each firm's bid under equilibrium is then determined by their best response functions $q_i^* = q_i^*(Q^*)$. The computations are further described by means of an illustration in Section 4.5.2.

Let q^* and Q^* be the optimal bids under equilibrium, then the equilibrium price becomes $P^* = P(L, Q^*) = \frac{L - Q^*}{m}$, whose mean and variance can be calculated accordingly. In the specific example above, $E[P^*] = \frac{E[L] - Q^*}{m}$ and $Var[P^*] = \frac{Var[L]}{m^2}$. Notice that the variance of the equilibrium price only depends on the variance of the load. Similarly to the expected cost, we can also recursively calculate the variance of profit under equilibrium:

$$Var[\pi_i(q_i | q_{-i})] = q_i^2 \int_{-\infty}^{\infty} [P(l, Q^*)^+]^2 f(l) dl - q_i^2 \left[\int_{-\infty}^{\infty} P(l, Q^*)^+ f(l) dl \right]^2 + Var_Y[Cost_i(q_i^*)].$$

Define

$$V_{i,j}(q) = \begin{cases} \text{Var}_Y[\text{Cost}_i(q)] & \text{if } j = 1, \\ \text{Var}_Y[\text{Cost}_i(q) \mid Y_{ik} = 0, \text{ for } k = 1, \dots, j-1] & \text{for } j = 2, \dots, N_i. \end{cases}$$

Then,

$$V_{i,N_i}(q) = 0,$$

and for $k = 1, 2, \dots, N_i - 1$,

$$V_{i,j}(q) = \begin{cases} (1 - p_{ij})V_{i,j+1}(q) + p_{ij}(1 - p_{ij})[d_{ij}q - C_{i,j+1}(q)]^2, & 0 \leq q \leq c_{ij}, \\ p_{ij}V_{i,j+1}(q - c_{ij}) + (1 - p_{ij})V_{i,j+1}(q) \\ + p_{ij}(1 - p_{ij})[d_{ij}c_{ij} + C_{i,j+1}(q - c_{ij}) - C_{i,j+1}(q)]^2, & q > c_{ij}. \end{cases}$$

4.4 LINEAR SUPPLY FUNCTION EQUILIBRIUM

In the SFE model, firms simultaneously bid their supply functions $S_i(P)$. After the supply bids are submitted, the actual demand function is observed. Thereafter, the market clearing price P^* is obtained such that $D(l, P^*) = \sum_{i=1}^n S_i(P^*)$, where l is the realization of uncertainty L . We assume that if $P^* < 0$, no trade is made. In this section, we restrict our attention to linear supply functions, i.e $S_i(P) = a_i + b_i P$, and a linear demand function $D(L, P) = L - mP$. Here, L is a random variable and m is a constant.

Again, firms choose their bids $S_i(P) = a_i + b_i P$ in order to maximize their expected profits. Given the sum of other firms' bids $S_{-i}(P) = a_{-i} + b_{-i} P$ and using the equation $D(L, P) = S_i(P) + S_{-i}(P)$, we can solve for the market clearing price $P^* = \frac{(L - a_i - a_{-i})^+}{m + b_i + b_{-i}}$. Define $x_i = \frac{b_i}{m + b_i + b_{-i}}$, we then have $P^* = \frac{(1 - x_i)(L - a_i - a_{-i})^+}{m + b_{-i}}$ and $S_i(P^*) = a_i + x_i(L - a_i - a_{-i})^+$. The profit of firm i is a function of $S_i(P)$, or equivalently, a function of a_i and x_i :

$$\begin{aligned}
\pi_i(a_i, x_i) &= S_i(P^*)P^* - Cost_i[S_i(P^*)] \\
&= \frac{(1-x_i)(L-a_i-a_{-i})^+[a_i+x_i(L-a_i-a_{-i})^+]}{m+b_{-i}} \\
&\quad - Cost_i[a_i+x_i(L-a_i-a_{-i})^+],
\end{aligned}$$

where $Cost_i(q)$ is the cost for firm i to produce the quantity of q , which now involves both demand side and supply side uncertainties. Therefore,

$$\begin{aligned}
E[\pi_i(a_i, x_i)] &= \frac{(1-x_i) \left\{ a_i E[L-a_i-a_{-i}]^+ + x_i E[(L-a_i-a_{-i})^+]^2 \right\}}{m+b_{-i}} \\
&\quad - E_{Y,L} \{ Cost_i[a_i+x_i(L-a_i-a_{-i})^+] \}.
\end{aligned}$$

Specifically, if L is uniformly distributed on $[L_1, L_2]$ (assuming $L_2 \geq a_i + a_{-i}$), then

$$\begin{aligned}
E[L-a_i-a_{-i}]^+ &= \frac{1}{L_1-L_2} \int_{\max(L_1, a_i+a_{-i})}^{L_2} (l-a_i-a_{-i}) dl \\
&= \frac{[L_2 - \max(L_1, a_i+a_{-i})][L_2 + \max(L_1, a_i+a_{-i}) - 2(a_i+a_{-i})]}{2(L_2-L_1)}
\end{aligned}$$

and

$$\begin{aligned}
E[(L-a_i-a_{-i})^+]^2 &= \frac{1}{L_1-L_2} \int_{\max(L_1, a_i+a_{-i})}^{L_2} (l-a_i-a_{-i})^2 dl \\
&= \frac{(L_2-a_i-a_{-i})^3 - [\max(L_1, a_i+a_{-i}) - a_i - a_{-i}]^3}{3(L_2-L_1)}.
\end{aligned}$$

As in the Cournot model, we again develop a recursive relationship for determining the expected cost under a given supply function. For x and $\alpha \geq 0$, define

$$\bar{C}_{i,j}^L(x, \alpha, \beta) = \begin{cases} E_{Y,L} \{ Cost_i[\alpha + (Lx - \beta)^+] \}, \\ E_{Y,L} \{ Cost_i[\alpha + (Lx - \beta)^+] \mid Y_{ik} = 0, k = 1, \dots, j-1 \} \text{ for } j = 2, \dots, N_i. \end{cases}$$

Then,

$$\bar{C}_{i,N_i}^L(x, \alpha, \beta) = E[\alpha + (Lx - \beta)^+] d_{N_i} \tag{4.2}$$

and for $j = 1, \dots, N_i - 1$:

$$\bar{C}_{i,j}^L(x, \alpha, \beta) = \begin{cases} p_{ij}d_{ij}E[\alpha + (Lx - \beta)^+] + (1 - p_{ij})\bar{C}_{i,j+1}^L(x, \alpha, \beta), & \alpha + (L_2x - \beta)^+ \leq c_{i,j}; \\ p_{ij}d_{ij}E\{c_{ij} - [c_{ij} - \alpha - (Lx - \beta)^+]^+\} & \alpha + (L_1x - \beta)^+ < c_{ij}, \\ + p_{ij}\bar{C}_{i,j+1}^L(x, 0, \beta + c_{ij} - \alpha) & c_{ij} < \alpha + (L_2x - \beta)^+; \\ + (1 - p_{ij})\bar{C}_{i,j+1}^L(x, \alpha, \beta) & \\ p_{ij}d_{ij}c_{ij} + p_{ij}\bar{C}_{i,j+1}^L(x, 0, \beta + c_{ij} - \alpha) & \alpha + (L_1x - \beta)^+ \geq c_{ij}, \\ + (1 - p_{ij})\bar{C}_{i,j+1}^L(x, \alpha, \beta) & \alpha \leq c_{ij}; \\ p_{ij}d_{ij}c_{ij} + p_{ij}\bar{C}_{i,j+1}^L(x, \alpha - c_{ij}, \beta) & \alpha > c_{ij}, \\ + (1 - p_{ij})\bar{C}_{i,j+1}^L(x, \alpha, \beta) & \alpha + (L_1x - \beta)^+ \geq c_{ij}. \end{cases} \quad (4.3)$$

Therefore, $E_{Y,L}\{Cost_i[a_i + x_i(L - a_i - a_{-i})^+]\} = \bar{C}_{i1}^L[x_i, a_i, (a_i + a_{-i})x_i]$ can be evaluated recursively. If L is uniformly distributed on $[L_1, L_2]$, then from (4.2) and (4.3) we obtain

$$E[\alpha + (Lx - \beta)^+] = \begin{cases} \alpha + (L_2x - \beta)^+ & x = 0, \\ & L_1 = L_2, \text{ or} \\ & L_2x \leq \beta; \\ \alpha + \frac{1}{L_2 - L_1} \int_{\max(L_1, \frac{\beta}{x})}^{L_2} (lx - \beta) dl & \\ = \alpha + \frac{[L_2 - \max(L_1, \frac{\beta}{x})][L_2x + \max(L_1x, \beta) - 2\beta]}{2(L_2 - L_1)} & \text{otherwise.} \end{cases}$$

In fact, the Cournot model is a special case of LSFE, where the supply function $S(P) = a$; also the expected cost function $C_{i,j}(q)$ in the Cournot model is a special case of $\bar{C}_{i,j}^L(x = 0, \alpha = q, \beta = 0)$.

Let a^* and b^* be the optimal bids under equilibrium (assuming $L_1 \geq \sum_{i=1}^n a_i^*$), then the equilibrium price becomes $P^* = \frac{L - \sum_{i=1}^n a_i^*}{m + \sum_{i=1}^n b_i^*}$, and $E[P^*] = \frac{E[L] - \sum_{i=1}^n a_i^*}{m + \sum_{i=1}^n b_i^*}$ and $Var[P^*] = \frac{Var[L]}{(m + \sum_{i=1}^n b_i^*)^2}$. Notice that here the variance of price under LSFE model is smaller than that under Cournot model. We do not obtain an analytical expression for the variance of profit

under LSFE model. Instead, we obtain the results shown in Section 4.5 using Monte Carlo simulation.

For the purpose of obtaining the equilibrium solution (a_i^*, b_i^*) , we adopt a sequential search procedure:

1. Set $k_i = 0$, $a_i^{k_i} = 0$, $b_i^{k_i} = 0$, for $i = 1, 2, \dots, n$. Select an $\epsilon > 0$.
2. For $i = 1, 2, \dots, n$,

$$(a_i^{k_i+1}, b_i^{k_i+1}) = \operatorname{argmax}_{a_i \in \mathbb{R}_+, b_i \in \mathbb{R}_+} E \left[\pi \left(a_i, b_i \left| \sum_{j \neq i} a_j^{k_j}, \sum_{j \neq i} b_j^{k_j} \right. \right) \right]$$

and set $k_i = k_i + 1$.

3. If $\Delta a_i = |a_i^{k_i} - a_i^{k_i-1}| \leq \epsilon$ and $\Delta b_i = |b_i^{k_i} - b_i^{k_i-1}| \leq \epsilon$ for $i = 1, 2, \dots, n$, stop; otherwise go to step 2.

Thus the starting point of the algorithm is monopoly, and the firm obtains its optimal linear supply function that will maximize its expected profit. And then the second firm enters the market and obtains its optimal supply function subject to the residual demand function. The third firm enters in a similar way as the second one, then it obtain its optimal supply function based on the other two firms' previous supply functions. Subsequently, the three firms bid in the same order iteratively until the coefficients a_i and b_i converge. We use two dimensional golden section search to solve the maximization problem in step 2. While function $E[\pi(\cdot)]$ is non-convex, one can only get a local optimal solution using this algorithm. However, we conjecture based on our extensive experiments that the two dimensional golden section search obtains the global optimal in most cases.

We illustrate the results for both Cournot and LSFE models and present comparisons in the following section.

4.5 NUMERICAL EXAMPLES

4.5.1 Demand and Supply

We consider a market which consists of three asymmetric firms with different mixes of generator types. Firm 1 has 12 generators, firm 2 has 8, and firm 3 has 10. The characteristics of the units and their numbers are given in Tables 17 and 18. The last row in Table 17 refers to the N_i^{th} unit of each firm. It has infinite capacity and is perfectly reliable. Its marginal cost is assumed to be higher than that of the firm's generators. The last two columns refer to the generating units' steady-state availability and the average 24-hour availability (under the assumption that at the beginning of the period the unit is up). The terms MTTF and MTTR refer to the mean uptime and mean downtime respectively. The values given in this table have been extracted from [43].

We give two examples using different coefficients. In the first example, $m = 38.5$ and L has a uniform distribution on $[769, 1154]$. This represents an 11.6% load variation. We also use the steady state availability p_{ij} . Our solution approach for Nash Cournot equilibrium is illustrated in Figures 16 to 19, and the results for both Cournot and LSFE models are given in Tables 19 to 22. In the second example, $m = 38.5$ and L has a uniform distribution on $[913, 1010]$. This represents a 2.9% load variation, a figure in agreement with the recent literature [8, 9] on the short term load forecast errors. We also use the average availability \bar{p}_{ij} . Results for this example are given in Tables 23 to 26.

Clearly, the results given in the second example are more relevant for the decision maker who is considering making a day-ahead bid. In contrast, the first example illustrates how varying assumptions on the load distribution and the generator availabilities affect the price and profit statistics.

4.5.2 Cournot Model

For a given q_{-i} , firm i 's expected profit is a function of q_i . Our approach for obtaining the Nash Cournot equilibrium is illustrated by the following figures. Figure 16 shows the expected profit (expected revenue less the expected production cost) for firm 3 as a function

Table 17: Generator unit data

Unit Group	Unit Type	Unit Capacity	Marginal Cost	MTTF	MTTR	Availability p_{ij}	Average Availability \bar{p}_{ij}
		c_{ij}	d_{ij}				
U12	Oil/Steam	12	14.8	2940	60	0.98	0.996
U20	Oil/CT	20	8.0	450	50	0.90	0.978
U50	Hydro	50	1.0	1980	20	0.99	0.996
U76	Coal/Stem	76	14	1960	40	0.98	0.995
U100	Oil/Steam	100	14.8	1200	50	0.96	0.991
U155	Coal/Steam	155	14	960	40	0.96	0.990
U197	Oil/Steam	197	14.8	950	50	0.95	0.989
U350	Coal/Steam	350	14	1150	100	0.92	0.990
U400	Nuclear	400	0.4	1100	150	0.88	0.990
U ∞	Market	∞	30	—	—	1.00	1.000

of q_3 when $q_{-3} = 480.75$. Figure 17 are the derivative functions $C'_{3,1}(q_3)$ and $R'_3(q_3|q_{-3})$, the intersection of which yields the best response q_3^* . Figure 18 is a plot of the piecewise linear optimal response function $q_3^*(q_{-3})$ vs. q_{-3} . Figure 19 illustrates the graphical solution of Nash Cournot equilibrium. The intersection of the dashed equiangular line and the summation of best response functions $q(Q) = \sum_{i=1}^n q_i^*(Q)$ yields the market supply Q^* , and the dashed vertical line starting from Q^* crosses each firm's best response function $q_i^*(Q)$ at its supply q_i^* under equilibrium. Firms' optimal bids and expected profits and standard deviation of profits under Nash equilibrium are shown in Tables 22 and 26.

Table 18: Firm unit data

Unit Group	Number of Units Owned by		
	Firm 1	Firm 2	Firm 3
U12	2	2	0
U20	1	1	1
U50	0	2	2
U76	2	1	1
U100	0	1	2
U155	2	0	0
U197	2	0	2
U350	2	0	0
U400	0	0	1
U_{∞}	1	1	1

4.5.3 LSFE Model

To determine the equilibrium solution for our numerical example, we use the sequential search procedure outlined at the end of Section 4.4. As we see by the successive values of the approximations in Tables 19 and 23, the solutions converged quite rapidly. The same final values were reached using different firms as the initial starting points in the iterations. Note that in general, even for LSFE with two decision variables a_i and b_i , the equilibrium solution may not necessarily exist, nor does it have to be unique [35]. In our experiments, however, we have been able to obtain the equilibria for a large range of parameter settings.

4.5.4 Model Comparisons

Table 20 gives a comparison of the mean and standard deviation of prices and the expected values of total market supply under Cournot, LSFE, “perfect” SFE and Bertrand models. In

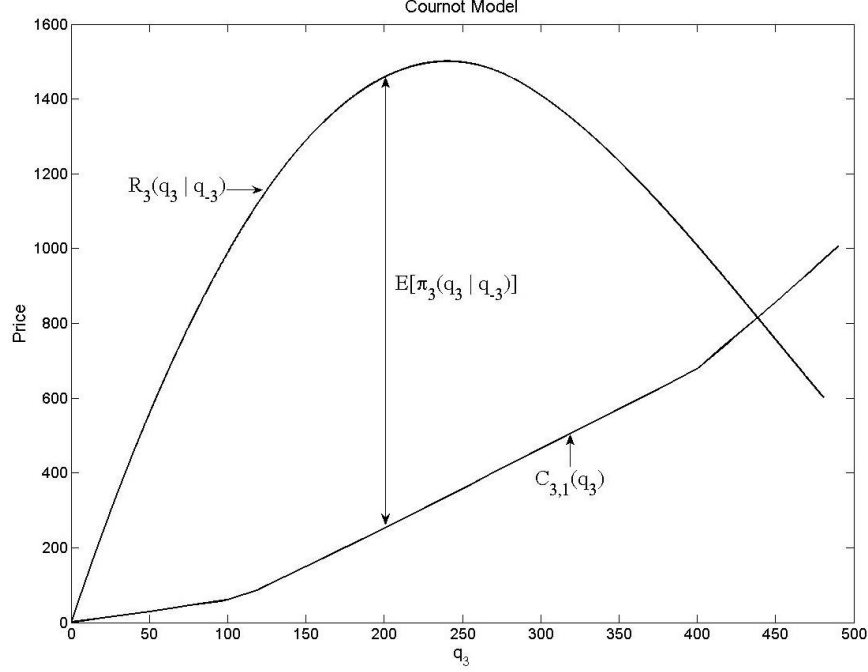


Figure 16: Expected profit for $q_{-3} = 480.75$ with $L \sim U(769, 1154)$ and $m = 38.5$

the perfect SFE model, we assume that the realized value of load (occurring according to the stipulated distribution) is known to each supplier who then offers its profit-maximizing bid according to a Cournot model including generator failure. Note that the perfect SFE solution in this case is identical to the corresponding Cournot equilibrium solution. In the Bertrand model, we assume that firms bid their expected cost functions as supply functions. Here, the expectation considers generator failure only. We observe that the LSFE model yields a smaller expected value and standard deviation of price. The values for perfect SFE have been obtained using Monte Carlo simulation. We hypothesize that this yields an upper bound to expected profit, because the shape of the perfect SFE is not restricted. Table 21 captures the effect of different assumptions on generator reliabilities. In the first row, the Cournot bids are made assuming that the generators do not fail. The expected profit is however obtained using the availability values, p_{ij} . In the second row, the generator capacities are derated. The maximum c_{ij} is now multiplied by p_{ij} and in the remainder of the computations the p_{ij}

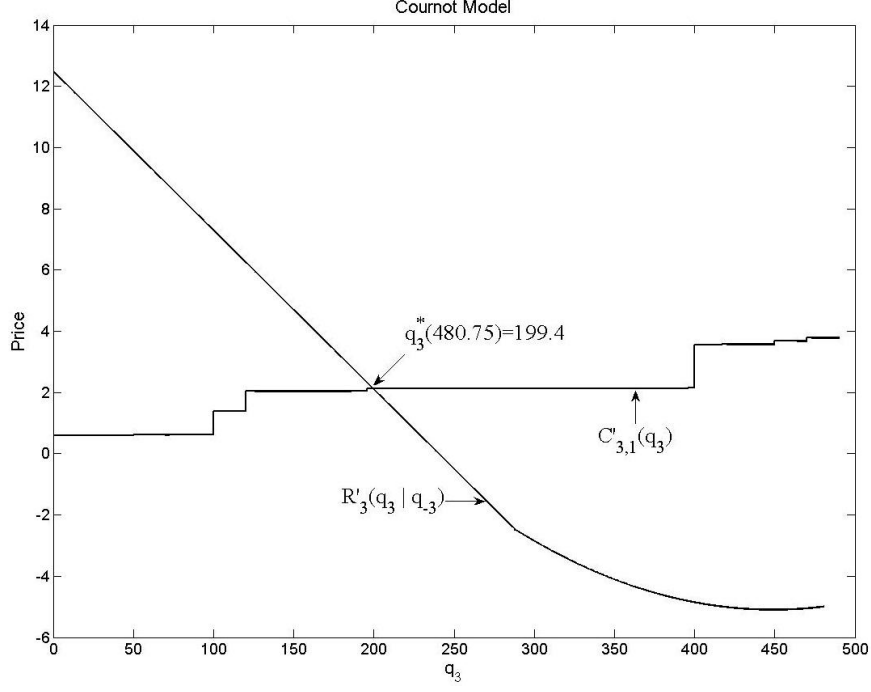


Figure 17: Best response of q_3^* to $q_{-3} = 480.75$ with $L \sim U(769, 1154)$ and $m = 38.5$

values are ignored. The last two rows of the tables repeat similar computations for the LSFE model. The model using derated capacities yields slightly higher values of the expected price and larger values for the expected profit when compared to the Cournot model (ignoring failures). The expected value for this case is less than that when failures are taken into account as shown in Table 20. The conclusions from comparing the three LSFE models are similar to those from the corresponding Cournot model. Table 22 gives the quantities (expected quantities for the LSFE) and the expected values and standard deviation of profit for each of the three different firms. Although the quantity values change very little, the expected profits are less for each firm when the bids are made ignoring failures.

Tables 23, 24, 25 and 26 are counterparts of tables 19, 20, 21 and 22, respectively, with p_{ij} substituted by \bar{p}_{ij} and the spread of the uniform load distribution reduced. They apply for the day-ahead bid situation. The conclusions from the inter-model comparisons for this situation remain the same as before. The LSFE model yields a smaller expected value and

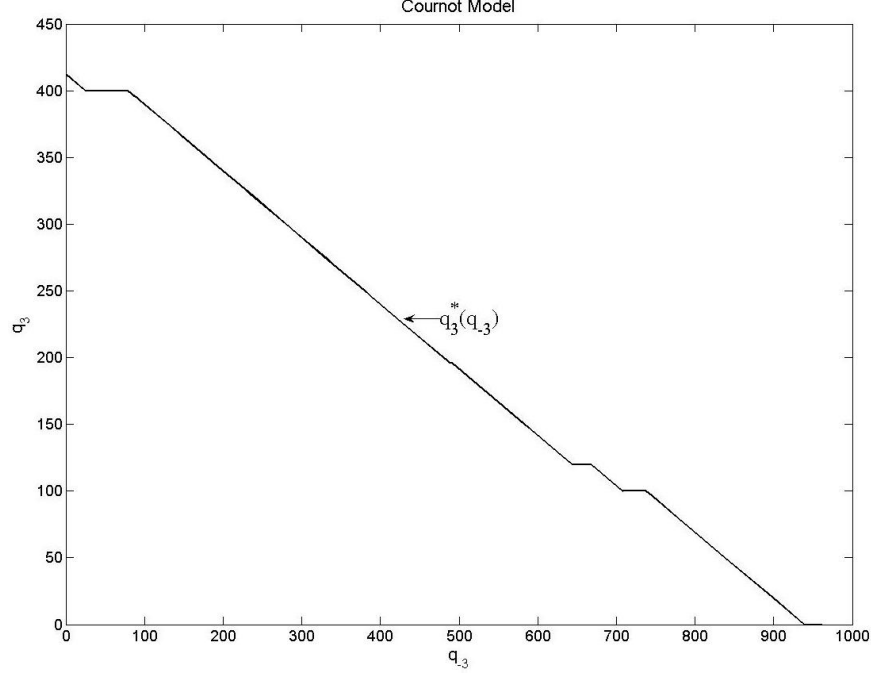


Figure 18: Best response function $q_3^*(q_{-3})$ with $L \sim U(769, 1154)$ and $m = 38.5$

standard deviation of profit than Cournot. The Bertrand model yields the lowest price, the highest supply quantity, but lowest expected profit. Accounting for the possibility of unit failures, the Cournot model yields a higher expected profit than when quantity bids are offered while ignoring this uncertainty. Comparing Tables 22 and 26, we observe that although statistics for firms 1 and 2 change very little, firm 3 has higher expected profit with much lower standard deviation. This is undoubtedly a consequence of the large difference between the values of p_{ij} and \bar{p}_{ij} for the base loaded nuclear unit, and its having a relatively large value for its MTTF.

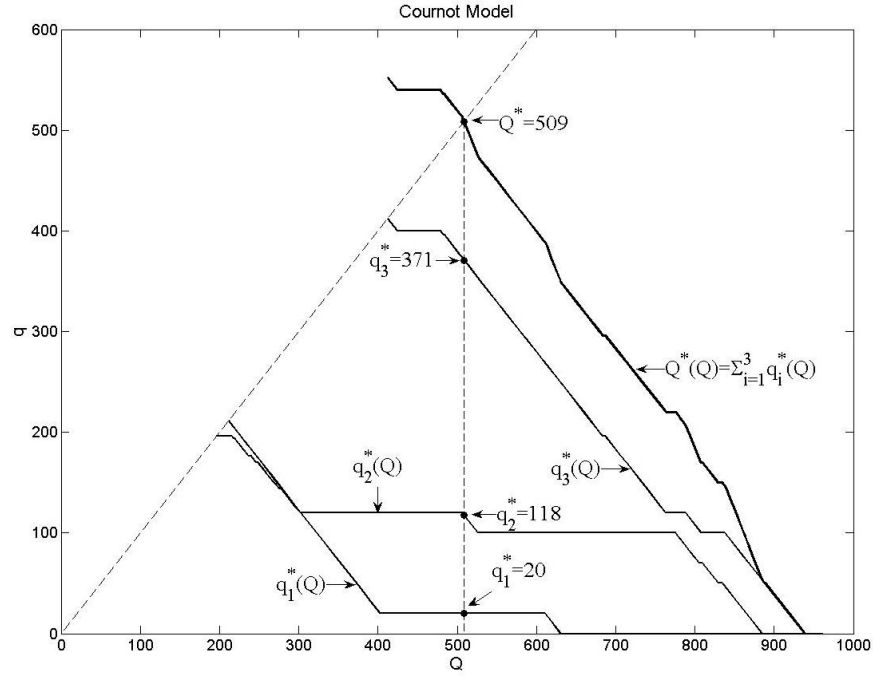


Figure 19: Nash equilibrium outcome with $L \sim U(769, 1154)$ and $m = 38.5$

Table 19: Sequential search iteration results using p_{ij} and $L \sim U[769, 1154]$

k	a_1	b_1	a_2	b_2	a_3	b_3	$\max\{ \Delta a_i , \Delta b_i \}$
0	56.2977	7.9560	61.2977	4.4223	261.1492	11.3414	—
1	14.5297	0.4658	67.4462	3.8744	247.8594	12.5006	41.7680
2	15.4563	0.3870	65.5544	4.0563	247.8594	12.5306	1.8918
3	15.4271	0.3885	65.5475	4.0588	247.8594	12.5318	0.0291
4	15.4271	0.3885	65.5475	4.0589	247.8594	12.5318	0.0001
5	15.4271	0.3885	65.5475	4.0589	247.8594	12.5318	0.0000

Table 20: Comparison of equilibrium outcomes under different models using p_{ij} and $L \sim U[769, 1154]$

Model	$E[P^*]$	$S.D.(P^*)$	$E[Q^*]$	$E[\Pi^*]$
Cournot	11.76	2.89	508.59	4943.2
LSFE	11.40	1.00	522.46	4986.6
Perfect SFE ¹	11.93	1.48	502.03	5217.3
Bertrand	8.94	2.46	617.10	4333.1

¹Same as perfect Cournot

Table 21: Comparison of equilibrium outcomes under different models using p_{ij} and $L \sim U[769, 1154]$

Model	$E[P^*]$	$S.D.(P^*)$	$E[Q^*]$	$E[\Pi^*]$
Cournot (Ignoring Failures)	11.03	2.89	536.75	4827.5
Cournot (Derated Capacities)	11.23	2.89	529.00	4876.2
LSFE (Ignoring Failures)	10.58	0.93	554.31	4821.7
LSFE (Derated Capacities)	10.95	0.99	539.87	4926.1

Table 22: Equilibrium outcomes for each firm using p_{ij} and $L \sim U[769, 1154]$

	Cournot			LSFE			
	q^*	$E[\pi^*]$	$S.D.(\pi^*)$	(a^*, b^*)	$E[q^*]$	$E[\pi^*]$	$S.D.(\pi^*)$
Firm 1	20	63	68	(15.43, 0.39)	20	56	40
Firm 2	118	1119	353	(65.55, 4.06)	112	1074	243
Firm 3	371	3761	1634	(247.86, 12.53)	391	3857	1016
	Cournot (Ignoring Failures)			LSFE (Ignoring Failures)			
	q^*	$E[\pi^*]$	$S.D.(\pi^*)$	(a^*, b^*)	$E[q^*]$	$E[\pi^*]$	$S.D.(\pi^*)$
Firm 1	20	49	68	(13.89, 0.53)	20	39	37
Firm 2	117	1031	350	(64.96, 4.40)	112	980	221
Firm 3	400	3748	1791	(251.49, 16.24)	423	3803	1035

Table 23: Sequential search iteration results using \bar{p}_{ij} and $L \sim U[913, 1010]$

k	a_1	b_1	a_2	b_2	a_3	b_3	$\max\{ \Delta a_i , \Delta b_i \}$
0	122.1574	4.5758	64.7189	3.5281	235.6314	16.1959	—
1	17.3470	0.2384	74.8778	3.9372	232.7896	16.6475	104.8104
2	17.3943	0.2386	74.2296	4.0065	232.7896	16.6747	0.6482
3	17.3883	0.2390	74.2296	4.0085	232.7896	16.6756	0.0060
4	17.3883	0.2390	74.2296	4.0085	232.7896	16.6756	0.0001
5	17.3883	0.2390	74.2296	4.0085	232.7896	16.6756	0.0000

Table 24: Comparison of equilibrium outcomes under different models using \bar{p}_{ij} and $L \sim U[913, 1010]$

Model	$E[P^*]$	$S.D.(P^*)$	$E[Q^*]$	$E[\Pi^*]$
Cournot	11.12	0.73	533.30	5353.7
LSFE	10.72	0.24	548.73	5265.1
Perfect SFE ²	11.18	0.39	531.09	5510.1
Bertrand	8.73	0.44	625.37	4763.2

²Same as perfect Cournot

Table 25: Comparison of equilibrium outcomes under different models using \bar{p}_{ij} and $L \sim U[913, 1010]$

Model	$E[P^*]$	$S.D.(P^*)$	$E[Q^*]$	$E[\Pi^*]$
Cournot (Ignoring Failures)	11.03	0.7273	536.75	5315.9
Cournot (Derated Capacities)	11.09	0.73	534.53	5309.8
LSFE (Ignoring Failures)	10.68	0.2372	550.40	5256.0
LSFE (Derated Capacities)	10.68	0.24	550.47	5265.5

Table 26: Equilibrium outcomes for each firm using \bar{p}_{ij} and $L \sim U[913, 1010]$

	Cournot			LSFE			
	q^*	$E[\pi^*]$	$S.D.(\pi^*)$	(a^*, b^*)	$E[q^*]$	$E[\pi^*]$	$S.D.(\pi^*)$
Firm 1	20	60	23	(17.39, 0.24)	20	52	10
Firm 2	113	1047	100	(74.23, 4.01)	117	1012	61
Firm 3	400	4247	509	(232.79, 16.68)	412	4201	274
	Cournot (Ignoring Failures)			LSFE (Ignoring Failures)			
	q^*	$E[\pi^*]$	$S.D.(\pi^*)$	(a^*, b^*)	$E[q^*]$	$E[\pi^*]$	$S.D.(\pi^*)$
Firm 1	20	58	23	(17.46, 0.23)	20	51	10
Firm 2	117	1047	103	(74.63, 3.91)	117	1008	61
Firm 3	400	4211	509	(238.09, 16.39)	413	4198	274

4.6 CONCLUSIONS AND DISCUSSIONS

In this chapter we have provided an analytical procedure for calculating a Nash equilibrium solution when firms submit bids (before the realization of uncertainties in demand and supply) that maximize their expected profits. Two different oligopoly market models have been considered, Cournot and LSFE. We have enhanced these conventional models by including supply side uncertainties in addition to the stochastic demand. The randomness on the supply side is assumed here to be caused by the unpredictable failures of the generators. We have not considered other important supply side uncertainties such as those affecting hydro generation or fuel prices. The stochasticity associated with fuel prices can be accounted for by assuming that the cost parameter d_{ij} has a probability distribution. [65] has used such an approach for the Cournot model. The numerical values given in our tables may give the reader the impression that inclusion of generation availabilities and load uncertainties in the various oligopoly models do not make much differences in the statistics related to electricity prices and the profits of individual firms. As a matter of fact, these comparisons depend greatly on the assumed values for generator reliabilities and the parameters of the load probability distribution. The contribution of this chapter has been in the development of a mathematical framework in which the effect of these uncertainties on prices and profits can be calculated for standard oligopoly models when the firms are not necessarily symmetric and supply side uncertainties prevail. The results given in the chapter indicate that lower prices and profits arise when the effects of generator failures are not considered in determining the bids. Notice that not including generator reliabilities is similar to assuming that all generators are perfectly reliable, and all will be competing in the market. Therefore, under this assumption the bids are determined assuming a more intense competition, which results in lower prices. The costs are also affected by these uncertainties. The costs increase because when the random demand is realized, some inexpensive generators may not be available and the firm may need to use more expensive units. The analysis given in this chapter can also enable one to compare the relative importance of load and capacity uncertainties [88].

5.0 SUMMARY, DISCUSSION, AND FUTURE RESEARCH DIRECTIONS

This thesis consists of three essays, representing three different but well connected facets of the sophisticated electric power systems, where strategic and operational decisions at various levels need to be made in different time frames. Due to the critical role of electricity as well as its special properties, many decisions need to be made under uncertainty. These essays thus serve as examples of using operations research techniques to assist decision making in the electric power system.

5.1 SUMMARY

Chapter 2 analyzes four factors that have significant influence on the locational marginal prices, and decomposes the mean and standard deviation of LMPs to contribution from individual factors and their interactions. This approach not only presents a novel angle to understand the LMPs, but also can be used to quantitatively evaluate the effectiveness of system expansion projects.

As opposed to the simplifying 90% capacity reserve criterion in Chapter 2, Chapter 3 attempts to find the “optimal” solution for the security constrained economic dispatch problem. Since an 100% secure and reliable dispatch strategy does not exist (it is conceptually possible for all generation and transmission units to break down simultaneously due to natural disasters), the problem becomes of resolving how much tradeoff between system security and economic benefit is appropriate. A key point in solving such a problem is to accurately evaluate the economic impact of the risk, so that the risk can be converted to dollars and combined with the generation cost as a single objective function for the system operator to

minimize. Using the MDP model, we evaluate the economic impact of a dispatch decision by calculating not only its immediate generation cost but also the risk imposed to the system by such decision. Different contingency scenarios are treated as various states of the system, and an optimal dispatch decision for each of the states is obtained from the solution to the MDP model.

Chapter 4 examines how power suppliers compete with each other under different oligopoly models as well as the presence of uncertainties (from both demand and supply sides). The results in this chapter show that the LSFE model, as a generalized case of Bertrand and Cournot, results in more competition than Cournot but less than Bertrand. The results on the effect of uncertainty on the market power exercise is open ended. On the one hand, for a single supplier, taking into account uncertainty improves its profitability. On the other hand, all suppliers considering the uncertainty in their bids may or may not generate a more favorable result than all suppliers ignoring the uncertainty.

These three essays present novelty from not only the methodological perspective, but also from the application perspective. Similar ideas of attributing electricity prices to various factors have been presented in the literature [21, 63, 70]. What enables Chapter 2 to take a further step in implementing the idea is the system model, which quantitatively decomposes the prices to the contribution of individual factors as well as their interactions. The application of sensitivity analysis results from parametric quadratic programming also plays an important role in making the computation accurate and efficient. Chapter 3 examines a well studied yet open problem, the security constrained economic dispatch. Instead of focusing on a short period of time as most other papers do, this chapter takes the impact of a dispatch decision to the entire future into the modeling consideration, and formulates the problem as a Markov decision process model with continuous action space, which is a relatively rarely studied model. The numerical example section in this chapter provides experimental examples for the computational study of such model. Chapter 4 raises the question of how demand and supply uncertainties affect the exercise of market power in the electric power system, creatively uses the recursive function to solve the piecewise linear expected cost function, and graphically obtains the Nash equilibrium.

5.2 INTERRELATIONSHIPS AMONG THREE ESSAYS

An electric power system is such a sophisticated system that people usually have to restrict their scope to small facets, make simplifying assumptions about certain details, and study separate problems, like what is being done in this thesis. However, the three essays can be integrated by a single market clearing problem presented in Section 2.2.6, which is rewritten here:

$$\min_{q,z} \quad \sum_{n \in \mathcal{S}} (\alpha_n q_n + \frac{1}{2} b_n q_n^2) \quad (5.1)$$

$$\text{s. t.} \quad q_n - z_n = d_{n,t}(1 + \epsilon_t), \quad (p_{n,t}) \quad \forall n \in \mathcal{N} \quad (5.2)$$

$$\sum_{n \in \mathcal{N}} H_{l,n} z_n \leq 0.9 T_l, \quad \forall l \in \mathcal{L} \quad (5.3)$$

$$-\sum_{n \in \mathcal{N}} H_{l,n} z_n \leq 0.9 T_l, \quad \forall l \in \mathcal{L} \quad (5.4)$$

$$\sum_{n \in \mathcal{N}} z_n = 0 \quad (5.5)$$

$$0 \leq q_n \leq 0.9 \bar{Q}_n, \quad \forall n \in \mathcal{S}. \quad (5.6)$$

The first essay assumes that (1) supply functions in (5.1) are constant and known, (2) the system security is simply taken care of by the 90% criterion in (5.3), (5.4) and (5.6), and transmission lines never fail. These (and other) simplifying assumptions enable one to take a systemic and strategic perspective, and to use the system model to calculate impact coefficients.

The second essay focuses on the dispatch decision making process at the operational level, keeps assumption (1), relaxes assumption (2), and searches for the dispatch decision that has the best tradeoff between cost efficiency and system security.

Assumption (1) is relaxed in the third essay, which examines the oligopoly competition from two perspectives: what is the best strategy for a supplier to maximize its own profit, and how the oligopoly competition will affect the price of electricity. Transmission constraints (5.3) and (5.4) are ignored to simplify the computation, but demand and supply side uncertainties are introduced. The existing literature has also studied the oligopoly competition with transmission constraints (5.3) and (5.4) but without demand and supply side uncertainties, which will result in the MPEC formulation to be briefly discussed in Section 5.3.3.

5.3 DISCUSSIONS AND FUTURE RESEARCH DIRECTIONS

The research in this thesis has been conducted with the hope that it will (1) shed light on a deeper understanding of decision making under uncertainty in electric power systems, (2) provide novel modeling and computational perspectives on solving some of the existing problems, and (3) outline or inspire future research on continuous improvement of the electric power system towards a more efficient and reliable direction.

5.3.1 Discussions and Future Research Directions for Chapter 2

- More factors that affect LMPs significantly need to be considered. These include fuel price change, transmission line failures, long term demand increase, etc. The assumption of constant fuel prices restricts the analysis to a short time horizon. The fuel prices having exhibited such volatile behavior during the past years, their impact on the electricity prices remains an important yet open question. The system model used in Chapter 2 provides a unique and appropriate approach to such problem, because it can quantitatively differentiate the sole contribution of fuel price change from that of its interaction among other factors.

It is assumed in the current model that, although capacity reserve criterion is used, transmission line failures do not actually occur. To study the effects of transmission line failures on the electricity prices, an extensive additional modeling and computational effort will be needed. Some results from Chapter 3 may be useful in such extension. Mean and standard deviation will not be sufficient in describing the random behavior of LMPs, because the delivery of electricity could be interrupted by transmission line failures. A risk index needs to be added to take such possibility into account. The calculation of mean and standard deviation will also be complicated by transmission line failures.

The computational techniques in Chapter 2 heavily depend on the assumption that demands at all nodes increase or decrease by the same percentage simultaneously. Although this is not completely unrealistic (according to the load data from PJM [1], the correlation

between PJM-E and PJM-W is 0.8632), it will be more accurate to relax this assumption and study non-perfect load correlation situations. The required computational effort remains an open question.

- For modeling simplicity, it is assumed in Chapter 2 that supply functions never change. However, it will be more interesting (and challenging) to study dynamic market power behavior under different scenarios. In such situation, the supply functions of all generators need to be calculated for each possible system input parameter $\mathbf{x} = \{x_1, x_2, x_3, x_4\}$. However, direct calculation of the Nash Equilibrium would lead to a sophisticated program Equilibrium Program with Equilibrium Constraints (EPEC), which is one of the most challenging mathematical programming problems, and to which no known algorithm is guaranteed a solution.
- The locational marginal price $p_{n,t}$ is calculated as the dual of the equality constraint (2.4) in the market clearing problem (2.3)-(2.8). However, unless certain constraint qualifications hold, the optimal dual $p_{n,t}^*$ is not guaranteed to be unique or bounded. For a nonlinear program $\min\{f(x) : g(x) \leq 0, h(x) = 0\}$, the Linear Independence Constraint Qualification(LICQ) [31] at a feasible solution x_0 requires that the gradients $\nabla g_i(x_0), \forall i : g_k(x_0) = 0$ and $\nabla h_j(x_0), \forall j$ are linearly independent. If LICQ holds for (2.3)-(2.8), then $p_{n,t}^*$ can be uniquely determined.

Theorem 2. *LICQ holds for (2.3)-(2.8) when the congested transmission lines are acyclic.*

Proof. The market clearing problem (2.3)-(2.8) can be written in matrix form as

$$\begin{aligned} \min_{q,z} \quad & c^\top q + \frac{1}{2} q^\top Q q \\ \text{s. t.} \quad & M \begin{bmatrix} q \\ z \end{bmatrix} - m \leq 0 \\ & N \begin{bmatrix} q \\ z \end{bmatrix} - n = 0, \end{aligned}$$

where

$$M = \begin{bmatrix} \mathbf{0}_{\mathcal{L} \times \mathcal{N}} & H_{\mathcal{L} \times \mathcal{N}} \\ \mathbf{0}_{\mathcal{L} \times \mathcal{N}} & -H_{\mathcal{L} \times \mathcal{N}} \\ I_{\mathcal{N} \times \mathcal{N}} & \mathbf{0}_{\mathcal{N} \times \mathcal{N}} \end{bmatrix}, m = \begin{bmatrix} 0.9T_{\mathcal{L} \times 1} \\ 0.9T_{\mathcal{L} \times 1} \\ 0.9\overline{Q}_{\mathcal{N} \times 1} \end{bmatrix},$$

$$N = \begin{bmatrix} I_{\mathcal{N} \times \mathcal{N}} & -I_{\mathcal{N} \times \mathcal{N}} \\ \mathbf{0}_{1 \times \mathcal{N}} & \mathbf{1}_{1 \times \mathcal{N}} \end{bmatrix}, \text{ and } n = \begin{bmatrix} d_{\mathcal{N} \times 1}(1 + \epsilon_t) \\ 0 \end{bmatrix}.$$

Let \mathcal{K} be any set of congested lines that are acyclic. Without loss of generality, we use $H_{\mathcal{K} \times \mathcal{N}} \cdot z = 0.9T_{\mathcal{K} \times 1}$ to represent the active thermal limit constraints, since a power flow has only one direction, and the two thermal limit constraints

$$H_{\mathcal{L} \times \mathcal{N}} \cdot z \leq 0.9T_{\mathcal{L} \times 1}$$

$$-H_{\mathcal{L} \times \mathcal{N}} \cdot z \leq 0.9T_{\mathcal{L} \times 1}$$

cannot both be active. Using only the constraints with plus signs does not change the argument about the linear independency that follows.

To prove LICQ, it suffices to show that all rows of the following matrix are linearly independent:

$$W = \begin{bmatrix} \mathbf{0}_{\mathcal{K} \times \mathcal{N}} & H_{\mathcal{K} \times \mathcal{N}} \\ I_{\mathcal{N} \times \mathcal{N}} & \mathbf{0}_{\mathcal{N} \times \mathcal{N}} \\ I_{\mathcal{N} \times \mathcal{N}} & -I_{\mathcal{N} \times \mathcal{N}} \\ \mathbf{0}_{1 \times \mathcal{N}} & \mathbf{1}_{1 \times \mathcal{N}} \end{bmatrix}.$$

For $i = 1, 2, 3, 4$, let W_i denote the i^{th} block of rows in W . The linear independence of $W_{\{2,3,4\}}$ is easy to see. If we can prove that $H_{\mathcal{K} \times \mathcal{N}}$ has a rank $|\mathcal{K}|$, then the linear independence of W_1 as well as W_1 with $W_{\{2,3,4\}}$ will be clear, which will also complete the proof.

The PTDF matrix H is calculated using the formula given in [76] on page 316:

$$\overline{H} = \Omega A (A^\top \Omega A)^{-1},$$

where $A_{\mathcal{L} \times (\mathcal{N}-1)}$ is the reduced arc-node incidence matrix, $\Omega_{\mathcal{L} \times \mathcal{L}}$ is a positive diagonal matrix, and the relation between $\overline{H}_{\mathcal{L} \times (\mathcal{N}-1)}$ and $H_{\mathcal{L} \times \mathcal{N}}$ is $H_{\mathcal{L} \times \mathcal{N}} = [\overline{H}_{\mathcal{L} \times (\mathcal{N}-1)} \ \mathbf{0}_{\mathcal{L} \times 1}]$. Showing that $H_{\mathcal{K} \times \mathcal{N}}$ has a rank $|\mathcal{K}|$ is equivalent to show that

$$\overline{H}_{\mathcal{K} \times (\mathcal{N}-1)} = \Omega_{\mathcal{K} \times \mathcal{K}} A_{\mathcal{K} \times (\mathcal{N}-1)} (A_{(\mathcal{N}-1) \times \mathcal{L}}^\top \Omega_{\mathcal{L} \times \mathcal{L}} A_{\mathcal{L} \times (\mathcal{N}-1)})^{-1}$$

has a rank $|\mathcal{K}|$. We know that $\overline{H}_{\mathcal{K} \times (\mathcal{N}-1)}$ has $|\mathcal{K}|$ rows, so $\text{rank}[\overline{H}_{\mathcal{K} \times (\mathcal{N}-1)}] \leq |\mathcal{K}|$. On the other hand, we have

$$\begin{aligned} & \text{rank}[\overline{H}_{\mathcal{K} \times (\mathcal{N}-1)}] \\ &= \text{rank} [\Omega_{\mathcal{K} \times \mathcal{K}} A_{\mathcal{K} \times (\mathcal{N}-1)} (A_{(\mathcal{N}-1) \times \mathcal{L}}^\top \Omega_{\mathcal{L} \times \mathcal{L}} A_{\mathcal{L} \times (\mathcal{N}-1)})^{-1}] \\ &= \text{rank} [(A_{(\mathcal{N}-1) \times \mathcal{L}}^\top \Omega_{\mathcal{L} \times \mathcal{L}} A_{\mathcal{L} \times (\mathcal{N}-1)})^{-1}] \\ &\quad - \dim \{ \text{Null}[\Omega_{\mathcal{K} \times \mathcal{K}} A_{\mathcal{K} \times (\mathcal{N}-1)}] \cap \text{Range}[(A_{(\mathcal{N}-1) \times \mathcal{L}}^\top \Omega_{\mathcal{L} \times \mathcal{L}} A_{\mathcal{L} \times (\mathcal{N}-1)})^{-1}] \} \\ &\geq \text{rank} [(A_{(\mathcal{N}-1) \times \mathcal{L}}^\top \Omega_{\mathcal{L} \times \mathcal{L}} A_{\mathcal{L} \times (\mathcal{N}-1)})^{-1}] - \dim \{ \text{Null}[\Omega_{\mathcal{K} \times \mathcal{K}} A_{\mathcal{K} \times (\mathcal{N}-1)}] \} \\ &= (|\mathcal{N}| - 1) - (|\mathcal{N}| - 1 - |\mathcal{K}|) \\ &= |\mathcal{K}|, \end{aligned} \tag{5.7}$$

where (5.7) follows because

$$\dim \{ \text{Null}[\Omega_{\mathcal{K} \times \mathcal{K}} A_{\mathcal{K} \times (\mathcal{N}-1)}] \} = |\mathcal{N}| - 1 - \text{rank}[\Omega_{\mathcal{K} \times \mathcal{K}} A_{\mathcal{K} \times (\mathcal{N}-1)}],$$

and $\Omega_{\mathcal{K} \times \mathcal{K}}$ is a positive diagonal matrix, also the rank of a reduced acyclic arc-node incidence matrix $A_{\mathcal{K} \times (\mathcal{N}-1)}$ equals $|\mathcal{K}|$. Therefore,

$$\text{rank}[\overline{H}_{\mathcal{K} \times (\mathcal{N}-1)}] = |\mathcal{K}|.$$

This completes the proof. □

5.3.2 Discussions and Future Research Directions for Chapter 3

- A larger system needs to be tested to study the efficiency and convergence of the algorithm, which could be computationally a challenging task. An alternative approach would be to study heuristic or approximation algorithms that overcome the curse of dimensionality.
- Instead of converting system risk into dollars, the multi-objective approach seems to provide a natural alternative perspective to examine the same problem. One objective is to minimize the generation cost, and the other objective is to minimize the risk of cascading failures. A dispatch decision that has larger objective values than another dispatch decision in both objective functions is called a dominated decision. The collection of all non-dominated dispatch decisions forms a Pareto frontier. The inevitable tradeoff between cost and risk is more apparent to observe from Figure 20. In this example of Pareto frontier, each point represents the cost minimizing dispatch for the given level of risk, or the risk minimizing dispatch for the given level of cost. The “optimal” dispatch will need to be selected from the Pareto frontier by the decision maker according to specific system requirements.

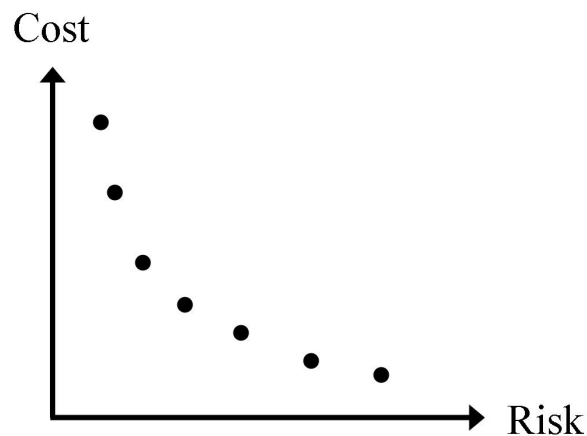


Figure 20: An example of a Pareto frontier

5.3.3 Discussions and Future Research Directions for Chapter 4

- The effect of uncertainty on the exercise of market power demands more study from the game theory perspective. The numerical examples in Chapter 4 do not demonstrate much difference between considering the uncertainty and ignoring it. However, not considering uncertainty while all other competitors do would hurt a supplier's profitability. Therefore, considering uncertainty is not only a rational option for any supplier, but also a necessary strategy to survive in the market competition.
- Transmission constraints could also be added into the model, resulting in a Mathematical Program with Equilibrium Constraints (MPEC) [64]. An MPEC [64] is defined as

$$\min\{f(x, y) : (x, y) \in Z, y \in \mathcal{S}(x)\},$$

where for each $x \in \mathbf{X}$, $\mathcal{S}(x)$ is the solution set of the variational inequality $\text{VI}(F(x, \cdot), C(x))$; i.e., $y \in \mathcal{S}(x)$ if and only if $y \in C(x)$ and $(v - y)^\top F(x, y) \geq 0, \forall v \in C(x)$.

The deterministic version of the game is a well studied problem (see [25, 53] for example, which are not considering demand and supply uncertainties), but both theoretical and computational techniques are still evolving, and no known algorithm is guaranteed to find a global optimal solution. As a matter of fact, MPEC is a subproblem in EPEC. MPEC represents the best response action of a supplier who tries to maximize its own profit assuming other suppliers' actions are known, while EPEC is the Nash Equilibrium state where no supplier has an incentive to unilaterally change its action. In the current literature, a local optimum is treated as the solution to MPEC, and different suppliers' MPECs are iteratively solved with the hope that an equilibrium occurs. Both convergence and cycle have been observed and reported in the literature [53]. A possible alternative could be a modified version of the game-theoretic model, where optimality conditions and Nash equilibria are easier to achieve.

BIBLIOGRAPHY

- [1] <http://www.pjm.com>.
- [2] ftp://www.nerc.com/pub/sys/all_updl/docs/blackout/814BlackoutReport.pdf.
- [3] <http://www.ilog.com>.
- [4] <http://www.mathworks.com>.
- [5] R.B. Adler, S.L. Daniel Jr., C.R. Heising, M.G. Lauby, R.P. Ludorf, and T.S. White. An IEEE survey of U.S. and Canadian overhead transmission outages at 230 kv and above. *IEEE Transactions on Power Delivery*, 9(1):21–39, 1994.
- [6] R. Allan and R. Billinton. Probabilistic assessment of power systems. *Proceedings of the IEEE*, 88(2):140–162, 2000.
- [7] O. Alsac and B. Stott. Optimal load flow with steady-state security. *IEEE Transactions on Power Apparatus and Systems*, 93(3):745–751, 1973.
- [8] N. Amjady. Short-term hourly load forecasting using time-series modeling with peak load estimation Capability. *IEEE Transactions on Power Systems*, 16(3):498–505, 2001.
- [9] N. Amjady. Short-term load forecasting via ARMA model identification including non-Gaussian process considerations. *IEEE Transactions on Power Systems*, 18(2):673–679, 2001.
- [10] J. Apt, L.B. Lave, S. Talukdar, M.G. Morgan, and M. Ilic. Electrical blackouts: a systemic problem. *Issues in Science and Technology*, Summer 2004.
- [11] R. Baldick, R. Grant, and E. Kahn. Linear supply function equilibrium: generalizations, application, and limitations. Technical report, University of California Energy Institute, Berkeley, CA, 2000. POWER Working Paper PWP-078.
- [12] R. Baldick, R. Grant, and E. Kahn. Theory and application of linear supply function equilibrium in electricity markets. *Journal of Regulatory Economics*, 25(2):143–167, 2004.

- [13] R. Baldick, W. Hogan, and E. Kahn. Capacity constrained supply function equilibrium models of electricity markets: stability, non-decreasing constraints, and function space iterations. Technical report, University of California Energy Institute, Berkeley, CA, 2001. POWER Working Paper PWP-089.
- [14] J.N. Bastian, J. Zhu, V. Banunarayana, and R. Mukerji. Forecasting energy prices in a competitive market. *IEEE Computer Applications in Power*, 13(3):40–45, 1999.
- [15] A.B. Berkelaar, B. Jansen, K. Roos, and T. Terlaky. Sensitivity analysis in (degenerate) quadratic programming. Technical report, Econometric Institute, Erasmus University Rotterdam, The Netherlands, 1996.
- [16] S. Borenstein and J. Bushnell. An empirical analysis of the potential for market power in California’s electricity industry. *The Journal of Industrial Economics*, 47(3):285–323, 1999.
- [17] F. Bouffard, F.D. Galiana, and J.M. Arroyo. Umbrella contingencies in security-constrained optimal power flow. *15th Power Systems Computation Conference (PSCC 05), Liège, Belgium*, 2005.
- [18] F. Bouffard, F.D. Galiana, and A.J. Conejo. Market-clearing with stochastic security part I: formulation. *IEEE Transactions on Power Systems*, 20(4):1818–1826, 2005.
- [19] F. Bouffard, F.D. Galiana, and A.J. Conejo. Market-clearing with stochastic security part II: case studies. *IEEE Transactions on Power Systems*, 20(4):1827–1835, 2005.
- [20] S. Bruno, E.D. Tuglie, and M.L. Scala. Transient security dispatch for the concurrent optimization of plural postulated contingencies. *IEEE Transactions on Power Systems*, 17(3):707–714, 2002.
- [21] M. Burger, B. Klar, A. Müller, and G. Schindlmayr. A spot market model for pricing derivatives in electricity markets. *Quantitative Finance*, 4:109–122, 2004.
- [22] J. Chen, J.S. Thorp, and I. Dobson. Cascading dynamics and mitigation assessment in power system disturbances via a hidden failure model. *Electrical Power and Energy Systems*, 27(4):318–326, 2005.
- [23] Q. Chen. *The probability, identification, and prevention of rare events in power systems*. PhD thesis, Iowa State University, 2004.
- [24] Q. Chen and J.D. McCalley. A cluster distribution as a model for estimating high-order-event probabilities in power systems. *Probability in the Engineering and Informational Sciences*, 19:489–505, 2005.
- [25] Y. Chen and B.F. Hobbs. An oligopolistic power market model with tradable NO_x permits. *IEEE Transactions on Power Systems*, 20(1):119–129, 2005.

- [26] Y. Chen, B.F. Hobbs, S. Leyffer, and T.S. Munson. Leader-follower equilibria for electric power and NO_x allowances markets. Technical report, Argonne National Laboratory, 9700 South Cass Avenue, Argonne, Illinois 60439, 2004. http://www.optimization-online.org/DB_HTML/2004/08/936.html.
- [27] B.H. Chowdhury and S. Rahman. A review of recent advances in economic dispatch. *IEEE Transactions on Power Systems*, 5(4):1248–1259, 1990.
- [28] R.D. Christie, B.F. Wollenberg, and I. Wangensteen. Transmission management in the deregulated environment. *Proceedings of the IEEE*, 88(2):170–195, 2000.
- [29] H.K. Clark. It’s time to challenge conventional wisdom, 2004. http://tdworld.com/mag/power_time_challenge_conventional.
- [30] A.J. Conejo, E. Castillo, R. Mínguez, and F. Milano. Locational marginal price sensitivities. *IEEE Transactions on Power Systems*, 20(4):2026–2033, 2005.
- [31] R.W. Cottle, J.S. Pang, and R.E. Stone. *The linear complementarity problem*. Academic Press, San Diego, 1992.
- [32] K.L. Croxton, B. Gendron, and T.L. Magnanti. A comparison of mixed-integer programming models for nonconvex piecewise linear cost minimization problems. *Management Science*, 49(9):1268–1273, 2003.
- [33] A.F. Daughety. *Cournot oligopoly*. Cambridge University Press, New York, USA, 1988.
- [34] A.K. David and F. Wen. Market power in electricity supply. *IEEE Transactions On Energy Conversion*, 16(4):352–360, 2001.
- [35] C.J. Day, B.F. Hobbs, and J.S. Pang. Oligopolistic competition in power networks: a conjectured supply function approach. *IEEE Transactions on Power Systems*, 17(3):597–607, 2002.
- [36] I.R. de Farias JR., M. Zhao, and H. Zhao. A special ordered set approach to discontinuous piecewise linear optimization. Technical report, 2005. State University of New York at Buffalo.
- [37] I. Dobson. Where is the edge for cascading failure?: challenges and opportunities for quantifying blackout risk. *IEEE Power Engineering Society General Meeting, Tampa FL*, June 2007.
- [38] K. Dragoon and V. Dvortsov. Z-method for power system resource adequacy applications. *IEEE Transactions on Power Systems*, 21(2):982–988, May 2006.
- [39] U.S.-Canada Power System Outage Task Force. Final report on the August 14, 2003 blackout in the United States and Canada: causes and recommendations. Technical report, 2004. <https://reports.energy.gov/BlackoutFinal-Web.pdf>.

- [40] R. Green and D. Newbery. Competition in the British electricity spot market. *Journal of Political Economy*, 100(5):929–953, 1992.
- [41] R.J. Green. Increasing competition in the British electricity spot market. *Journal of Industrial Economics*, XLIV(2):205–216, 1992.
- [42] R.J. Green. The electricity contract market in England and Wales. *Journal of Industrial Economics*, XLVII(1):107–124, 1999.
- [43] C. Grigg, P. Wong, P. Albrecht, R. Allan, M. Bhavaraju, R. Billinton, Q. Chen, C. Fong, S. Haddad, S. Kuruganty, W. Li, R. Mukerji, D. Patton, N. Rau, D. Reppen, A. Schneider, M. Shahidehpour, and C. Singh. The IEEE reliability test system-1996. A report prepared by the reliability test system task force of the application of the probability methods subcommittee. *IEEE Transactions on Power Systems*, 14(3):1010–1020, 1999.
- [44] O. Güler and Y. Ye. Convergence behavior of interior-point algorithms. *Mathematical Programming*, 60:215–228, 1993.
- [45] G. Hamoud and I. Bradley. Assessment of transmission congestion cost and locational marginal pricing in a competitive electricity market. *IEEE Transactions on Power Systems*, 19(2):769–775, 2004.
- [46] K.E. Harris and W.E. Strongman. A probabilistic method for reliability, economic and generator interconnection transmission planning studies. *Power Systems Conference and Exposition, 2004. IEEE PES*, 1:486– 490, 2004.
- [47] P. Hines, J. Apt, H. Liao, and S. Talukdar. The frequency of large blackouts in the united states electrical transmission system: an empirical study. Technical report, Carnegie Mellon University, 2006.
- [48] P. Hines and S. Talukdar. Controlling cascading failures with cooperative autonomous agents. Technical report, Carnegie Mellon University, 2006.
- [49] E. Hirst and B. Kirby. Operating reserves and bulk-power reliability. *Energy*, 23(11):949–959, 1998.
- [50] B.F. Hobbs. Linear complementarity models of Nash-Cournot competition in bilateral and POLLCO power markets. *IEEE Transactions on Power Systems*, 16(2):194–202, 2001.
- [51] B.F. Hobbs, U. Hehnan, and J.S. Pang. Equilibrium market power modeling for large scale power systems. *IEEE Transactions on Power Systems*, 1(15-19):558–563, 2001.
- [52] B.F. Hobbs, S. Jitrapaikulsarn, S. Konda, V. Chankong, K.A. Loparo, and D.J. Maratukulam. Analysis of the value for unit commitment of improved load forecasts. *IEEE Transactions on Power Systems*, 14(4):1342–1348, 1999.

- [53] B.F. Hobbs, C.B. Metzler, and J.S. Pang. Strategic gaming analysis for electric power system: an MPEC approach. *IEEE Transactions on Power Systems*, 15(2):638–645, 2000.
- [54] W.W. Hogan. Markets in real electric networks require reactive prices. *The Energy Journal*, 14(3):171–200, 1993.
- [55] Y.Y. Hong and C.Y. Hsiao. Locational marginal price forecasting in deregulated electricity markets using a recurrent neural network. *Proceedings of the Power Engineering Society Winter Meeting*, 2:539–544, 2001.
- [56] Y.Y. Hong and C.Y. Hsiao. Locational marginal price forecasting in deregulated electricity markets using artificial intelligence. *IEE Proceedings of the Generation, Transmission and Distribution*, 149:621–626, 2002.
- [57] M. Huneault and F.D. Galiana. A survey of the optimal power flow literature. *IEEE Transactions on Power Systems*, 6(2):762–770, 1991.
- [58] D. Kirschen and G. Strbac. Why investments do not prevent blackouts. Technical report, UMIST, Manchester, UK, 2003.
- [59] P. Klemperer and M. Meyer. Supply function equilibria in oligopoly under uncertainty. *Econometrica*, 57(6):1243–1277, 1989.
- [60] L.M. Leemis. *Reliability: probabilistic models and statistical methods*. Prentice Hall, New Jersey, USA, 1995.
- [61] B.C. Lesieutre, H. Oh, R.J. Thomas, and V. Donde. Identification of market power in large-scale electric energy markets. *Proceedings of the 39th Hawaii International Conference on System Sciences*, 10:240b, 2006.
- [62] T. Li and M. Shahidehpour. Market power analysis in electricity markets using supply function equilibrium model. *IMA Journal of Management Mathematics*, 15:339–354, 2004.
- [63] F.A. Longstaff and A.W. Wang. Electricity forward prices: a high-frequency empirical analysis. *The Journal of Finance*, 59(4):1877–1900, 2004.
- [64] Z.Q. Luo, J.S. Pang, and D. Ralph. *Mathematical programs with equilibrium constraints*. Cambridge University Press, Cambridge, 1996.
- [65] M. Mazumdar, L. Wang, M. Bailey, and J. Valenzuela. A stochastic Cournot model for market price of electricity. *IEEE Power Engineering Society General Meeting, June 12-16, 2005, San Francisco, CA*, pages 2479–2483, 2005.
- [66] L. McLinden. An analogue of Moreau’s proximation theorem, with application to the nonlinear complementary problem. *Pacific Journal of Mathematics*, 88:101–161, 1980.

- [67] NERC. Disturbances analysis working group database. north american electric reliability council, 2002. <http://www.nerc.com/~database.html>.
- [68] T.J. Overbye, X. Cheng, and Y. Sun. A comparison of the AC and DC power flow models for LMP calculations. *Proceedings of the 37th Hawaii International Conference on System Sciences, 2004*, 2004.
- [69] G. Peters, T. DiGioia Jr., C. Hendrickson, and J. Apt. Transmission line reliability, climate change and extreme weather. Technical report, Carnegie Mellon University, 2006.
- [70] J. Popova. Spatial pattern in modeling electricity prices: evidence from the PJM market. 2004. 24th USAEE and IAEE North American Conference, July 8-10, Washington, DC.
- [71] M.L. Puterman. *Markov decision processes*. John Wiley & Sons, Inc., New York, 1994.
- [72] R. Ragupathi and T.K. Das. A stochastic game approach for modeling wholesale energy bidding in deregulated power markets. *IEEE Transactions On Power Systems*, 19(2):849–856, 2004.
- [73] D. Ralph and S.J. Wright. Some properties of regularization and penalization schemes for MPECs. *Optimization Methods and Software*, 19(5):527–556, 2004.
- [74] A. Rudkevich. Supply function equilibrium in power markets: learning all the way. Technical report, Cambridge, Massachusetts, USA, 1999.
- [75] A. Rudkevich. Supply function equilibrium: theory and applications. *Proceedings of the 36th Hawaii International Conference on System Sciences (HICSS'03)*, pages 107–124, 2003.
- [76] F.C. Schweppe, M.C. Caramanis, R.E. Tabors, and R.E. Bohn. *Spot pricing of electricity*. Kluwer Academics Publishers, Boston, 1998.
- [77] M. Shahidehpour, F. Tinney, and Y. Fu. Impact of security on power systems operation. *Proceedings of the IEEE*, 93(11):2013–2025, 2005.
- [78] P. Skantze, A. Gubina, and M.D. Ilic. Bid-based stochastic model for electricity prices: the impact of fundamental drivers on market dynamics. Energy Laboratory Publications MIT.EL 00-004, Massachusetts Institute of Technology, 2000.
- [79] H. Song, C.C. Liu, J. Lawarrée, and R.W. Dahlgren. Optimal electricity supply bidding by markov decision process. *IEEE Transactions on Power Systems*, 15(2):618–624, 2000.
- [80] Y.H. Song, X. Wang, and J.Z. Liu. *Operation of market-oriented power systems*. Springer, London, 2003.
- [81] S. Stoft. *Power system economics*. IEEE Press, Piscataway, 2002.

- [82] S. Stoft. The demand for operating reserves: key to price spikes and investment. *IEEE Transactions on Power Systems*, 18(2):470–477, 2003.
- [83] J.H. Talag, F., and M.E. El-Harwary. A summary of environmental/economic dispatch algorithms. *IEEE Transactions on Power Systems*, 9(3):1508–1516, 1994.
- [84] S. Talukdar, D. Jia, P. Hines, and B.H. Krogh. Distributed model predictive control for the mitigation of cascading failures. *Proceedings of the 44th IEEE Conference on Decision and Control, and the European Control Conference 2005*, pages 4440–4445, December 2005.
- [85] S.N. Talukdar, J. Apt, M. Ilic, L.B. Lave, and M.G. Morgan. Cascading failures: survival versus prevention. *The Electricity Journal*, 16(9):25–31, 2003.
- [86] J. Valenzuela and M. Mazumdar. Commitment of electric power generators under stochastic market prices. *Operations Research*, 51(6):880–893, 2003.
- [87] J. Valenzuela and M. Mazumdar. A probability model for the electricity price duration curve under an oligopoly market. *IEEE Transactions on Power Systems*, 20:1250–1256, 2005.
- [88] J. Valenzuela, M. Mazumdar, and A. Kapoor. Influence of Temperature and Load Forecast Uncertainty on Estimates of Power Generation Production Costs. *IEEE Transactions on Power Systems*, 15(2):668 – 674, 2000.
- [89] L. Wang, M. Mazumdar, M. Bailey, and J. Valenzuela. Oligopoly models for market price of electricity under demand uncertainty and unit reliability. *European Journal of Operational Research*, 181(3):1309–1321, 2007.
- [90] J.-Y. Wei and Y. Smeers. Spatial oligopolistic electricity models with Cournot generators and regulated transmission prices. *Operations Research*, 47(1):102–112, 1999.
- [91] B.F. Wollenberg. From blackout to blackout. *IEEE Power and Energy Magazine*, 2004.
- [92] A.J. Wood and B.F. Wollenberg. *Power generation operation and control*. John Wiley and Sons, New York, 1996.
- [93] J. Yao, S.S. Oren, and I. Adler. Computing Cournot equilibria in two settlement electricity markets with transmission constraints. *Proceedings of the 37th Hawaii International Conference on System Sciences*, 2004.
- [94] M. Zima and G. Andersson. On security criteria in power systems operation. *Proceedings of the IEEE Power Engineering Society General Meeting*, 3:3089–3093, June 2005.